Short-range-correlation physics at low RG resolution

Dick Furnstahl

Workshop on Quantitative SRC Physics

March 2022

The Ohio State University

U.S. Department of Energy

NUCLEI

Nuclear Computational Low-Energy Initiative

Most recent: Tropiano, Bogner, and rjf, Phys. Rev. C **104**, 034311 (2021);
Tropiano, Bogner, rjf, Hisham, Phys. Rev. C **106**, 024324 (2022);

What is renormalization group (RG) resolution?

Here: RG resolution is set by the largest momentum in low-energy wave functions

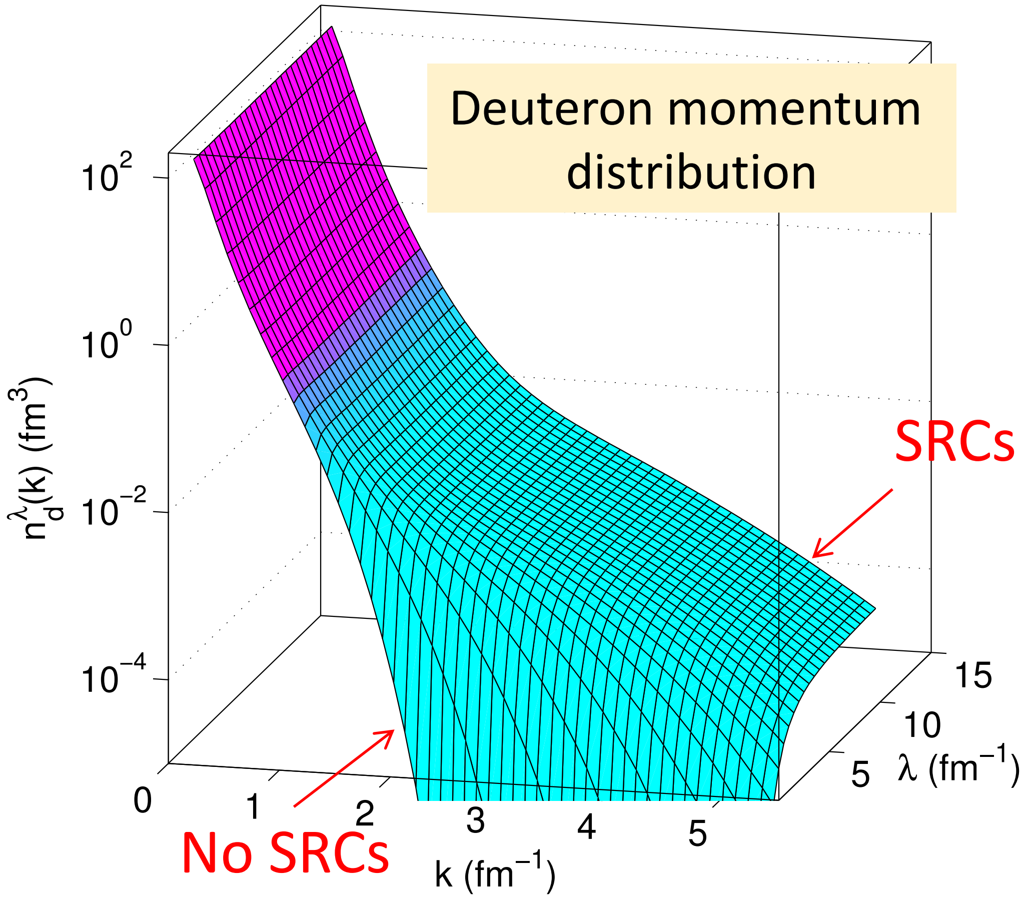

RG resolution on λ axis

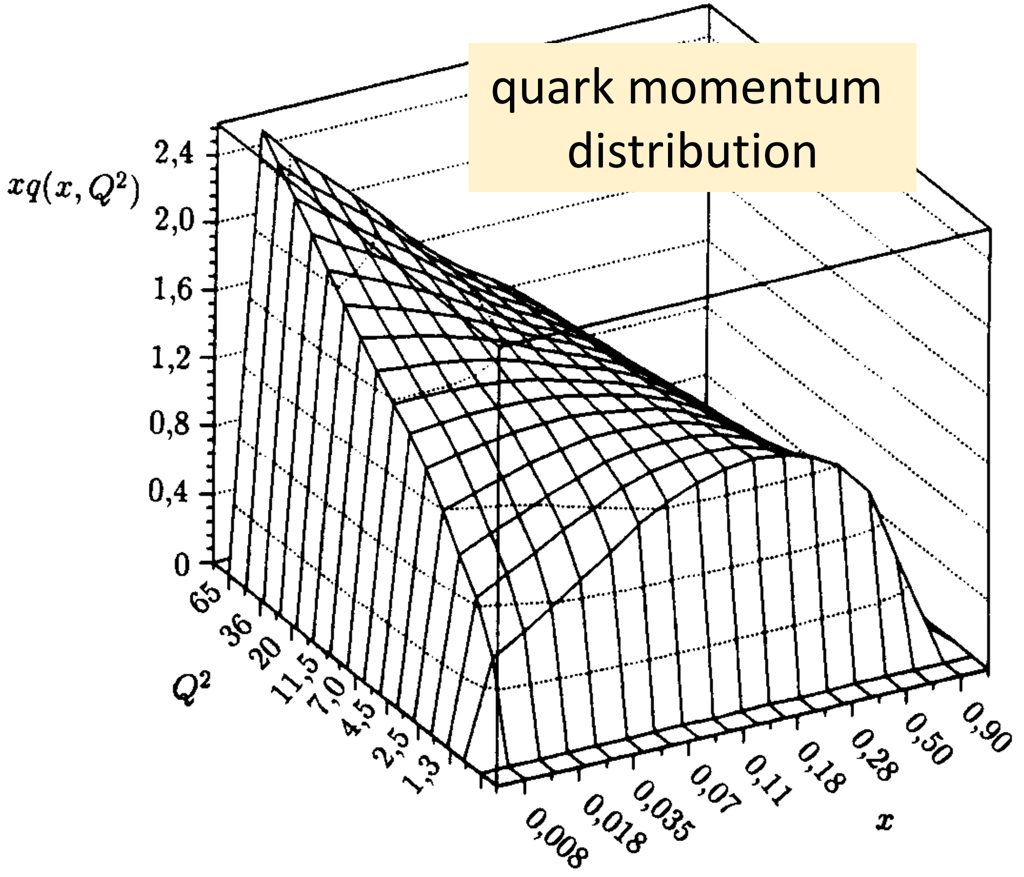

Resolution set by $\mu^2 \approx Q^2$

High and low RG resolution

- **High RG resolution:** One-body current operators suffice but with highly *correlated* wave functions

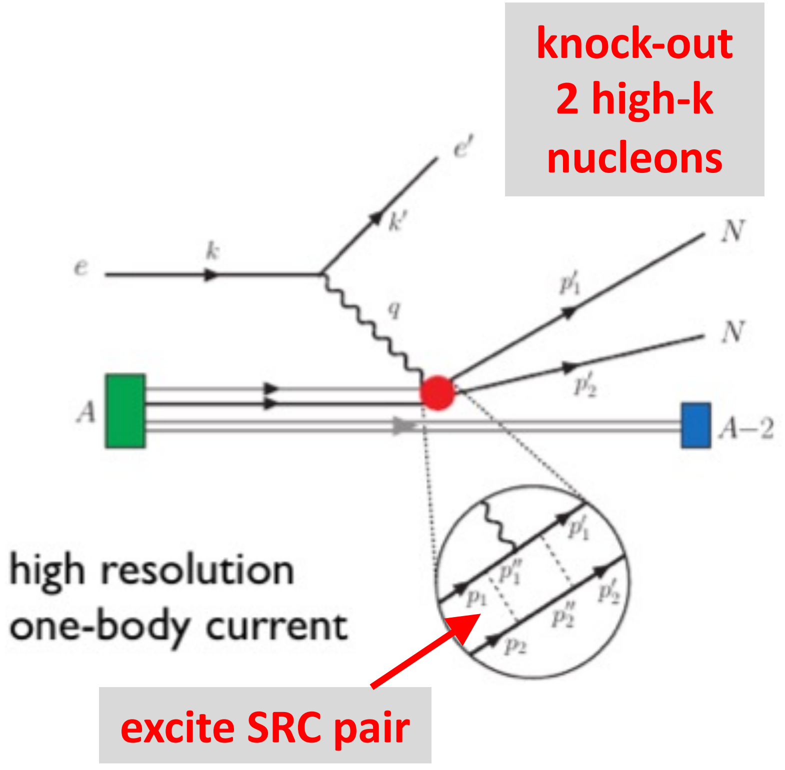

High and low RG resolution

- **High RG resolution:** One-body current operators suffice but with highly *correlated* wave functions
- **Low RG resolution:** Two-body current operators needed but with (comparatively) *uncorrelated* wave functions
  - Operators do NOT become hard, which simplifies calculations!

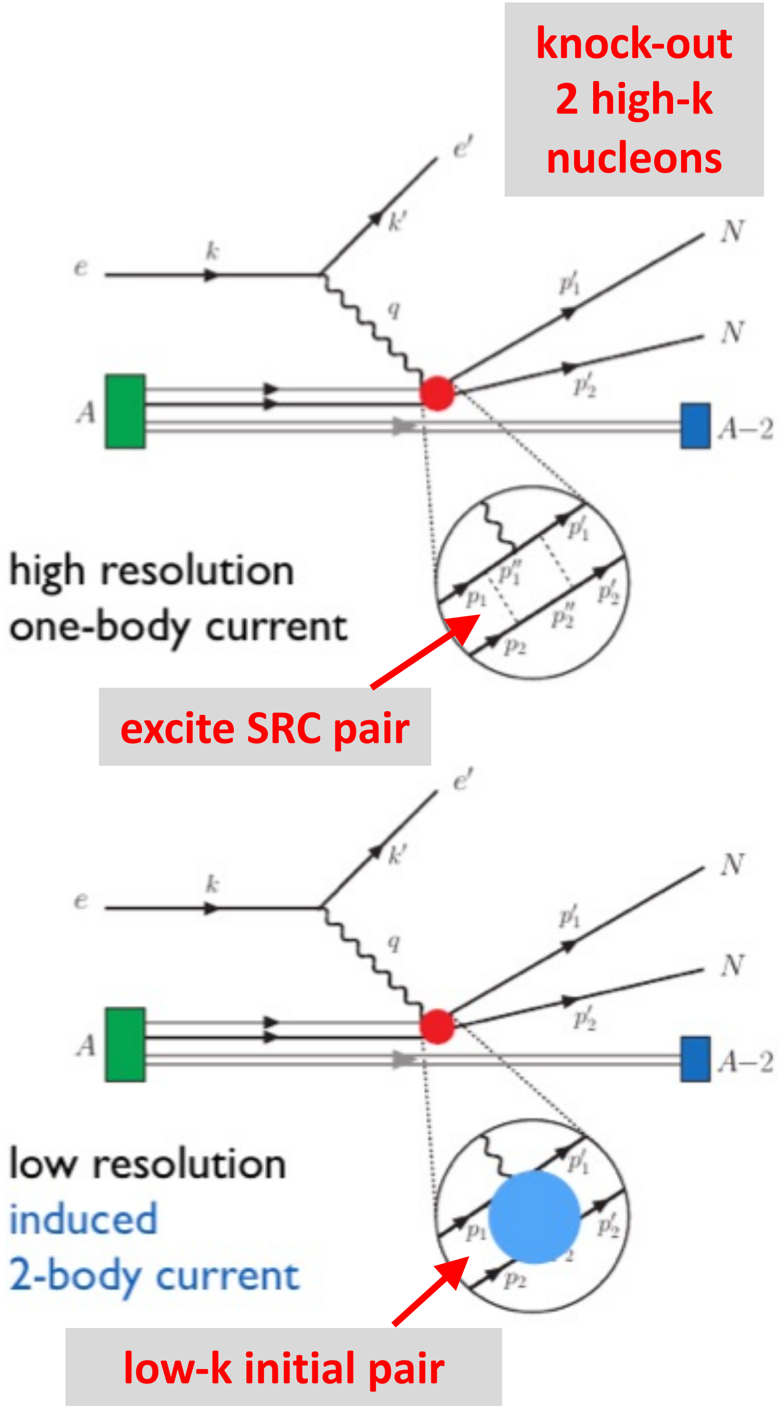

High and low RG resolution

- **High RG resolution:** One-body current operators suffice but with highly *correlated* wave functions
- **Low RG resolution:** Two-body current operators needed but with (comparatively) *uncorrelated* wave functions
  - Operators do NOT become hard, which simplifies calculations!
- ***Experimental resolution*** is set by kinematics of probe → same at both RG resolutions
- **Same observables** but different physical interpretation!

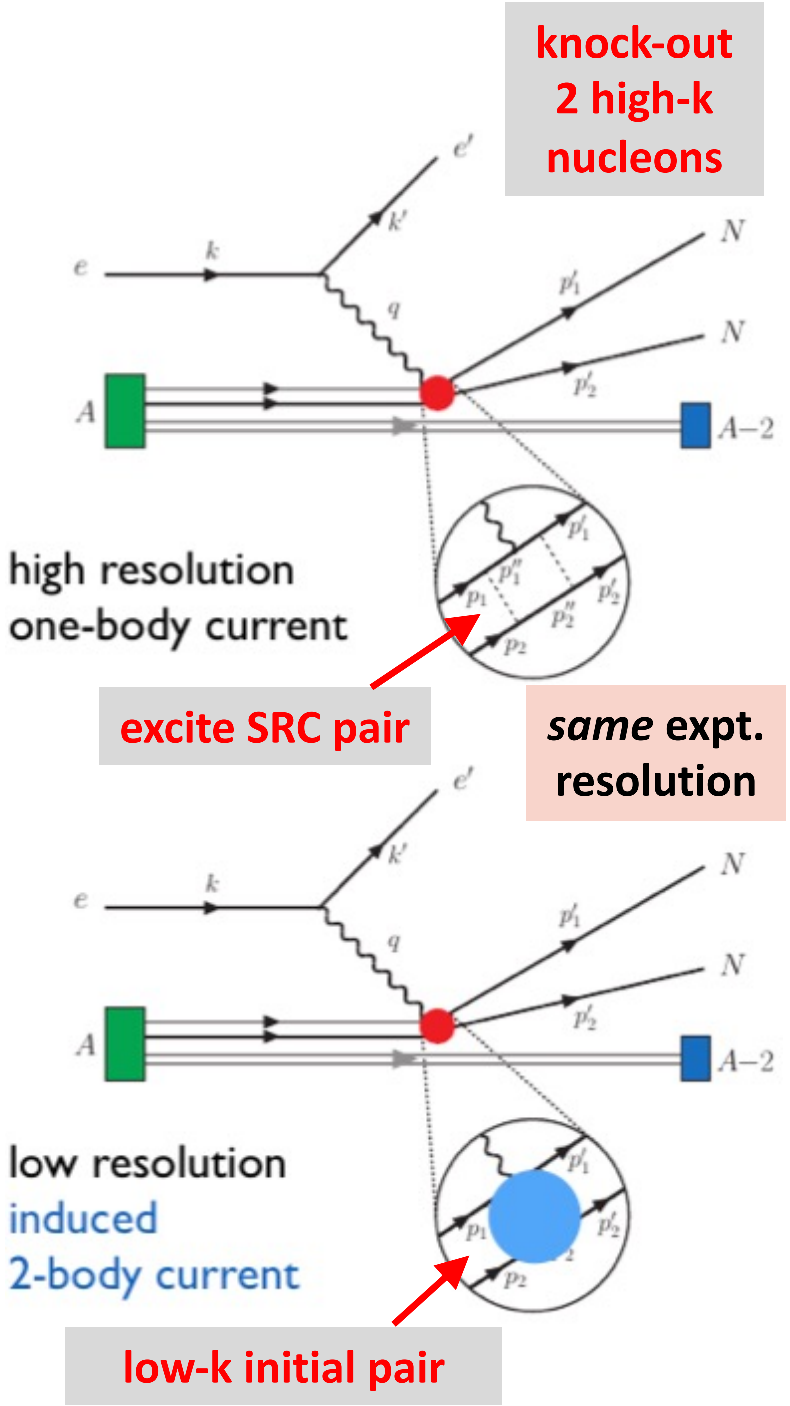

High and low RG resolution

- **High RG resolution:** One-body current operators suffice but with highly *correlated* wave functions
- **Low RG resolution:** Two-body current operators needed but with (comparatively) *uncorrelated* wave functions
    - Operators do NOT become hard, which simplifies calculations!
- ***Experimental resolution*** is set by kinematics of probe → same at both RG resolutions
- **Same observables** but different physical interpretation!

- **Rest of this talk:**
    - How can SRC calculations be carried out at low RG resolution?
    - What can we describe with simple approximations?
    - Connections to existing SRC phenomenology (e.g., GCF or LCA)
    - Levinger constant example: scale/scheme dependence

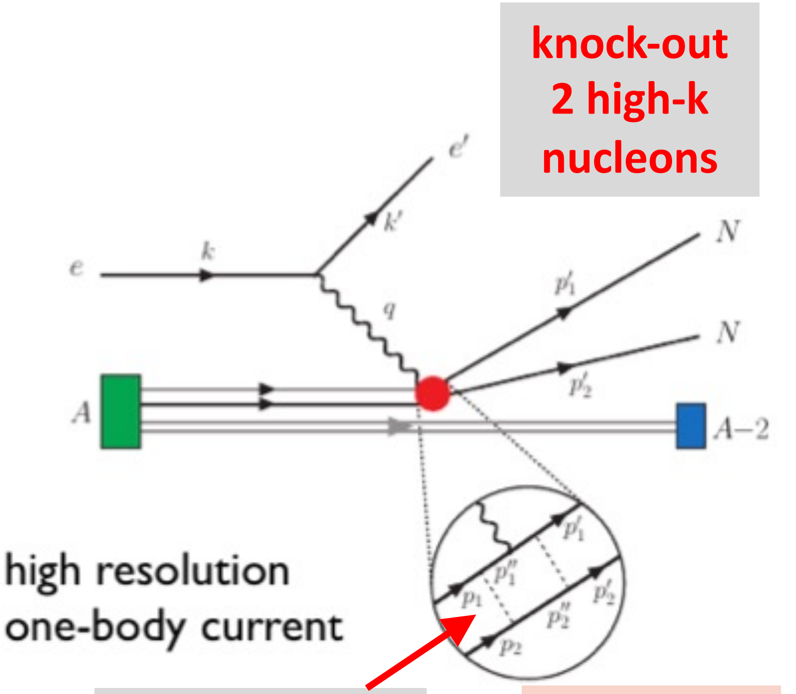

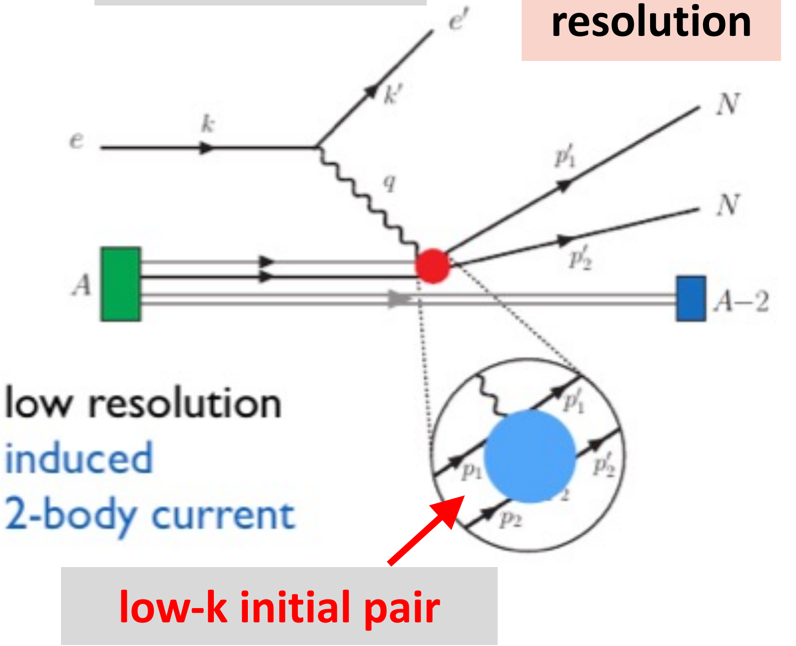

Changing RG resolution: Similarity RG (or SRG)

- Evolve to low RG resolution using the SRG

$$O(s) = U(s)O(0)U^{\dagger}(s)$$

where $s = 0 \to \infty$ and $U(s)$ is unitary

- SRG transformations decouple high- and low-momenta in the Hamiltonian

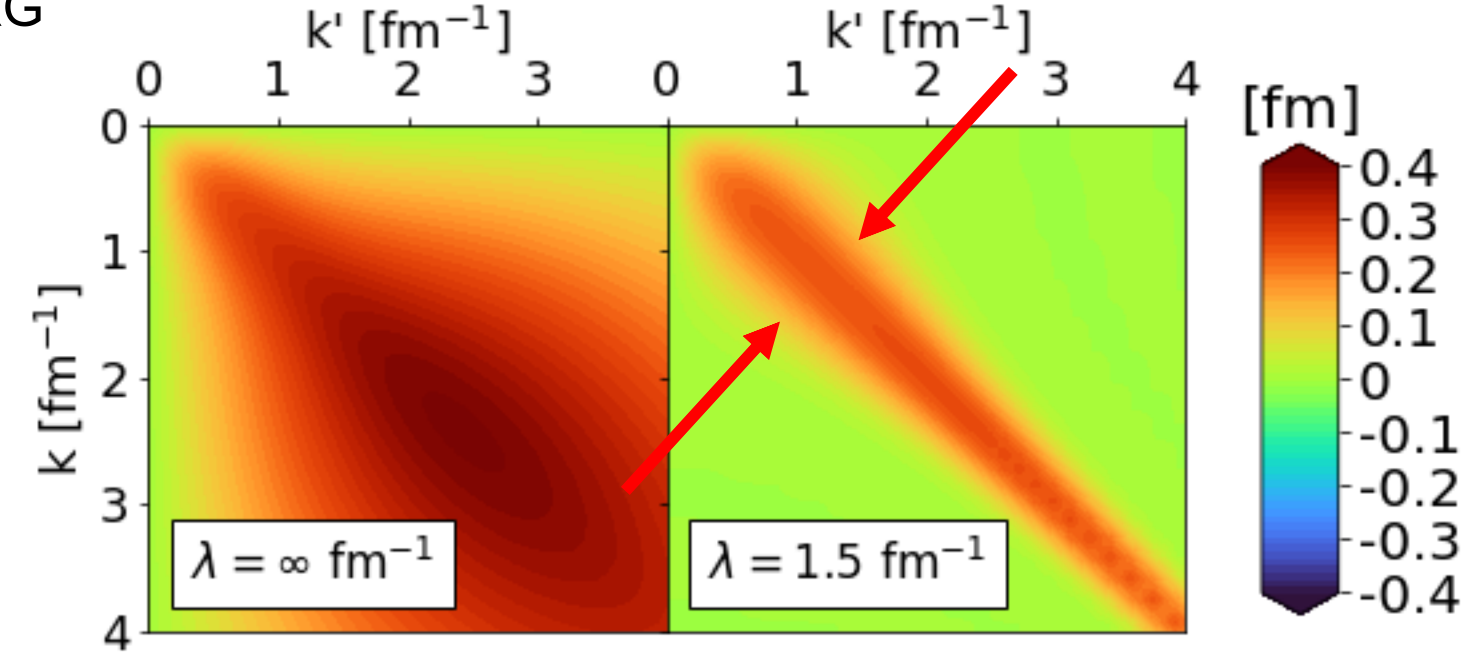

Fig. 1: Momentum space matrix elements of Argonne v18 (AV18) under SRG evolution in $^1P_1$ channel.

[e.g., see Hergert, arXiv:2008.05061]

Changing RG resolution: Similarity RG (or SRG)

- Evolve to low RG resolution using the SRG
$$O(s) = U(s)O(0)U^{\dagger}(s)$$
where $s = 0 \to \infty$ and $U(s)$ is unitary
- SRG transformations *decouple* high- and low-momenta in the Hamiltonian
- *Decoupling scale* given by $\lambda = s^{-1/4}$
- In practice, solve differential flow equation
$$\frac{dO(s)}{ds} = [\eta(s), O(s)]$$
where $\eta(s) \equiv \frac{dU(s)}{ds}U^{\dagger}(s) = [G, H(s)]$ is the SRG generator

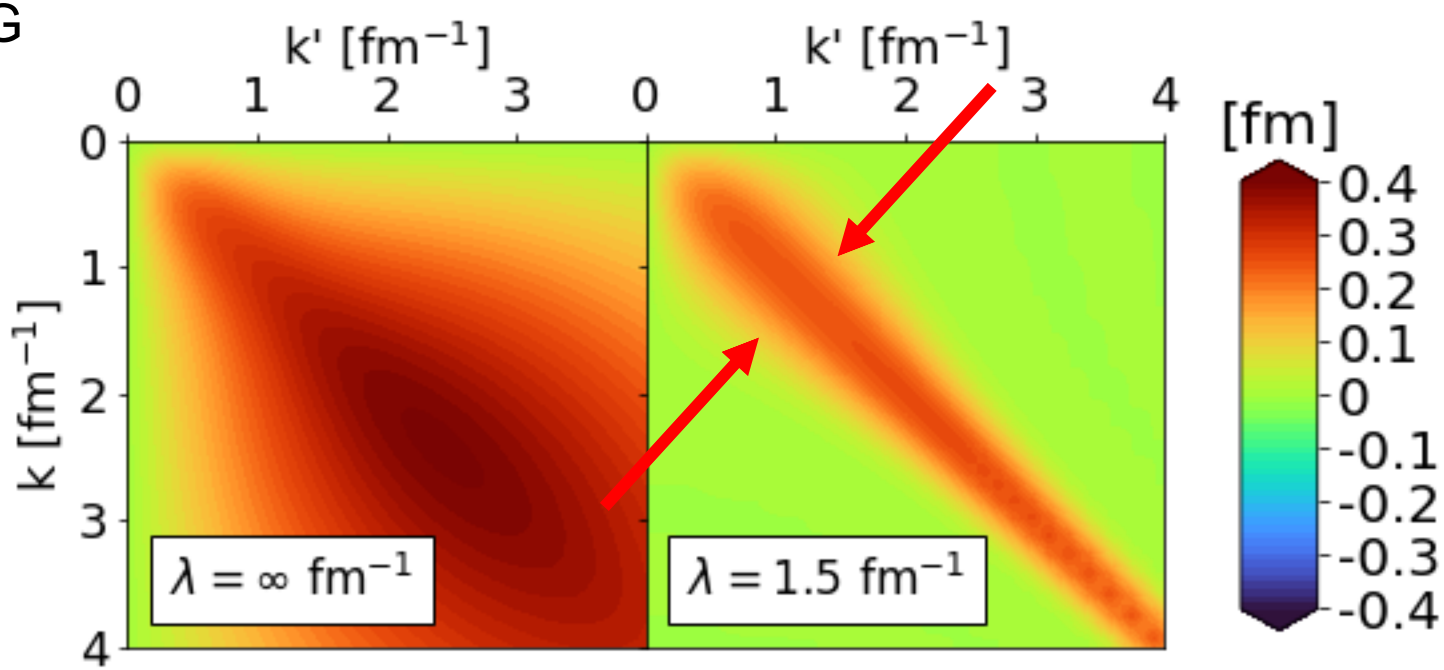

Fig. 1: Momentum space matrix elements of Argonne v18 (AV18) under SRG evolution in $^1P_1$ channel.

[e.g., see Hergert, arXiv:2008.05061]

Changing RG resolution: Similarity RG (or SRG)

- Evolve to low RG resolution using the SRG
$$O(s) = U(s)O(0)U^{\dagger}(s)$$
where $s = 0 \to \infty$ and $U(s)$ is unitary
- SRG transformations decouple high- and low-momenta in the Hamiltonian
- *Decoupling scale* given by $\lambda = s^{-1/4}$
- In practice, solve differential flow equation
$$\frac{dO(s)}{ds} = [\eta(s), O(s)]$$
where $\eta(s) \equiv \frac{dU(s)}{ds} U^{\dagger}(s) = [G, H(s)]$ is the SRG generator
- Trivial for one and two-body operators; routine for three-body operators

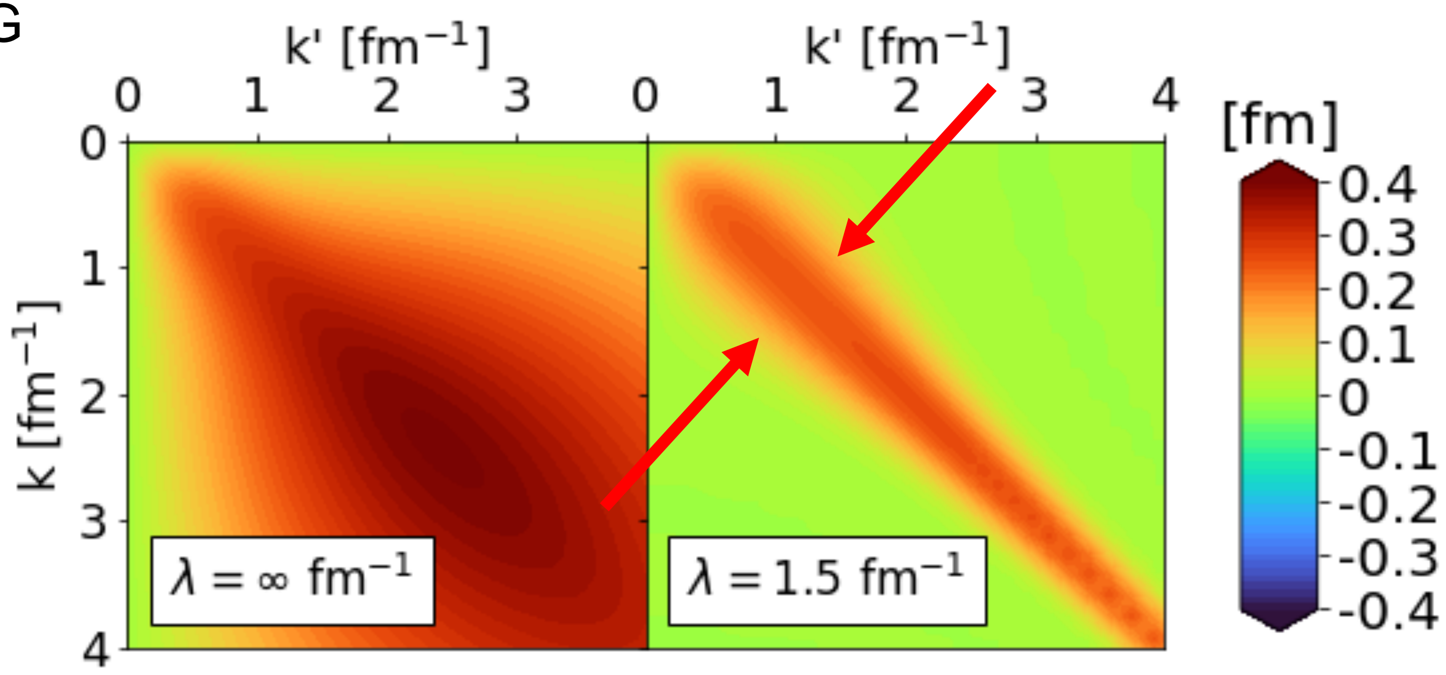

Fig. 1: Momentum space matrix elements of Argonne v18 (AV18) under SRG evolution in $^1P_1$ channel.

[e.g., see Hergert, arXiv:2008.05061]

Similarity RG evolution in action (visualization)

$\langle \hbar k | V(\lambda) | \hbar k' \rangle$

partial-wave momentum basis

Flow parameter λ (momentum)

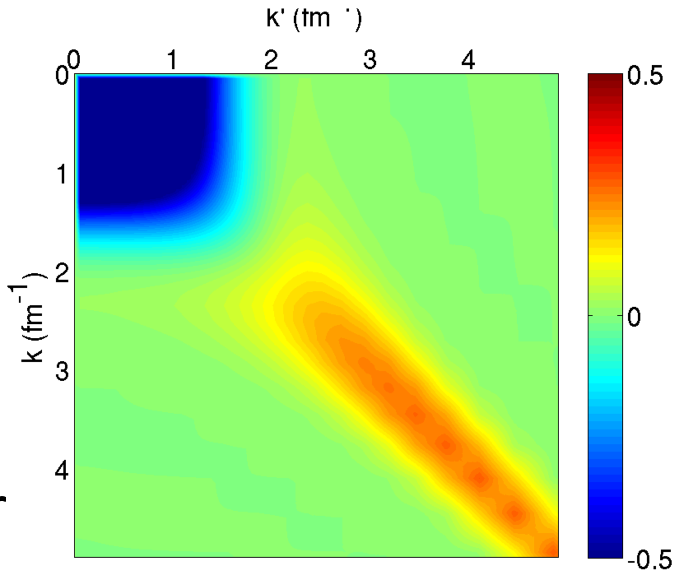

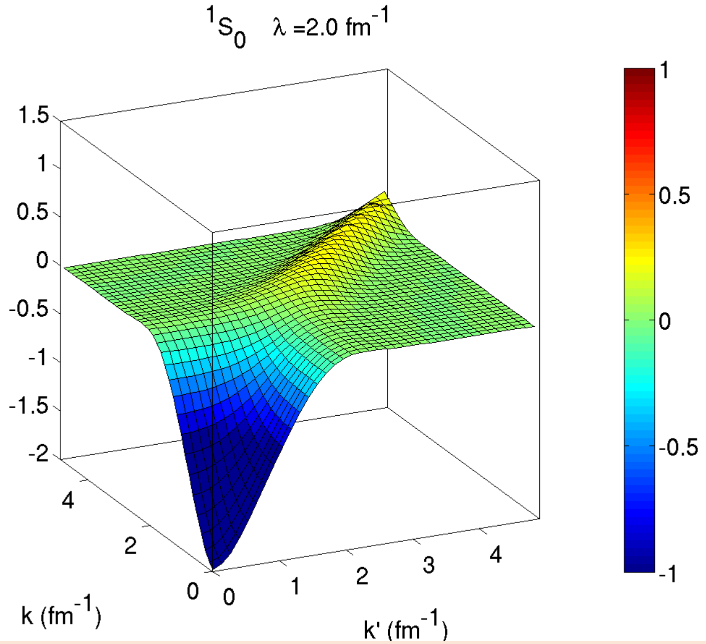

Band diagonalization of Hamiltonian

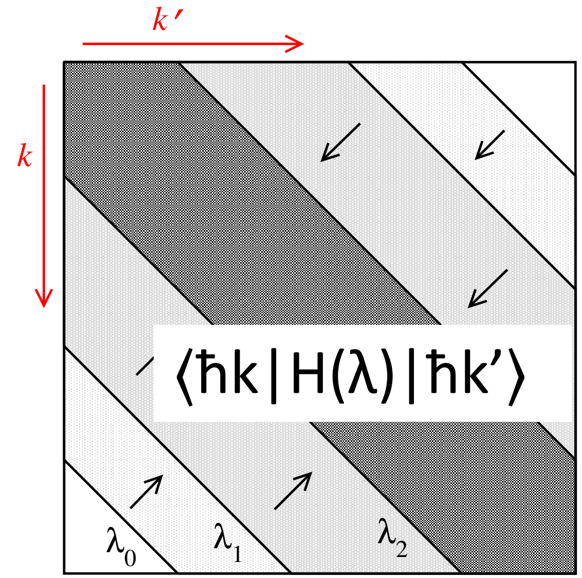

Kyle Wendt
PRC 86 (2012)

Local projection: action of potential between low-momentum nucleons

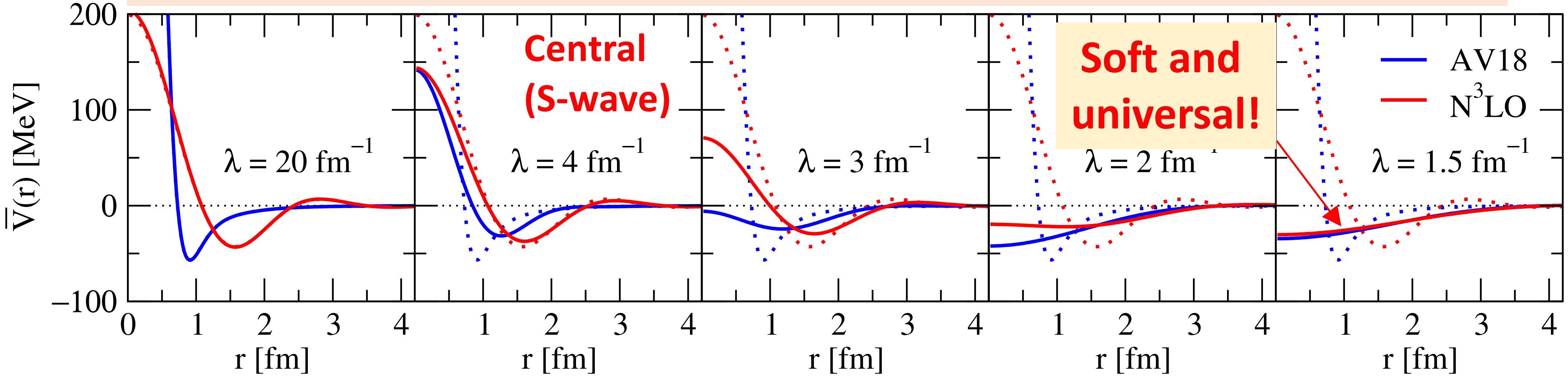

Similarity RG evolution in action (visualization)

⟨ħk|V(λ)|ħk’⟩

partial-wave momentum basis

Flow parameter λ (momentum)

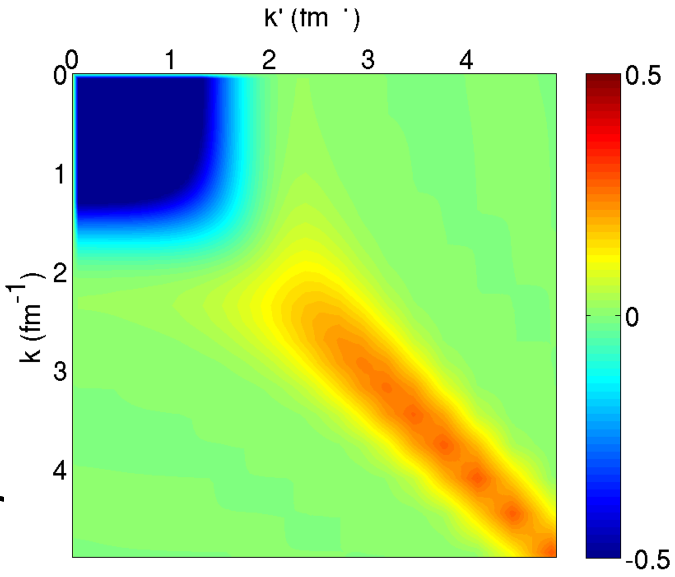

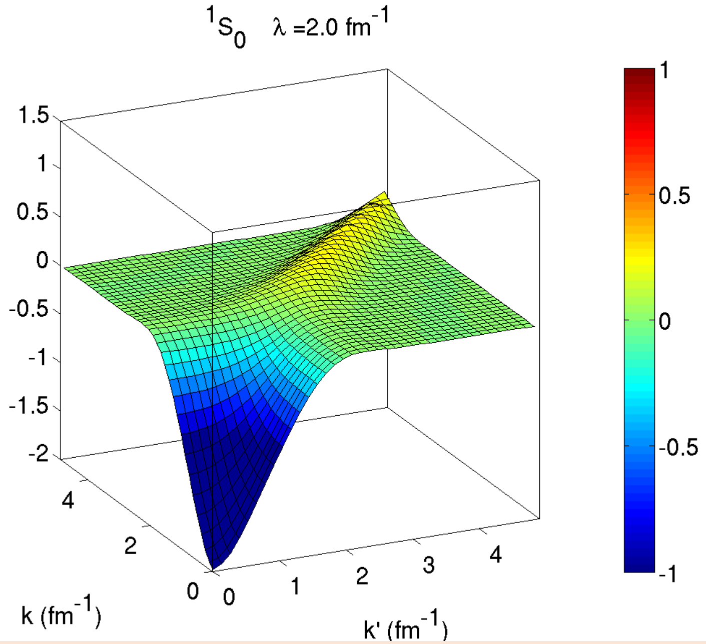

Band diagonalization of Hamiltonian

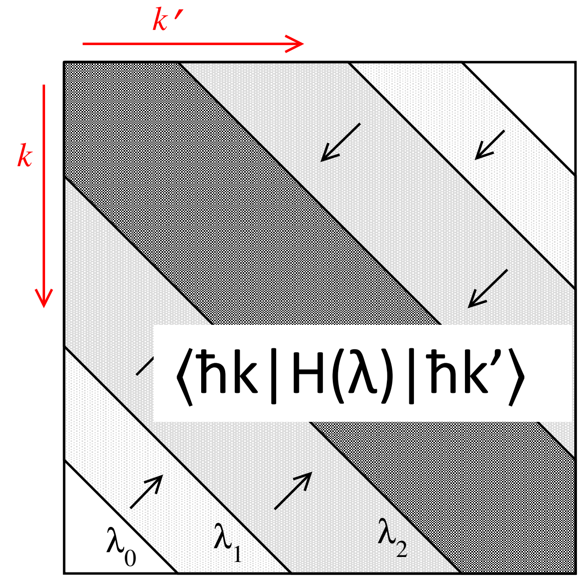

Local projection: action of potential between low-momentum nucleons

Kyle Wendt
PRC 86 (2012)

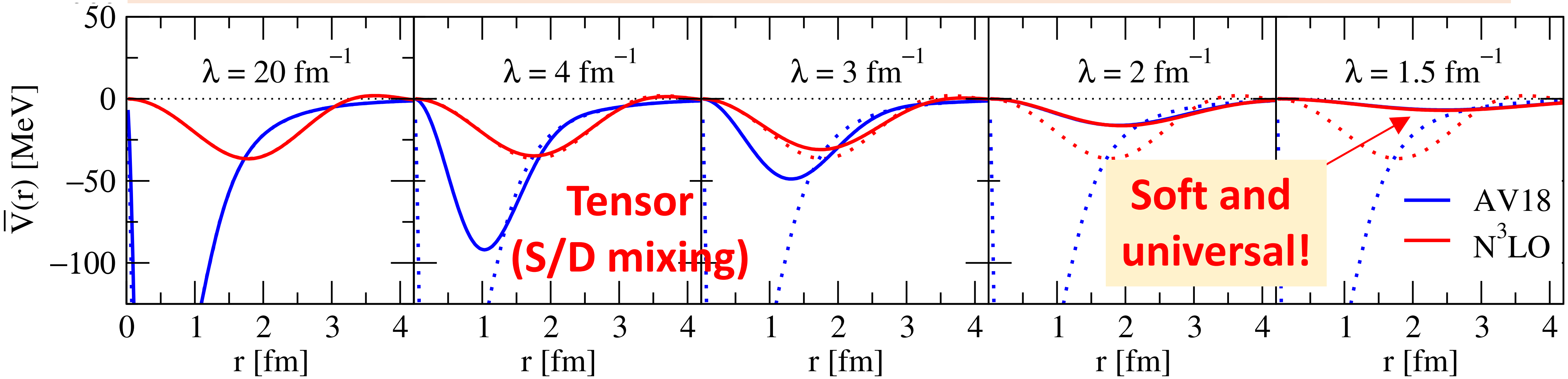

Changing RG resolution: Similarity RG (or SRG)

- AV18 wave functions have significant SRCs
- What happens to the wave functions under SRG transformations?

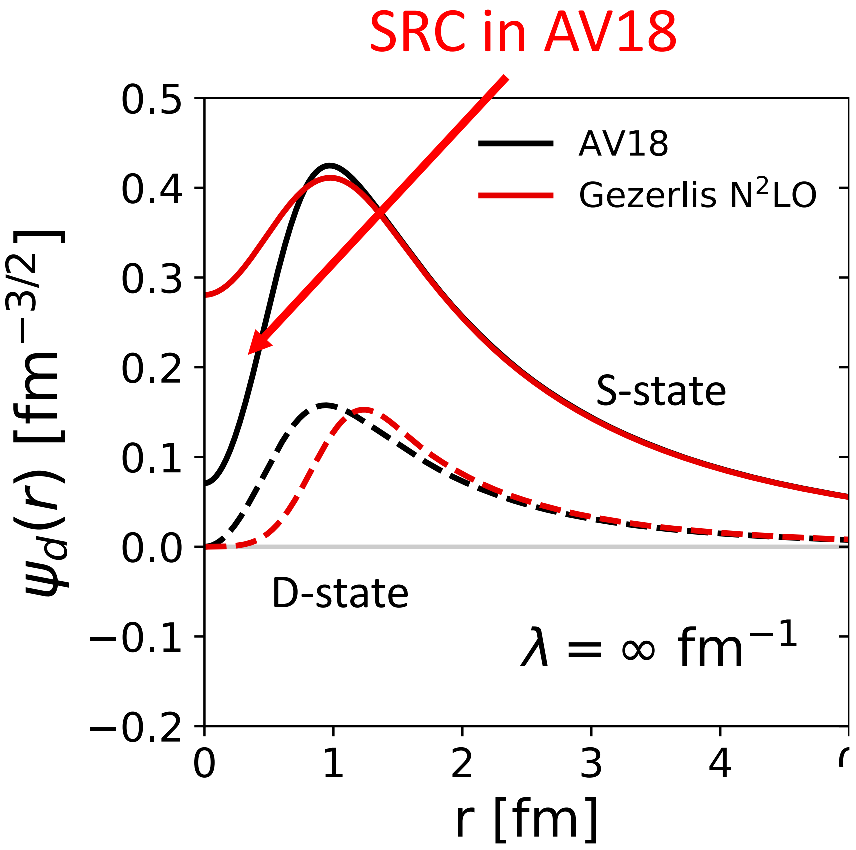

Fig. 2: SRG evolution of deuteron wave function in coordinate space for AV18 and Gezerlis N^{2}LO[1].

[1]A. Gezerlis et al., Phys. Rev. C **90**, 054323 (2014)

Changing RG resolution: Similarity RG (or SRG)

- SRC physics in AV18 is gone from wave function at low RG resolution
- Deuteron wave functions become soft and D-state probability decreases
- Observables such as asymptotic D-S ratio do not change
- Universal low-energy V → same wave functions

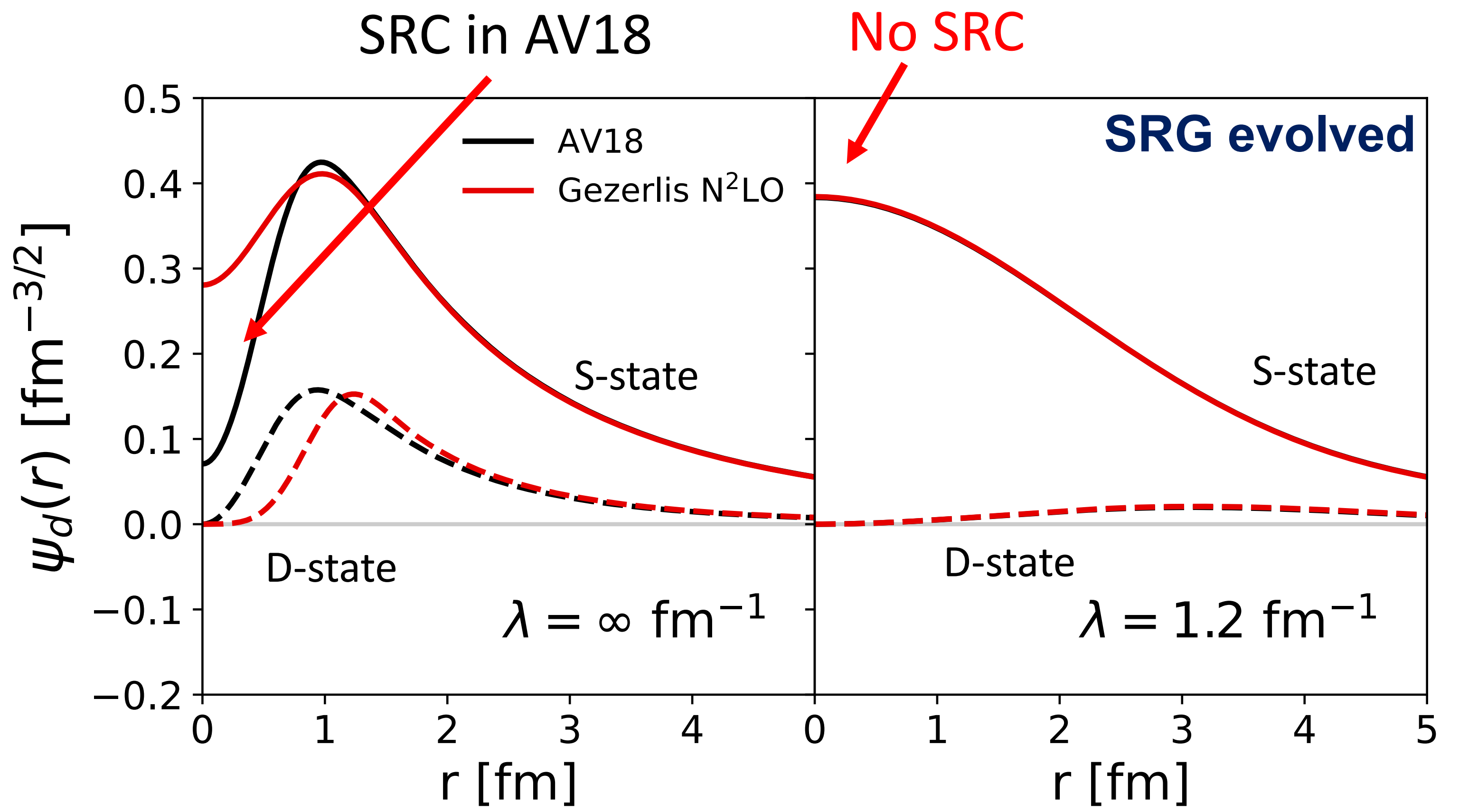

Fig. 2: SRG evolution of deuteron wave function in coordinate space for AV18 and Gezerlis N²LO[1].

[1]A. Gezerlis et al., Phys. Rev. C **90**, 054323 (2014)

Consistent operator evolution

- Soft wave functions at low RG resolution
- SRC physics shifts to the operators

$$\langle \psi_f^{hi} | O^{hi} | \psi_i^{hi} \rangle = \langle \psi_f^{hi} | U_\lambda^\dagger U_\lambda O^{hi} U_\lambda^\dagger U_\lambda | \psi_i^{hi} \rangle = \langle \psi_f^{low} | O^{low} | \psi_i^{low} \rangle$$

Consistent operator evolution

- Soft wave functions at low RG resolution
- SRC physics shifts to the operators

$$\langle \psi_f^{hi} | O^{hi} | \psi_i^{hi} \rangle = \langle \psi_f^{hi} | U_\lambda^\dagger U_\lambda O^{hi} U_\lambda^\dagger U_\lambda | \psi_i^{hi} \rangle = \langle \psi_f^{low} | O^{low} | \psi_i^{low} \rangle$$

- **Example:** Calculate high RG resolution single-nucleon momentum distribution at low RG res. by evolving momentum projection operator $a_q^\dagger a_q$:

$$n_d(q) = \langle \psi_d | a_q^\dagger a_q | \psi_d \rangle = \langle \psi_d^\lambda | U_\lambda a_q^\dagger a_q U_\lambda^\dagger | \psi_d^\lambda \rangle$$

Consistent operator evolution

Fig. 3: Evolved momentum projection operator $U_\lambda a_q^\dagger a_q U_\lambda^\dagger$ for several λ values where $q = 3$ fm-1.

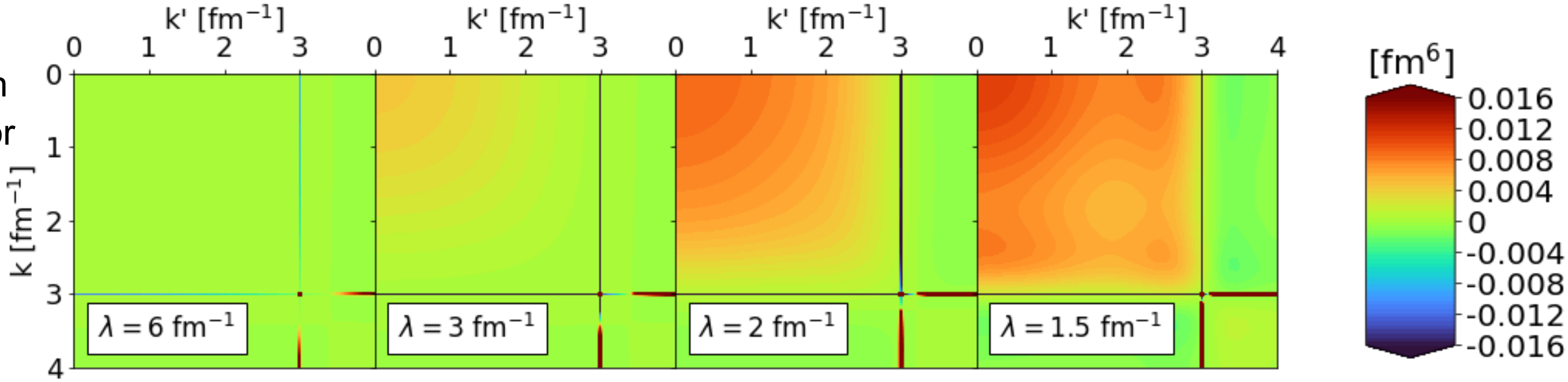

Consistent operator evolution

Fig. 3: Evolved momentum projection operator $U_\lambda a_q^\dagger a_q U_\lambda^\dagger$ for several λ values where $q = 3$ fm-1.

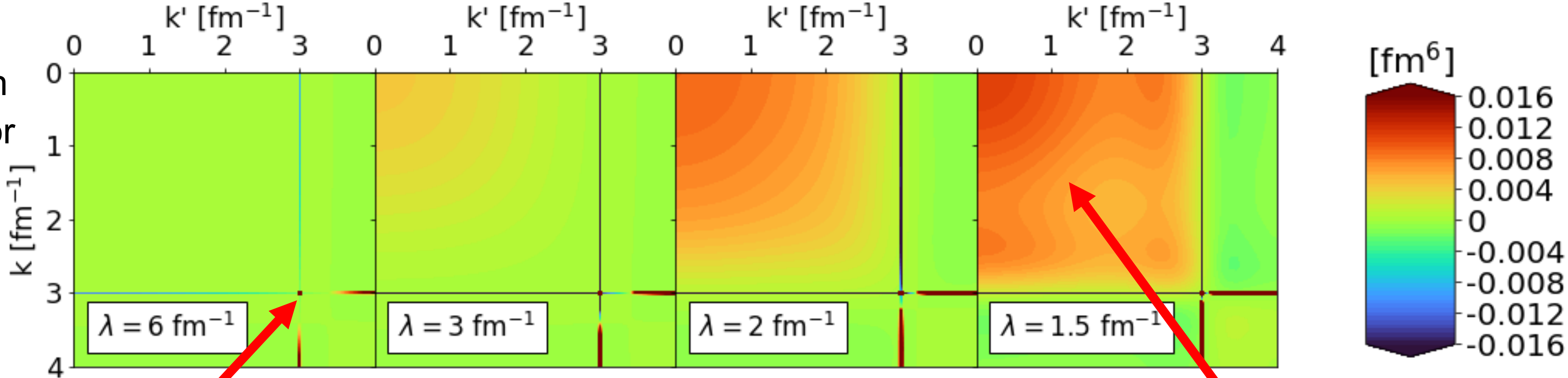

RG Scale

Initial operator is a discretized delta function in momentum space
$$\sim\delta(k-q)\delta(k'-q)$$

SRG evolution induces smooth, low-momentum contributions

Consistent operator evolution

Fig. 3: Evolved momentum projection operator $U_\lambda a_q^\dagger a_q U_\lambda^\dagger$ for several λ values where $q = 3$ fm[-1].

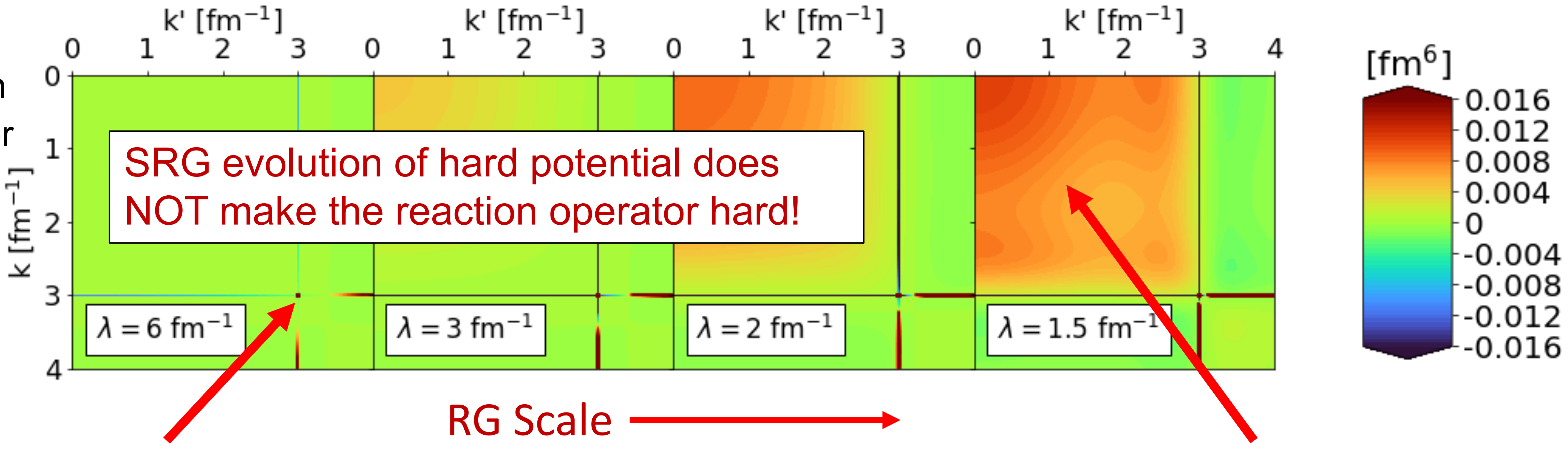

Initial operator is a discretized delta function in momentum space
$\sim\delta(k-q)\delta(k'-q)$

SRG evolution induces smooth, low-momentum contributions

Consistent operator evolution

Fig. 3: Evolved momentum projection operator $U_\lambda a_q^\dagger a_q U_\lambda^\dagger$ for several λ values where $q = 3$ fm-1.

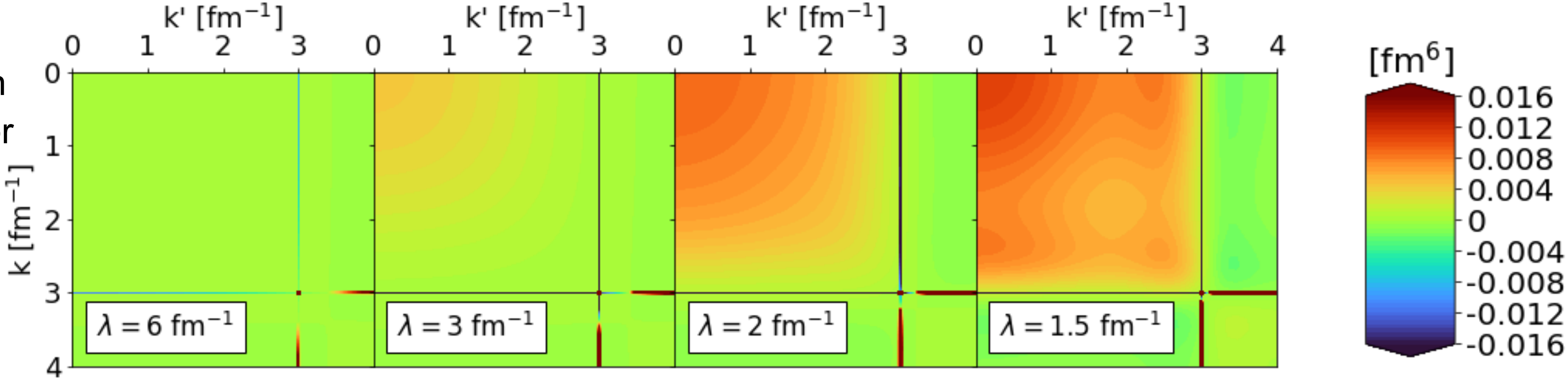

Fig. 4: *Integrand* of $\langle \psi_d^\lambda | U_\lambda a_q^\dagger a_q U_\lambda^\dagger | \psi_d^\lambda \rangle$ where $q = 3$ fm-1.

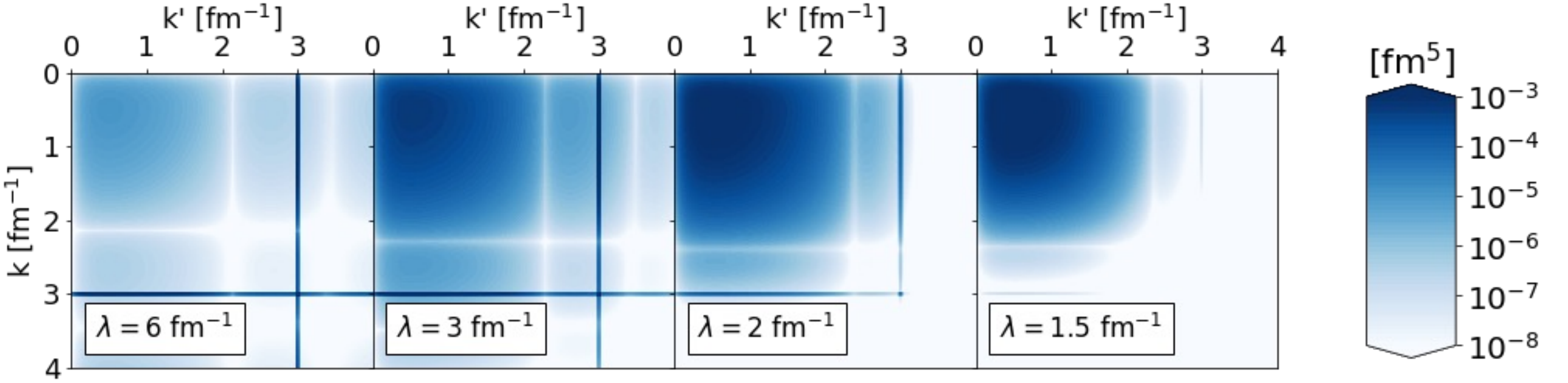

Consistent operator evolution

- Each panel gives the correct expectation value from unitarity
- At high RG resolution, $^3S_1$- $^3S_1$ channel contributes only ~25% of the expectation value $\langle \psi_d | a_q^\dagger a_q | \psi_d \rangle$ (heavy contribution from tensor force)

Fig. 3: Evolved momentum projection operator $U_\lambda a_q^\dagger a_q U_\lambda^\dagger$ for several λ values where $q = 3$ fm^{-1}.

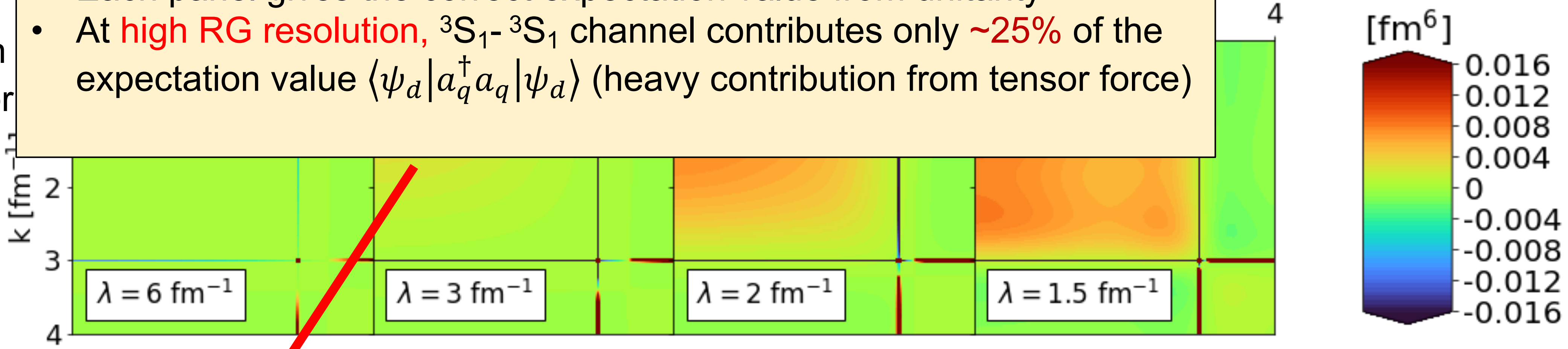

Fig. 4: *Integrand* of $\langle \psi_d^\lambda | U_\lambda a_q^\dagger a_q U_\lambda^\dagger | \psi_d^\lambda \rangle$ where $q = 3$ fm^{-1}.

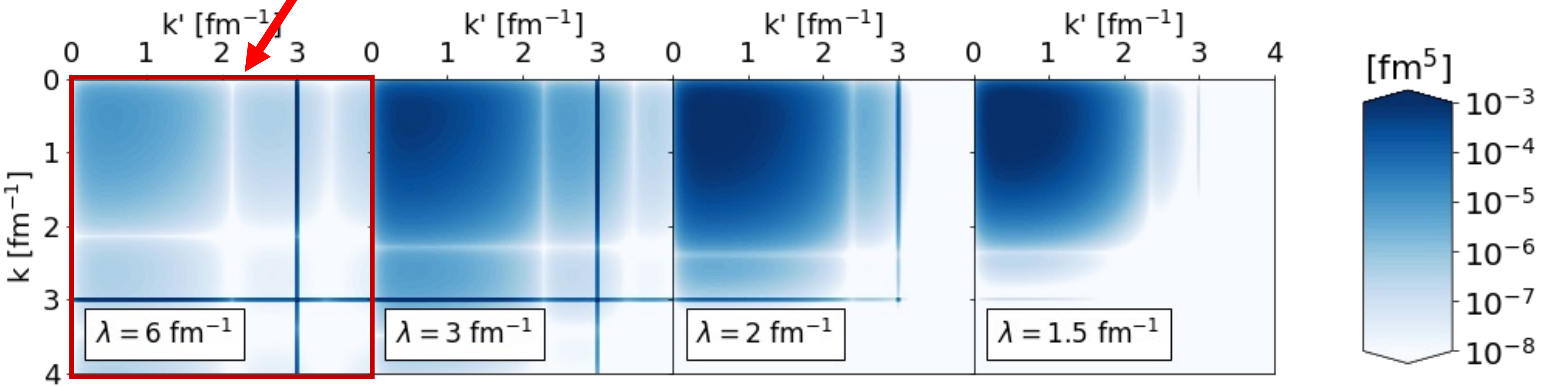

Consistent operator evolution

Fig. 3: Evolved momentum projection operator $U_\lambda a_q^\dagger a_q U_\lambda^\dagger$ for several λ values where $q = 3$ fm^{-1}.

- Each panel gives the correct expectation value from unitarity
- At high RG resolution, $^3S_1$- $^3S_1$ channel contributes only ~25% of the expectation value $\langle \psi_d | a_q^\dagger a_q | \psi_d \rangle$ (heavy contribution from tensor force)
- Expectation value is filtered to lower momentum at low RG resolution
- At low RG resolution, $^3S_1$- $^3S_1$ channel contributes to ~95% of the expectation value

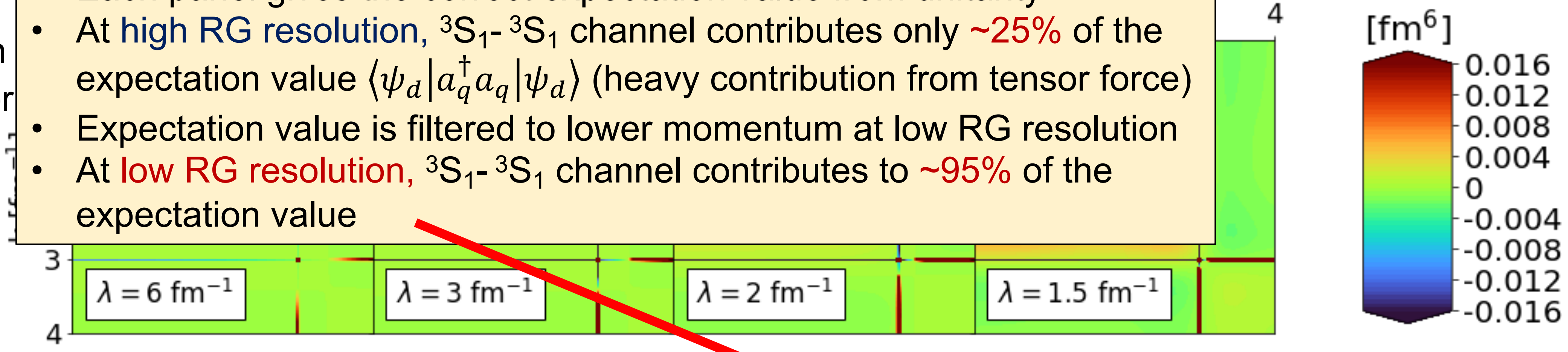

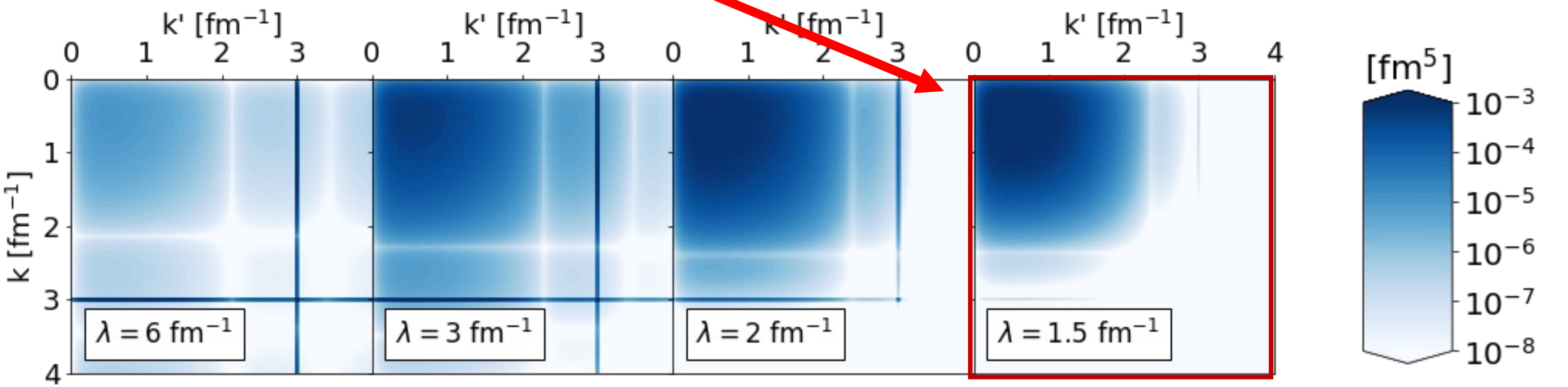

Fig. 4: *Integrand* of $\langle \psi_d^\lambda | U_\lambda a_q^\dagger a_q U_\lambda^\dagger | \psi_d^\lambda \rangle$ where $q = 3$ fm^{-1}.

Momentum distributions at low RG resolution

- Apply SRG transformations to momentum distribution operators
  - Single-nucleon momentum distribution: $\hat{n}^{hi}(\boldsymbol{q}) = a_{\boldsymbol{q}}^{\dagger} a_{\boldsymbol{q}}$
  - Pair momentum distribution: $\hat{n}^{hi}(\boldsymbol{q}, \boldsymbol{Q}) = a_{\frac{\boldsymbol{Q}}{2}+\boldsymbol{q}}^{\dagger} a_{\frac{\boldsymbol{Q}}{2}-\boldsymbol{q}}^{\dagger} a_{\frac{\boldsymbol{Q}}{2}-\boldsymbol{q}} a_{\frac{\boldsymbol{Q}}{2}+\boldsymbol{q}}$

Momentum distributions at low RG resolution

- Apply SRG transformations to momentum distribution operators
  - Single-nucleon momentum distribution: $\hat{n}^{hi}(\boldsymbol{q}) = a_{\boldsymbol{q}}^{\dagger} a_{\boldsymbol{q}}$
  - Pair momentum distribution: $\hat{n}^{hi}(\boldsymbol{q}, \boldsymbol{Q}) = a_{\frac{\boldsymbol{Q}}{2}+\boldsymbol{q}}^{\dagger} a_{\frac{\boldsymbol{Q}}{2}-\boldsymbol{q}}^{\dagger} a_{\frac{\boldsymbol{Q}}{2}-\boldsymbol{q}} a_{\frac{\boldsymbol{Q}}{2}+\boldsymbol{q}}$
- Expand SRG transformation to 2-body level

$$\widehat{U}_{\lambda} = 1 + \frac{1}{4} \sum_{\boldsymbol{K},\boldsymbol{k},\boldsymbol{k}'} \delta U_{\lambda}^{(2)}(\boldsymbol{k}, \boldsymbol{k}') a_{\frac{\boldsymbol{K}}{2}+\boldsymbol{k}}^{\dagger} a_{\frac{\boldsymbol{K}}{2}-\boldsymbol{k}}^{\dagger} a_{\frac{\boldsymbol{K}}{2}-\boldsymbol{k}'} a_{\frac{\boldsymbol{K}}{2}+\boldsymbol{k}'} + \cdots$$

- $\delta U_{\lambda}^{(2)}$ term is fixed by SRG evolution on $A = 2$ and inherits the symmetries of V_{NN}

Momentum distributions at low RG resolution

- Apply SRG transformations to momentum distribution operators
  - Single-nucleon momentum distribution: $\hat{n}^{hi}(\boldsymbol{q}) = a_{\boldsymbol{q}}^{\dagger} a_{\boldsymbol{q}}$
  - Pair momentum distribution: $\hat{n}^{hi}(\boldsymbol{q}, \boldsymbol{Q}) = a_{\frac{\boldsymbol{Q}}{2}+\boldsymbol{q}}^{\dagger} a_{\frac{\boldsymbol{Q}}{2}-\boldsymbol{q}}^{\dagger} a_{\frac{\boldsymbol{Q}}{2}-\boldsymbol{q}} a_{\frac{\boldsymbol{Q}}{2}+\boldsymbol{q}}$
- Expand SRG transformation to 2-body level

$$\widehat{U}_{\lambda} = 1 + \frac{1}{4} \sum_{\boldsymbol{K},\boldsymbol{k},\boldsymbol{k}'} \delta U_{\lambda}^{(2)}(\boldsymbol{k}, \boldsymbol{k}') a_{\frac{\boldsymbol{K}}{2}+\boldsymbol{k}}^{\dagger} a_{\frac{\boldsymbol{K}}{2}-\boldsymbol{k}}^{\dagger} a_{\frac{\boldsymbol{K}}{2}-\boldsymbol{k}'} a_{\frac{\boldsymbol{K}}{2}+\boldsymbol{k}'} + \cdots$$

- $\delta U_{\lambda}^{(2)}$ term is fixed by SRG evolution on $A = 2$ and inherits the symmetries of V_{NN}.
- **Strategy for leading contributions**: Apply Wick's theorem to evaluate $\widehat{U}_{\lambda}\hat{n}^{hi}(\boldsymbol{q})\widehat{U}_{\boldsymbol{\lambda}}^{\dagger}$ and $\widehat{U}_{\lambda}\hat{n}^{hi}(\boldsymbol{q}, \boldsymbol{Q})\widehat{U}_{\boldsymbol{\lambda}}^{\dagger}$, truncating 3-body and higher terms.

Momentum distributions at low-RG resolution

- **Example**: Evolved single-nucleon momentum distribution

$$\widehat{U}_\lambda \hat{n}^{hi}(\boldsymbol{q}) \widehat{U}_{\boldsymbol{\lambda}}^\dagger$$

$$\approx a_{\boldsymbol{q}}^\dagger a_{\boldsymbol{q}} + \frac{1}{2}\sum_{\boldsymbol{K},\boldsymbol{k}} [\delta U_\lambda^{(2)}\left(\boldsymbol{k}, \boldsymbol{q} - \frac{\boldsymbol{K}}{2}\right) a_{\frac{\boldsymbol{K}}{2}+\boldsymbol{k}}^\dagger a_{\frac{\boldsymbol{K}}{2}-\boldsymbol{k}}^\dagger a_{\boldsymbol{K}-\boldsymbol{q}} a_{\boldsymbol{q}} + \delta U_\lambda^{\dagger(2)}\left(\boldsymbol{q} - \frac{\boldsymbol{K}}{2}, \boldsymbol{k}\right) a_{\boldsymbol{q}}^\dagger a_{\boldsymbol{K}-\boldsymbol{q}}^\dagger a_{\frac{\boldsymbol{K}}{2}-\boldsymbol{k}} a_{\frac{\boldsymbol{K}}{2}+\boldsymbol{k}}]$$

$$+ \frac{1}{4}\sum_{\boldsymbol{K},\boldsymbol{k},\boldsymbol{k}'} \delta U_\lambda^{(2)}\left(\boldsymbol{k}, \boldsymbol{q} - \frac{\boldsymbol{K}}{2}\right) \delta U_\lambda^{\dagger(2)}\left(\boldsymbol{q} - \frac{\boldsymbol{K}}{2}, \boldsymbol{k}'\right) a_{\frac{\boldsymbol{K}}{2}+\boldsymbol{k}}^\dagger a_{\frac{\boldsymbol{K}}{2}-\boldsymbol{k}}^\dagger a_{\frac{\boldsymbol{K}}{2}-\boldsymbol{k}'} a_{\frac{\boldsymbol{K}}{2}+\boldsymbol{k}'}$$

- For an operator that probes high momentum ($q \gg \lambda$), the low-RG resolution wave function filters out the first few terms, leaving only the $\delta U \delta U^\dagger$ term

Momentum distributions at low RG resolution

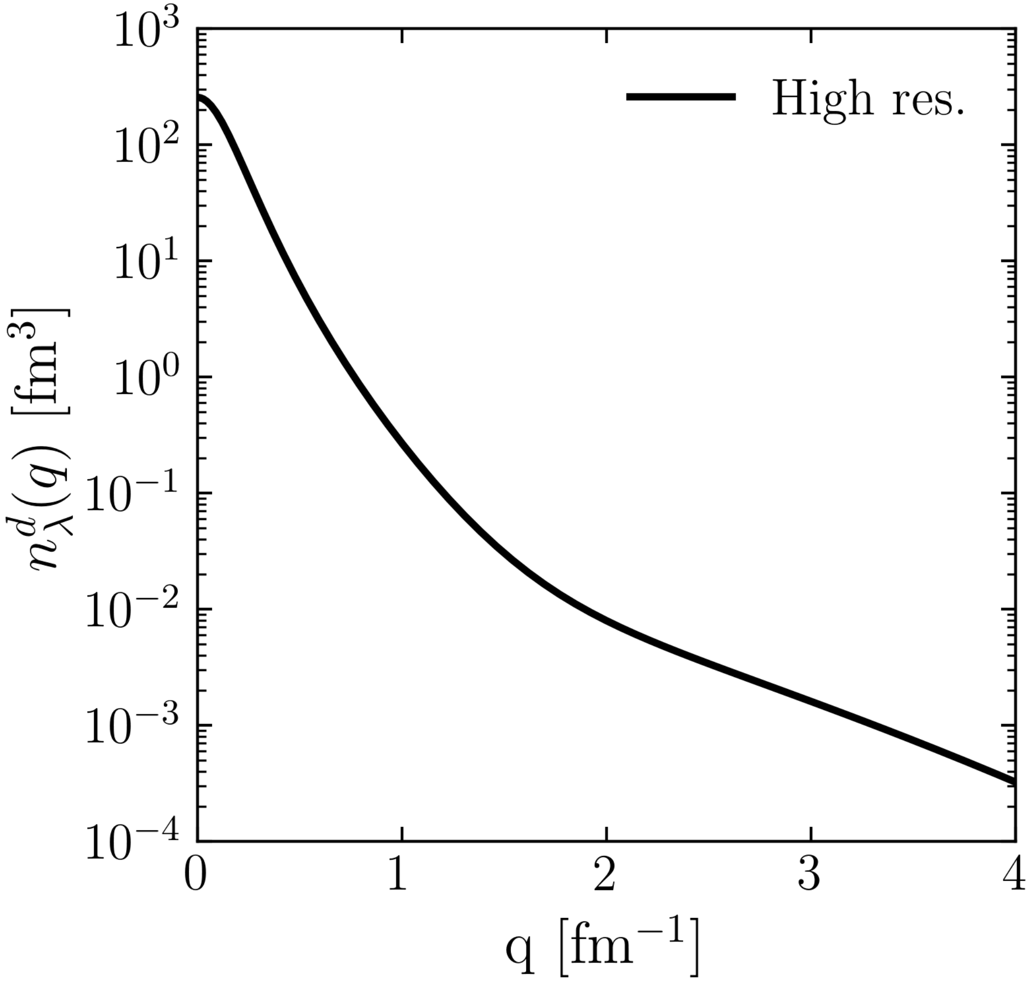

Fig. 5: Contributions to deuteron momentum distribution with AV18 and $\lambda = 1.35$ fm^{-1}.

- Deuteron example

$$n^{lo}(\boldsymbol{q}) = (1 + \delta U) a_{\boldsymbol{q}}^{\dagger} a_{\boldsymbol{q}} (1 + \delta U^{\dagger})$$

$$\langle \psi_d^{hi} | a_{\boldsymbol{q}}^{\dagger} a_{\boldsymbol{q}} | \psi_d^{hi} \rangle$$

Momentum distributions at low RG resolution

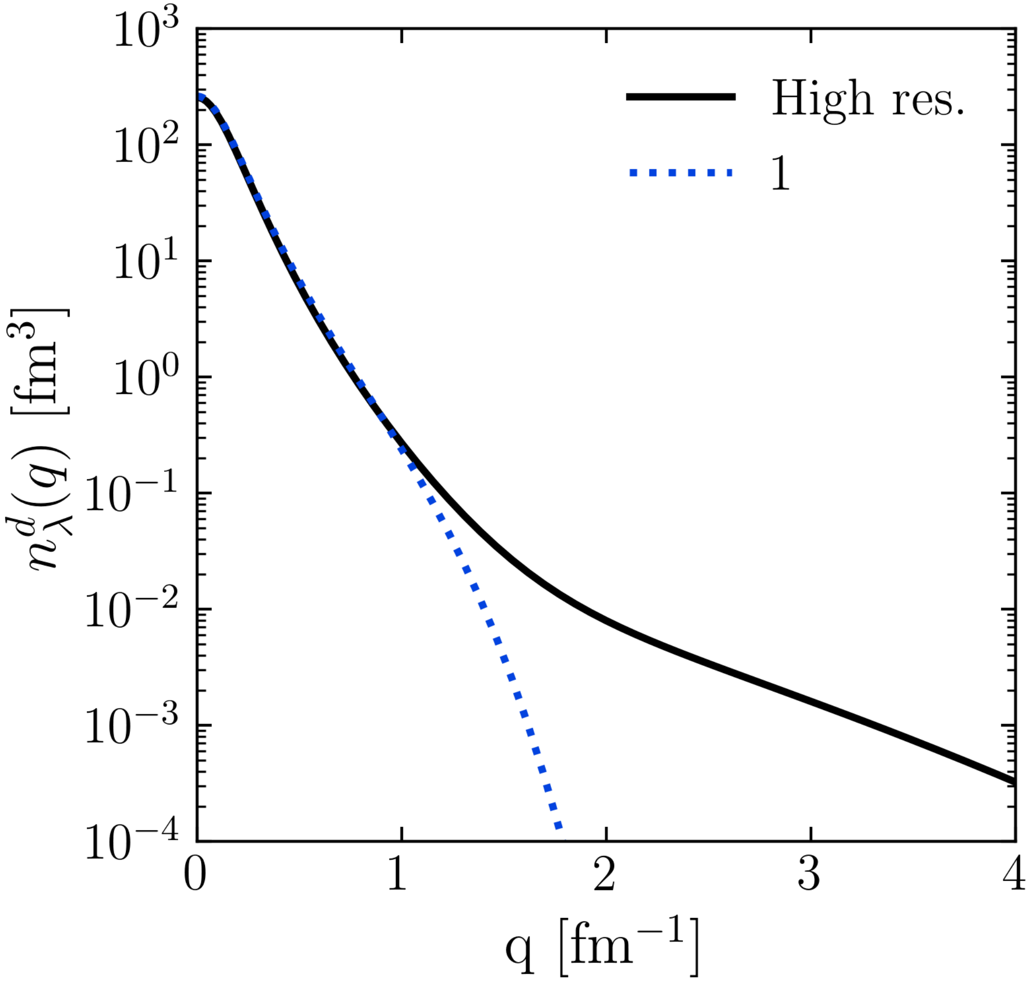

Fig. 5: Contributions to deuteron momentum distribution with AV18 and λ = 1.35 fm^{-1}.

- Deuteron example

$$n^{lo}(\boldsymbol{q}) = (1 + \delta U) a_{\boldsymbol{q}}^\dagger a_{\boldsymbol{q}} (1 + \delta U^\dagger)$$

$$\langle \psi_d^{hi} | a_{\boldsymbol{q}}^\dagger a_q | \psi_d^{hi} \rangle$$

$$\langle \psi_d^{lo} | a_{\boldsymbol{q}}^\dagger a_{\boldsymbol{q}} | \psi_d^{lo} \rangle$$

Momentum distributions at low RG resolution

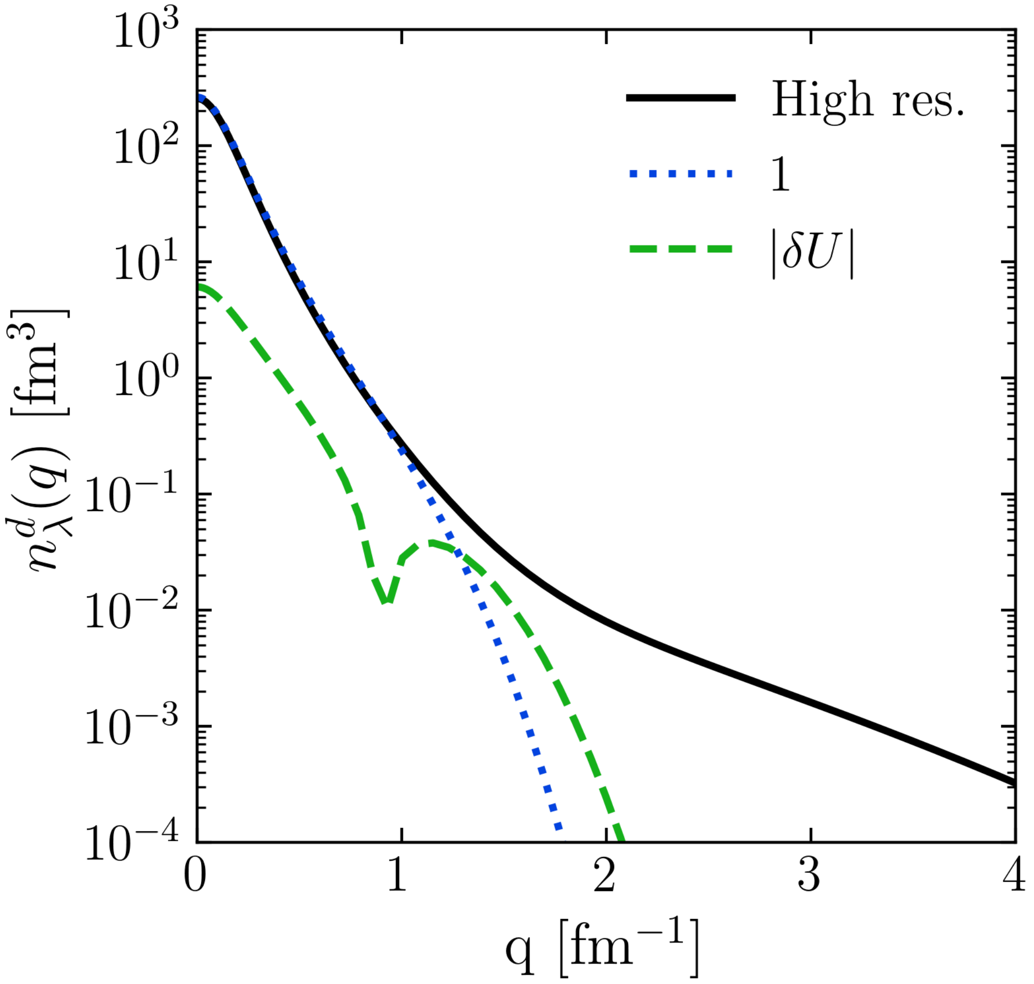

Fig. 5: Contributions to deuteron momentum distribution with AV18 and $\lambda = 1.35$ fm^{-1}.

- Deuteron example

$$n^{lo}(\boldsymbol{q}) = (1 + \delta U) a^\dagger_{\boldsymbol{q}} a_{\boldsymbol{q}} (1 + \delta U^\dagger)$$

$$\langle \psi_d^{hi} | a^\dagger_{\boldsymbol{q}} a_{\boldsymbol{q}} | \psi_d^{hi} \rangle$$

$$\langle \psi_d^{lo} | a^\dagger_{\boldsymbol{q}} a_{\boldsymbol{q}} | \psi_d^{lo} \rangle$$

$$\langle \psi_d^{lo} | \delta U a^\dagger_{\boldsymbol{q}} a_{\boldsymbol{q}} + a^\dagger_{\boldsymbol{q}} a_{\boldsymbol{q}} \delta U^\dagger | \psi_d^{lo} \rangle$$

Momentum distributions at low RG resolution

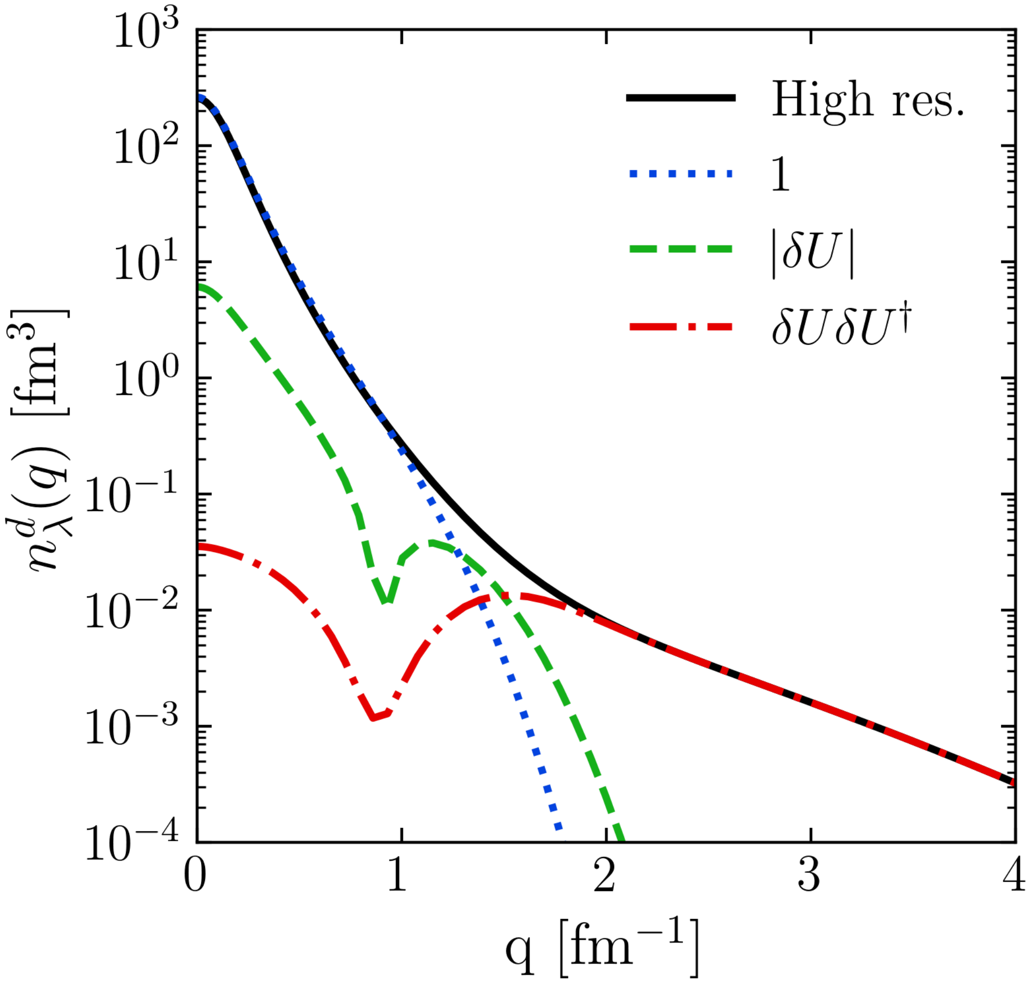

Fig. 5: Contributions to deuteron momentum distribution with AV18 and $\lambda = 1.35$ fm^{-1}.

- Deuteron example

$$n^{lo}(\boldsymbol{q}) = (1 + \delta U) a_{\boldsymbol{q}}^\dagger a_{\boldsymbol{q}} (1 + \delta U^\dagger)$$

$$\langle \psi_d^{hi} | a_{\boldsymbol{q}}^\dagger a_{\boldsymbol{q}} | \psi_d^{hi} \rangle$$

$$\langle \psi_d^{lo} | a_{\boldsymbol{q}}^\dagger a_{\boldsymbol{q}} | \psi_d^{lo} \rangle$$

$$\langle \psi_d^{lo} | \delta U a_{\boldsymbol{q}}^\dagger a_{\boldsymbol{q}} + a_{\boldsymbol{q}}^\dagger a_{\boldsymbol{q}} \delta U^\dagger | \psi_d^{lo} \rangle$$

$$\langle \psi_d^{lo} | \delta U a_{\boldsymbol{q}}^\dagger a_{\boldsymbol{q}} \delta U^\dagger | \psi_d^{lo} \rangle$$

Momentum distributions at low RG resolution

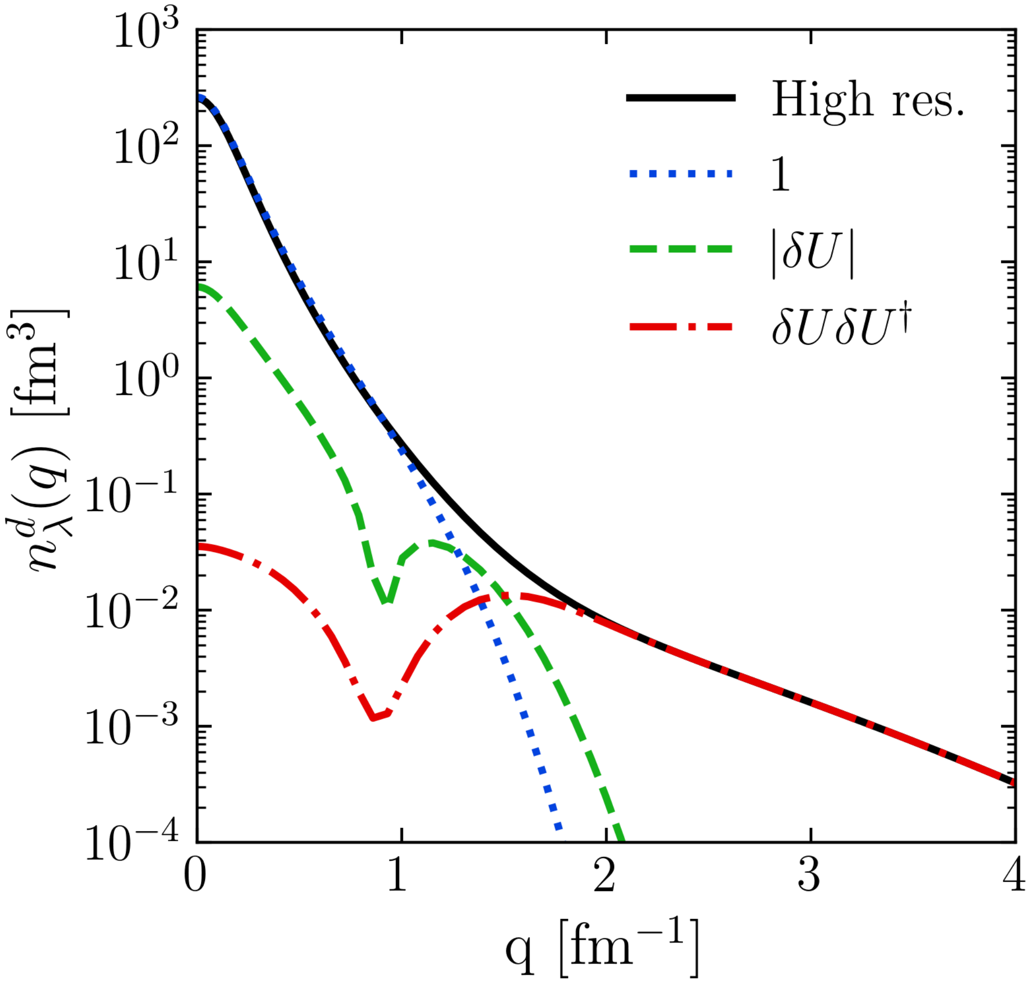

Fig. 5: Contributions to deuteron momentum distribution with AV18 and λ = 1.35 fm^{-1}.

- For high-q, the $\delta U_\lambda \delta U_\lambda^\dagger$ term dominates

$$\approx \sum_{\boldsymbol{K},\boldsymbol{k},\boldsymbol{k}'}^{\lambda} \delta U_\lambda(\boldsymbol{k},\boldsymbol{q}) \delta U_\lambda^\dagger(\boldsymbol{q},\boldsymbol{k}') a^\dagger_{\frac{\boldsymbol{K}}{2}+\boldsymbol{k}} a^\dagger_{\frac{\boldsymbol{K}}{2}-\boldsymbol{k}} a_{\frac{\boldsymbol{K}}{2}-\boldsymbol{k}'} a_{\frac{\boldsymbol{K}}{2}+\boldsymbol{k}'}$$

Momentum distributions at low RG resolution

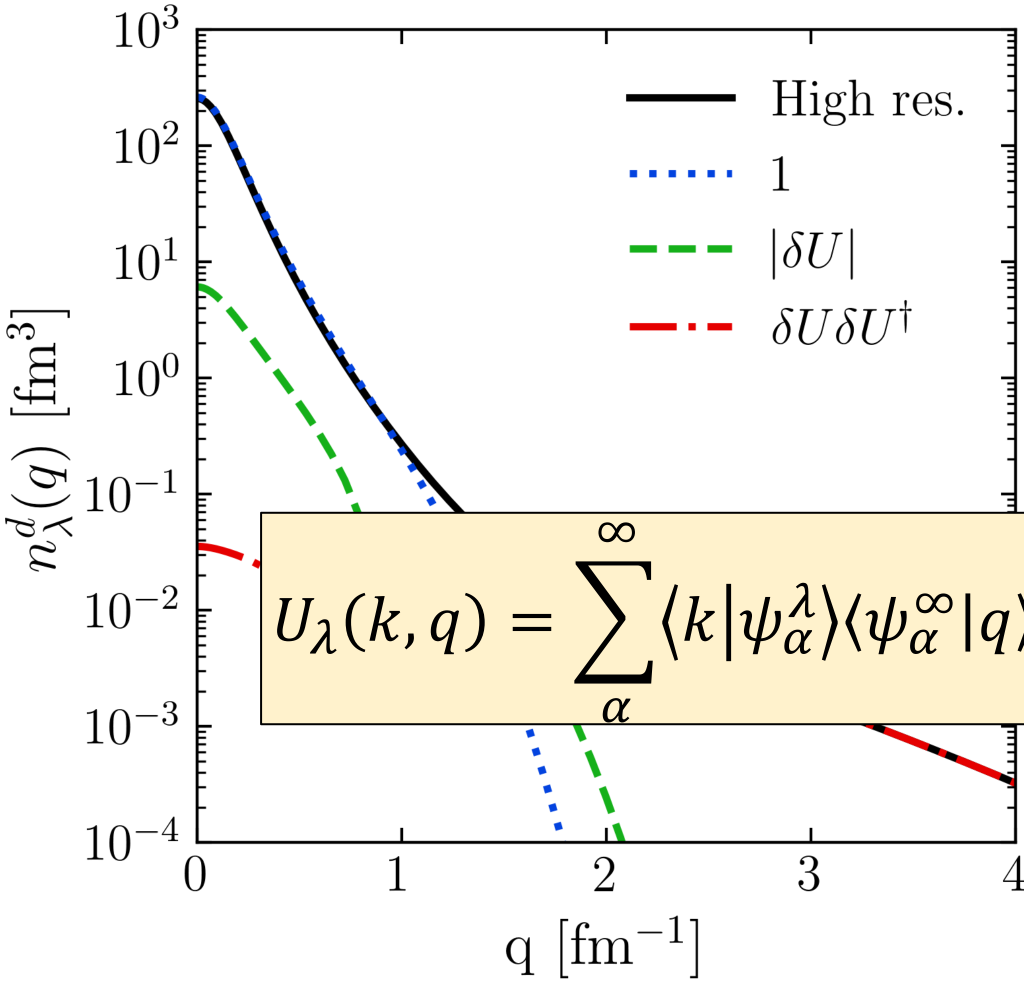

$$U_\lambda(k,q) = \sum_\alpha^\infty \langle k|\psi_\alpha^\lambda\rangle\langle\psi_\alpha^\infty|q\rangle$$

Fig. 5: Contributions to deuteron momentum distribution with AV18 and $\lambda = 1.35$ fm^{-1}.

- For high-q, the $\delta U_\lambda \delta U_\lambda^\dagger$ term dominates

$$\approx \sum_{\boldsymbol{K},\boldsymbol{k},\boldsymbol{k'}}^{\lambda} \delta U_\lambda(\boldsymbol{k},\boldsymbol{q})\delta U_\lambda^\dagger(\boldsymbol{q},\boldsymbol{k'}) a^\dagger_{\frac{\boldsymbol{K}}{2}+\boldsymbol{k}} a^\dagger_{\frac{\boldsymbol{K}}{2}-\boldsymbol{k}} a_{\frac{\boldsymbol{K}}{2}-\boldsymbol{k'}} a_{\frac{\boldsymbol{K}}{2}+\boldsymbol{k'}}$$

Factorization: $\delta U_\lambda(\boldsymbol{k},\boldsymbol{q}) \approx F_\lambda^{lo}(\boldsymbol{k}) F_\lambda^{hi}(\boldsymbol{q})$

$$\approx \left|F_\lambda^{hi}(\boldsymbol{q})\right|^2 \sum_{\boldsymbol{K},\boldsymbol{k},\boldsymbol{k'}}^{\lambda} F_\lambda^{lo}(\boldsymbol{k}) F_\lambda^{lo}(\boldsymbol{k'}) a^\dagger_{\frac{\boldsymbol{K}}{2}+\boldsymbol{k}} a^\dagger_{\frac{\boldsymbol{K}}{2}-\boldsymbol{k}} a_{\frac{\boldsymbol{K}}{2}-\boldsymbol{k'}} a_{\frac{\boldsymbol{K}}{2}+\boldsymbol{k'}}$$

Anderson et al., PRC (2010); Bogner/Roscher, PRC (2012)

Momentum distributions at low RG resolution

- Factorization of SRG transformations implies scaling of high-q tails
- Consider ratio $\frac{n^A(\boldsymbol{q})}{n^d(\boldsymbol{q})}$ for $q \gg \lambda$,

$$\frac{\langle \Psi_\lambda^A | U_\lambda a_q^\dagger a_q U_\lambda^\dagger | \Psi_\lambda^A \rangle}{\langle \Psi_\lambda^d | U_\lambda a_q^\dagger a_q U_\lambda^\dagger | \Psi_\lambda^d \rangle} = \cancel{\frac{\left| F_\lambda^{hi}(\boldsymbol{q}) \right|^2}{\left| F_\lambda^{hi}(\boldsymbol{q}) \right|^2}} \times \frac{\left\langle \Psi_\lambda^A \middle| \sum_{\boldsymbol{K},\boldsymbol{k},\boldsymbol{k}'}^{\lambda} F_\lambda^{lo}(\boldsymbol{k}) F_\lambda^{lo}(\boldsymbol{k}') a_{\frac{\boldsymbol{K}}{2}+\boldsymbol{k}}^\dagger a_{\frac{\boldsymbol{K}}{2}-\boldsymbol{k}}^\dagger a_{\frac{\boldsymbol{K}}{2}-\boldsymbol{k}'} a_{\frac{\boldsymbol{K}}{2}+\boldsymbol{k}'} \middle| \Psi_\lambda^A \right\rangle}{\left\langle \Psi_\lambda^d \middle| \sum_{\boldsymbol{K},\boldsymbol{k},\boldsymbol{k}'}^{\lambda} F_\lambda^{lo}(\boldsymbol{k}) F_\lambda^{lo}(\boldsymbol{k}') a_{\frac{\boldsymbol{K}}{2}+\boldsymbol{k}}^\dagger a_{\frac{\boldsymbol{K}}{2}-\boldsymbol{k}}^\dagger a_{\frac{\boldsymbol{K}}{2}-\boldsymbol{k}'} a_{\frac{\boldsymbol{K}}{2}+\boldsymbol{k}'} \middle| \Psi_\lambda^d \right\rangle}$$

- High-q dependence cancels, leaving a ratio only sensitive to low-momentum physics

Anderson et al., PRC (2010); Bogner/Roscher, PRC (2012); Chen et al., PRL (2017); Lynn et al., JPhysG (2020)

Figure from R. Cruz-Torres et al., Nat. Phys. **17**, 306 (2021)

Factorization

- Factorization of SRG transformations implies

Factorization built into GCF model seen by flat ratio of pair momentum distributions $n^A(q)$ over universal two-body wave functions $|\tilde{\varphi}(q)|^2$ at high q

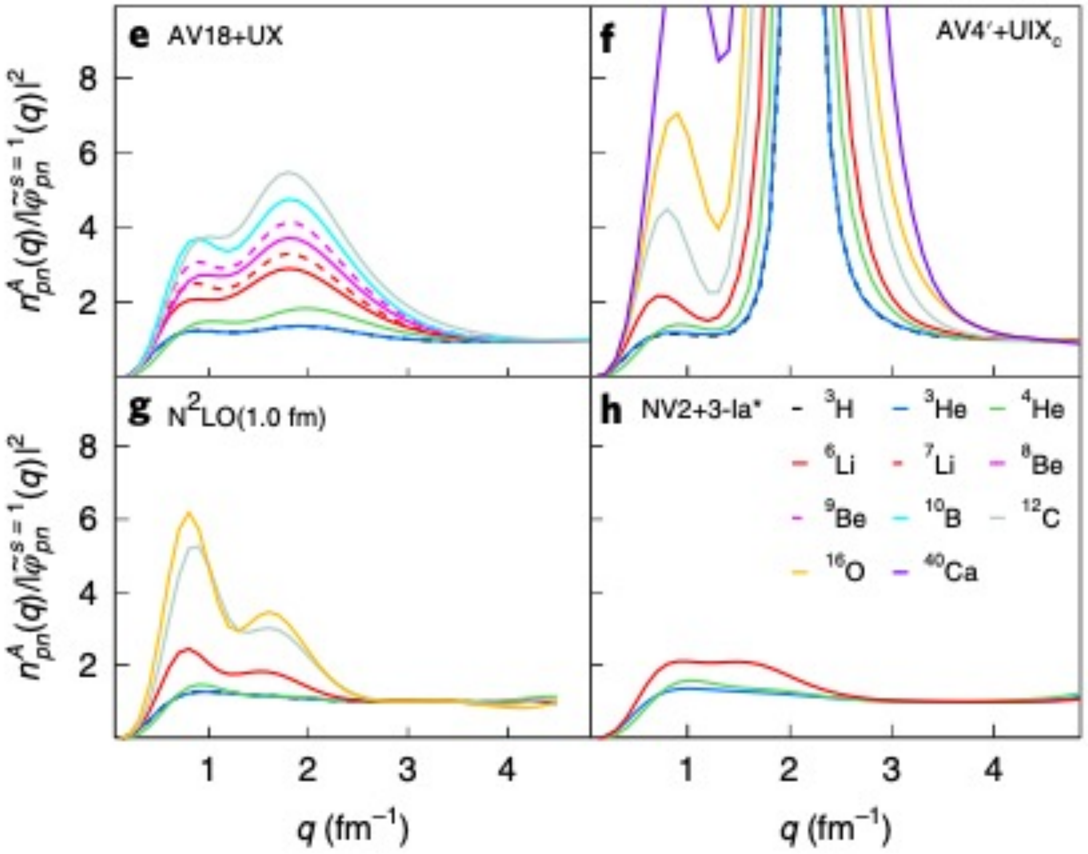

- High-q dependence cancels leaving ratio only sensitive to low-momentum physics

Why use low RG resolution?

- Ab initio methods that rely on low RG (soft) interactions can be widely applied!
- NOTE: SRC physics is *not* missing from energies.

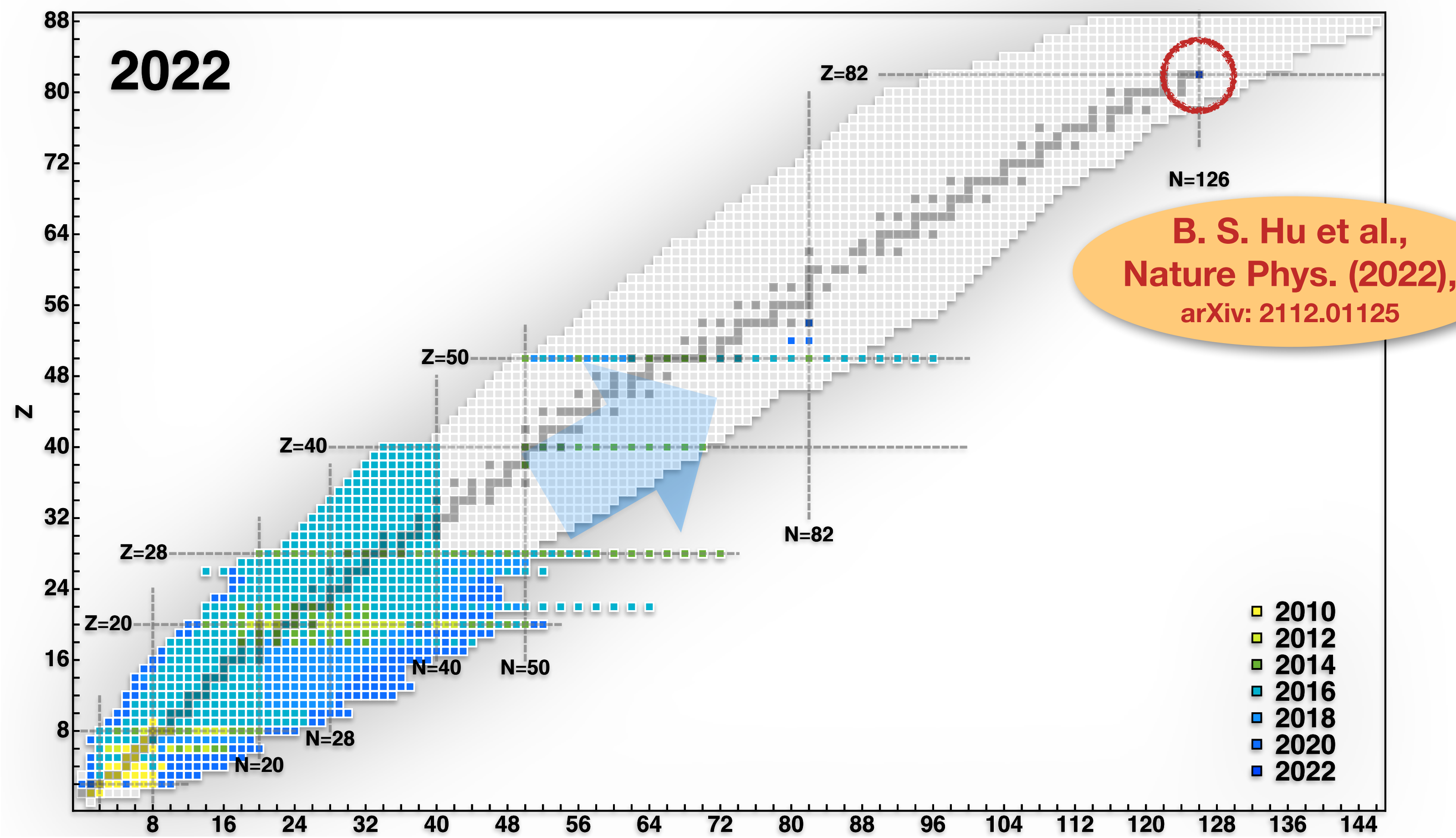

Heiko Hergert, 2023

Why use low RG resolution?

- Ab initio methods that rely on low RG (soft) interactions can be widely applied!
- NOTE: SRC physics is *not* missing from energies.
- What SRC physics can we describe using (very!) simple approximations at low res.?

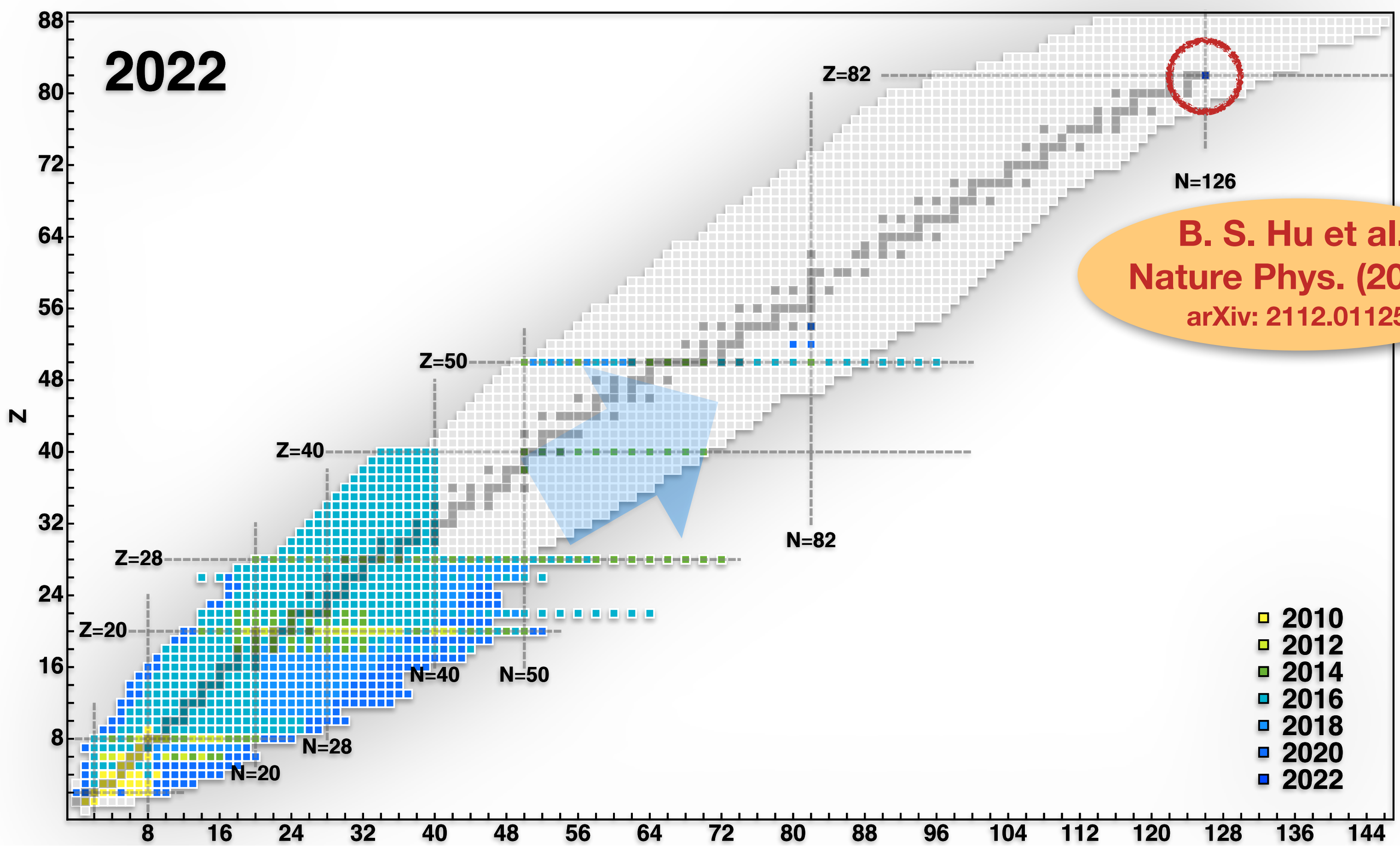

B. S. Hu et al., Nature Phys. (2022), arXiv: 2112.01125

Heiko Hergert, 2023

Why use low RG resolution?

- Ab initio methods that rely on low RG (soft) interactions can be widely applied!
- NOTE: SRC physics is *not* missing from energies.
- What SRC physics can we describe using (very!) simple approximations at low res.?
- Try Hartree-Fock (HF) with a local density approximation (LDA) to evaluate nuclear matrix elements.

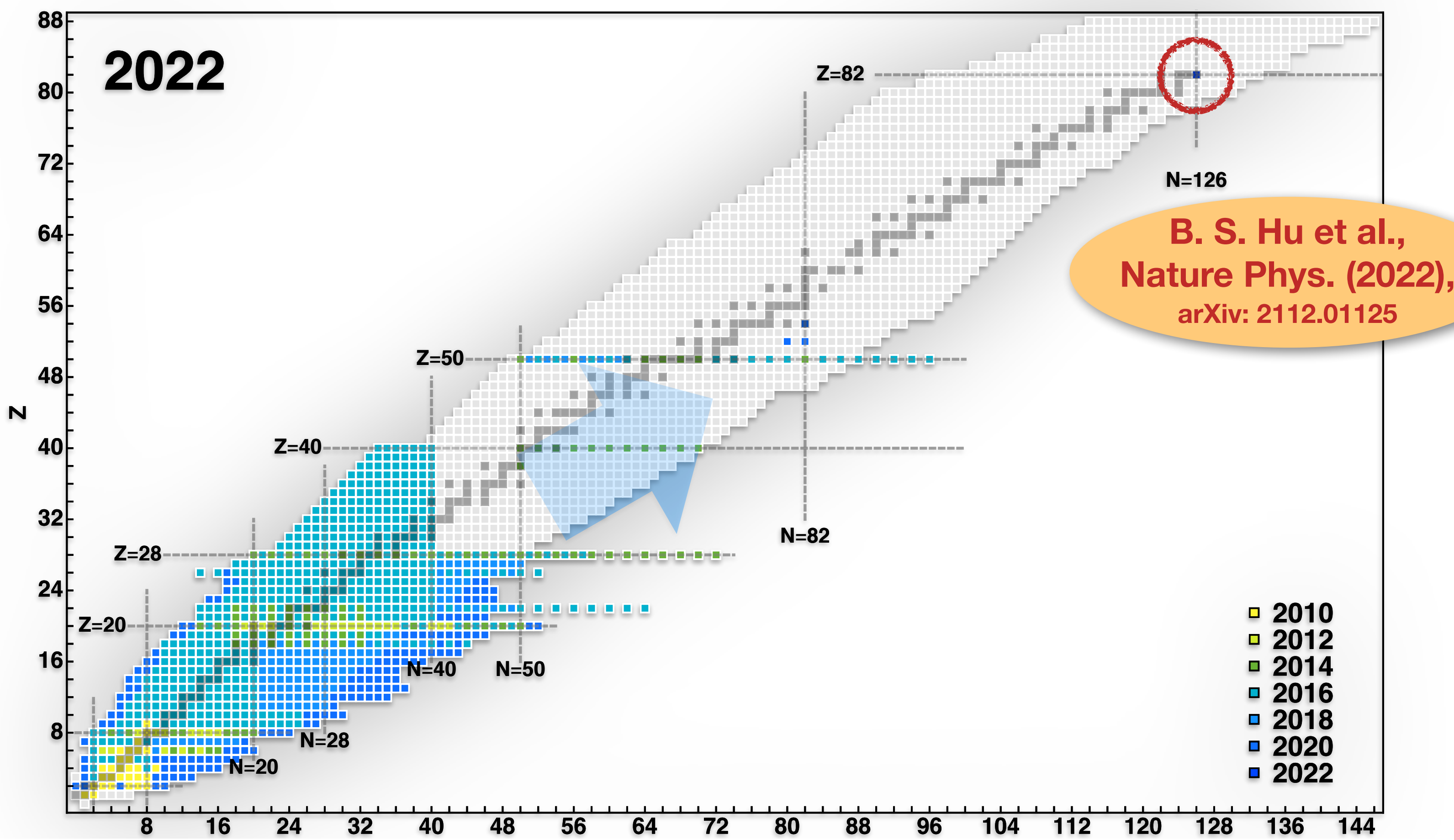

Heiko Hergert, 2023

HF and LDA calculation (details)

- Evaluating SRG-evolved operator with low RG resolution wave functions $\langle\Psi_\lambda^A|\widehat{U}_\lambda \hat{n}^{hi}(\boldsymbol{q})\widehat{U}_\lambda^\dagger|\Psi_\lambda^A\rangle$

$$
\begin{aligned}
&\approx \langle\Psi_\lambda^A| \Big[a_{\mathbf{q}}^\dagger a_{\mathbf{q}} + \frac{1}{2}\sum_{\mathbf{K},\mathbf{k}} \Big(\delta U_\lambda(\mathbf{k}, \mathbf{q}-\mathbf{K}/2) a^\dagger_{\mathbf{K}/2+\mathbf{k}} a^\dagger_{\mathbf{K}/2-\mathbf{k}} a_{\mathbf{K}-\mathbf{q}} a_{\mathbf{q}} \\
&\qquad + \delta U_\lambda^\dagger(\mathbf{q}-\mathbf{K}/2, \mathbf{k}) a^\dagger_{\mathbf{q}} a^\dagger_{\mathbf{K}-\mathbf{q}} a_{\mathbf{K}/2-\mathbf{k}} a_{\mathbf{K}/2+\mathbf{k}} \Big) \\
&\qquad + \frac{1}{4}\sum_{\mathbf{K},\mathbf{k},\mathbf{k}'} \delta U_\lambda(\mathbf{k}, \mathbf{q}-\mathbf{K}/2) \delta U_\lambda^\dagger(\mathbf{q}-\mathbf{K}/2, \mathbf{k}') a^\dagger_{\mathbf{K}/2+\mathbf{k}} a^\dagger_{\mathbf{K}/2-\mathbf{k}} a_{\mathbf{K}/2-\mathbf{k}'} a_{\mathbf{K}/2+\mathbf{k}'} \Big] |\Psi_\lambda^A\rangle
\end{aligned}
$$

Tropiano et al. (2021)

HF and LDA calculation (details)

- Evaluating SRG-evolved operator with low RG resolution wave functions $\langle\Psi_\lambda^A|\widehat{U}_\lambda \hat{n}^{hi}(\boldsymbol{q})\widehat{U}_\lambda^\dagger|\Psi_\lambda^A\rangle$

$$\approx \langle\Psi_\lambda^A| \Big[a_{\mathbf{q}}^\dagger a_{\mathbf{q}} + \frac{1}{2}\sum_{\mathbf{K},\mathbf{k}}\Big(\delta U_\lambda(\mathbf{k},\mathbf{q}-\mathbf{K}/2) a_{\mathbf{K}/2+\mathbf{k}}^\dagger a_{\mathbf{K}/2-\mathbf{k}}^\dagger a_{\mathbf{K}-\mathbf{q}} a_{\mathbf{q}}$$
$$+ \delta U_\lambda^\dagger(\mathbf{q}-\mathbf{K}/2,\mathbf{k}) a_{\mathbf{q}}^\dagger a_{\mathbf{K}-\mathbf{q}}^\dagger a_{\mathbf{K}/2-\mathbf{k}} a_{\mathbf{K}/2+\mathbf{k}}\Big)$$
$$+ \frac{1}{4}\sum_{\mathbf{K},\mathbf{k},\mathbf{k}'} \delta U_\lambda(\mathbf{k},\mathbf{q}-\mathbf{K}/2)\delta U_\lambda^\dagger(\mathbf{q}-\mathbf{K}/2,\mathbf{k}') a_{\mathbf{K}/2+\mathbf{k}}^\dagger a_{\mathbf{K}/2-\mathbf{k}}^\dagger a_{\mathbf{K}/2-\mathbf{k}'} a_{\mathbf{K}/2+\mathbf{k}'}\Big] |\Psi_\lambda^A\rangle$$

- Take continuum limit (suppressing spin and isospin labels): $\sum_{\boldsymbol{k}} \to \int d\boldsymbol{k}$

- Evaluate matrix elements assuming $|\Psi_\lambda^A\rangle$ is occupied up to momentum k_F averaging over local Fermi momentum $k_F^\tau(R) = (3\pi^2\rho^\tau(R))^{1/3}$:

$$\left\langle\Psi_\lambda^A\middle| a_{\frac{\boldsymbol{K}}{2}+\boldsymbol{k}}^\dagger a_{\frac{\boldsymbol{K}}{2}-\boldsymbol{k}}^\dagger a_{\frac{\boldsymbol{K}}{2}-\boldsymbol{k}'} a_{\frac{\boldsymbol{K}}{2}+\boldsymbol{k}'}\middle|\Psi_\lambda^A\right\rangle \approx \int d\boldsymbol{R}\, \delta(\boldsymbol{k}'-\boldsymbol{k})\, \theta(k_F^\tau(R) - |\boldsymbol{K}/2+\boldsymbol{k}|)\theta(k_F^{\tau'}(R) - |\boldsymbol{K}/2-\boldsymbol{k}|)$$

Tropiano et al. (2021)

HF and LDA calculation (details)

- Angle-average to evaluate angular dependence of $\boldsymbol{q} \cdot \boldsymbol{k}$, $\boldsymbol{q} \cdot \boldsymbol{K}$, and $\boldsymbol{K} \cdot \boldsymbol{k}$ (defines angles x, y, and z)

E.g, $$\int_{-1}^{1} \frac{dz}{2}\, \theta(k_{\mathrm{F}}^{\tau} - |\mathbf{K}/2 + \mathbf{k}|)\theta(k_{\mathrm{F}}^{\tau'} - |\mathbf{K}/2 - \mathbf{k}|) = \begin{cases} 1 & \text{if } k < k_{\mathrm{F}}^{\min} - \frac{K}{2} \\ \frac{(k_{\mathrm{F}}^{\min})^2 - (k - K/2)^2}{2kK} & \text{if } k < k_{\mathrm{F}}^{\min} + \frac{K}{2} \text{ and} \\ & k_{\mathrm{F}}^{\min} - \frac{K}{2} < k < k_{\mathrm{F}}^{\max} - \frac{K}{2} \\ \frac{(k_{\mathrm{F}}^{\mathrm{avg}})^2 - k^2 - K^2/4}{kK} & \text{if } k_{\mathrm{F}}^{\max} - \frac{K}{2} < k \text{ and} \\ & k < \sqrt{(k_{\mathrm{F}}^{\mathrm{avg}})^2 - \frac{K^2}{4}} \\ 0 & \text{otherwise} \end{cases}$$

where $\left|\frac{\boldsymbol{K}}{2} + \boldsymbol{k}\right| = \sqrt{\frac{K^2}{4} + k^2 + Kkz}$

Tropiano et al. (2021)

HF and LDA calculation (details)

- Angle-average to evaluate angular dependence of $\boldsymbol{q}\cdot\boldsymbol{k}$, $\boldsymbol{q}\cdot\boldsymbol{K}$, and $\boldsymbol{K}\cdot\boldsymbol{k}$ (defines angles x, y, and z)

E.g, $$\int_{-1}^{1}\frac{dz}{2}\,\theta(k_{\rm F}^{\tau}-|\mathbf{K}/2+\mathbf{k}|)\theta(k_{\rm F}^{\tau'}-|\mathbf{K}/2-\mathbf{k}|)=\begin{cases}1 & \text{if } k<k_{\rm F}^{\rm min}-\frac{K}{2}\\ \frac{(k_{\rm F}^{\rm min})^2-(k-K/2)^2}{2kK} & \text{if } k<k_{\rm F}^{\rm min}+\frac{K}{2} \text{ and}\\ & k_{\rm F}^{\rm min}-\frac{K}{2}<k<k_{\rm F}^{\rm max}-\frac{K}{2}\\ \frac{(k_{\rm F}^{\rm avg})^2-k^2-K^2/4}{kK} & \text{if } k_{\rm F}^{\rm max}-\frac{K}{2}<k \text{ and}\\ & k<\sqrt{(k_{\rm F}^{\rm avg})^2-\frac{K^2}{4}}\\ 0 & \text{otherwise}\end{cases}$$

where $\left|\frac{\boldsymbol{K}}{2}+\boldsymbol{k}\right|=\sqrt{\frac{K^2}{4}+k^2+Kkz}$

- Finally write in terms of partial waves using

$$|\boldsymbol{k}_1\sigma_1\tau_1\boldsymbol{k}_2\sigma_2\tau_2\rangle=\frac{1}{\sqrt{2}}\sum_{S,M_S}\sum_{L,M_L}\sum_{J,M_J}\sum_{T,M_T}\langle\sigma_1\sigma_2|SM_S\rangle\langle\tau_1\tau_2|TM_T\rangle\sqrt{\frac{2}{\pi}}Y^*_{L,M_L}(\hat{k})\langle LM_LSM_S|JM_J\rangle[1-(-1)^{L+S+T}]\,|\boldsymbol{K}k(LS)JM_JTM_T\rangle$$

where $\boldsymbol{k}\equiv\frac{1}{2}(\boldsymbol{k}_1-\boldsymbol{k}_2)$ and $\boldsymbol{K}\equiv\boldsymbol{k}_1+\boldsymbol{k}_2$

Tropiano et al. (2021)

HF and LDA calculation (details)

- Final formula for single-nucleon momentum distribution (τ specifies proton or neutron) given by:

$$
\begin{aligned}
n^{\tau}_{\lambda}(q) = \int d^3R \Bigg\{ & 2\theta\left(k_{\mathrm{F}}^{\tau} - q\right) + 32 \sum_{L,S,T}{}' \sum_{J} (2J+1) \frac{2}{\pi} \int_0^{\infty} dk\, k^2 (k(LS)JT|\delta U|k(LS)JT) \sum_{\tau'} |\langle \tau\tau' | T\, \tau+\tau' \rangle|^2 \theta\left(k_{\mathrm{F}}^{\tau} - q\right) \\
& \times \int_{-1}^{1} \frac{dx}{2} \theta\left(k_{\mathrm{F}}^{\tau'} - |\mathbf{q} - 2\mathbf{k}|\right) + 2 \sum_{L,L',S,T}{}' \sum_{J} (2J+1) \left(\frac{2}{\pi}\right)^2 \int_0^{\infty} dk\, k^2 \int_0^{\infty} dK\, K^2 \int_{-1}^{1} \frac{dy}{2} \\
& \times \int_{-1}^{1} \frac{dz}{2} (k(LS)JT|\delta U||\mathbf{q} - \mathbf{K}/2|(L'S)JT)(|\mathbf{q} - \mathbf{K}/2|(L'S)JT|\delta U^{\dagger}|k(LS)JT) \\
& \times \sum_{\tau'} |\langle \tau\tau' | T\, \tau+\tau' \rangle|^2\, \theta\left(k_{\mathrm{F}}^{\tau} - |\mathbf{K}/2 + \mathbf{k}|\right) \theta\left(k_{\mathrm{F}}^{\tau'} - |\mathbf{K}/2 - \mathbf{k}|\right) \Bigg\},
\end{aligned}
$$

Tropiano et al. (2021)

[1]R.B. Wiringa et al., Phys. Rev. C **89**, 024305 (2014)
https://www.phy.anl.gov/theory/research/momenta/
[2]K. Bennaceur et al., Comput. Phys. Commun. **168**, 96 (2005)

Example: proton momentum distributions

- Low RG resolution calculations reproduce momentum distributions of AV18 QMC calculations[1] (high RG resolution) with no adjusted parameters or scaling!

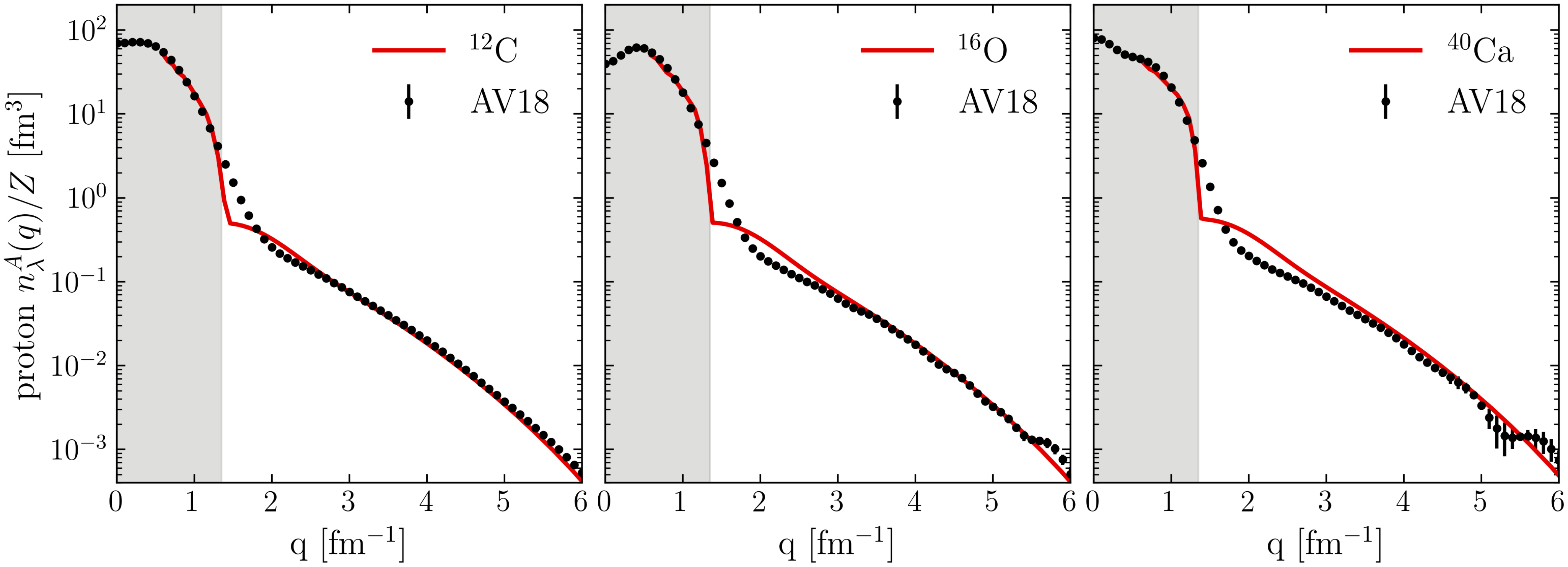

Fig. 6: Proton momentum distributions for ^{12}C, ^{16}O, and ^{40}Ca under HF+LDA with AV18, $\lambda = 1.35$ fm^{-1}, and densities from Skyrme EDF SLy4 using the HFBRAD code[2].

Tropiano et al. (2021)

[1]R.B. Wiringa et al., Phys. Rev. C **89**, 024305 (2014)
https://www.phy.anl.gov/theory/research/momenta/
[2]K. Bennaceur et al., Comput. Phys. Commun. **168**, 96 (2005)

Example: proton momentum distributions

- Low RG resolution calculations reproduce momentum distributions of AV18 QMC calculations[1] (high RG resolution) with no adjusted parameters or scaling!

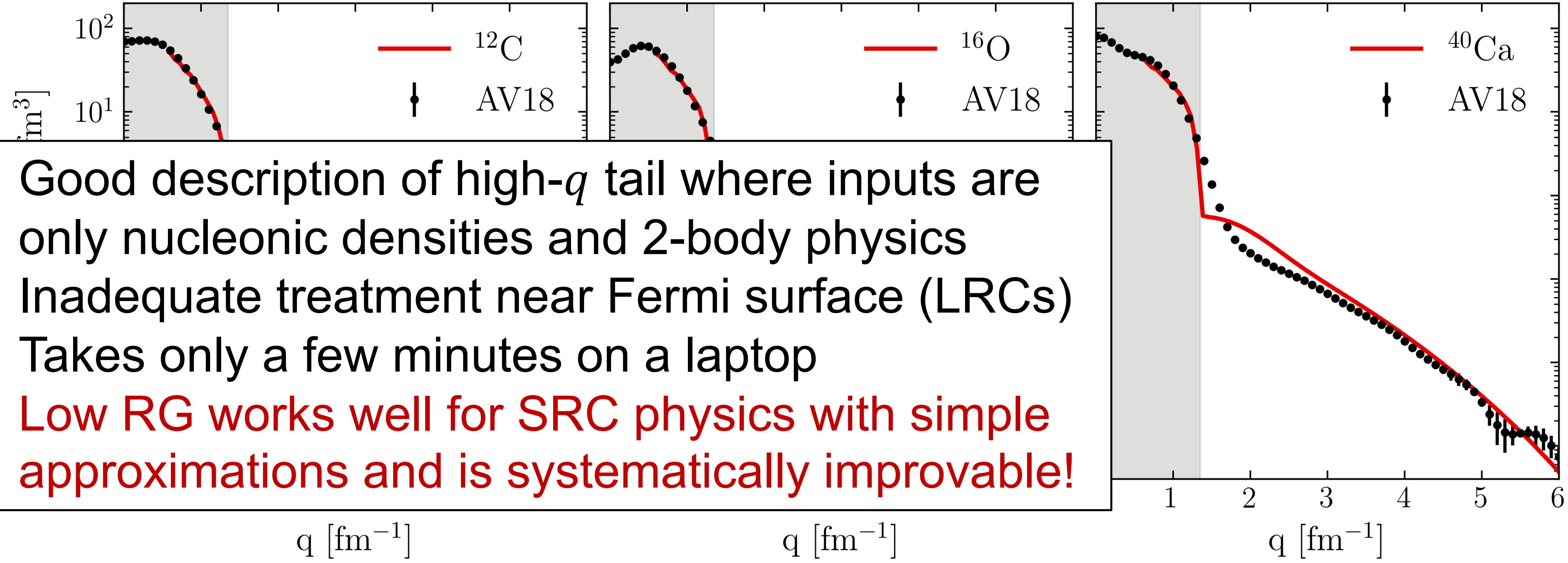

- Good description of high-q tail where inputs are only nucleonic densities and 2-body physics
- Inadequate treatment near Fermi surface (LRCs)
- Takes only a few minutes on a laptop
- Low RG works well for SRC physics with simple approximations and is systematically improvable!

Fig. 6: Proton momentum distributions for ^{12}C, ^{16}O, and ^{40}Ca under HF+LDA with AV18, $\lambda = 1.35$ fm^{-1}, and densities from Skyrme EDF SLy4 using the HFBRAD code[2].

Tropiano et al. (2021)

Example: proton momentum distributions

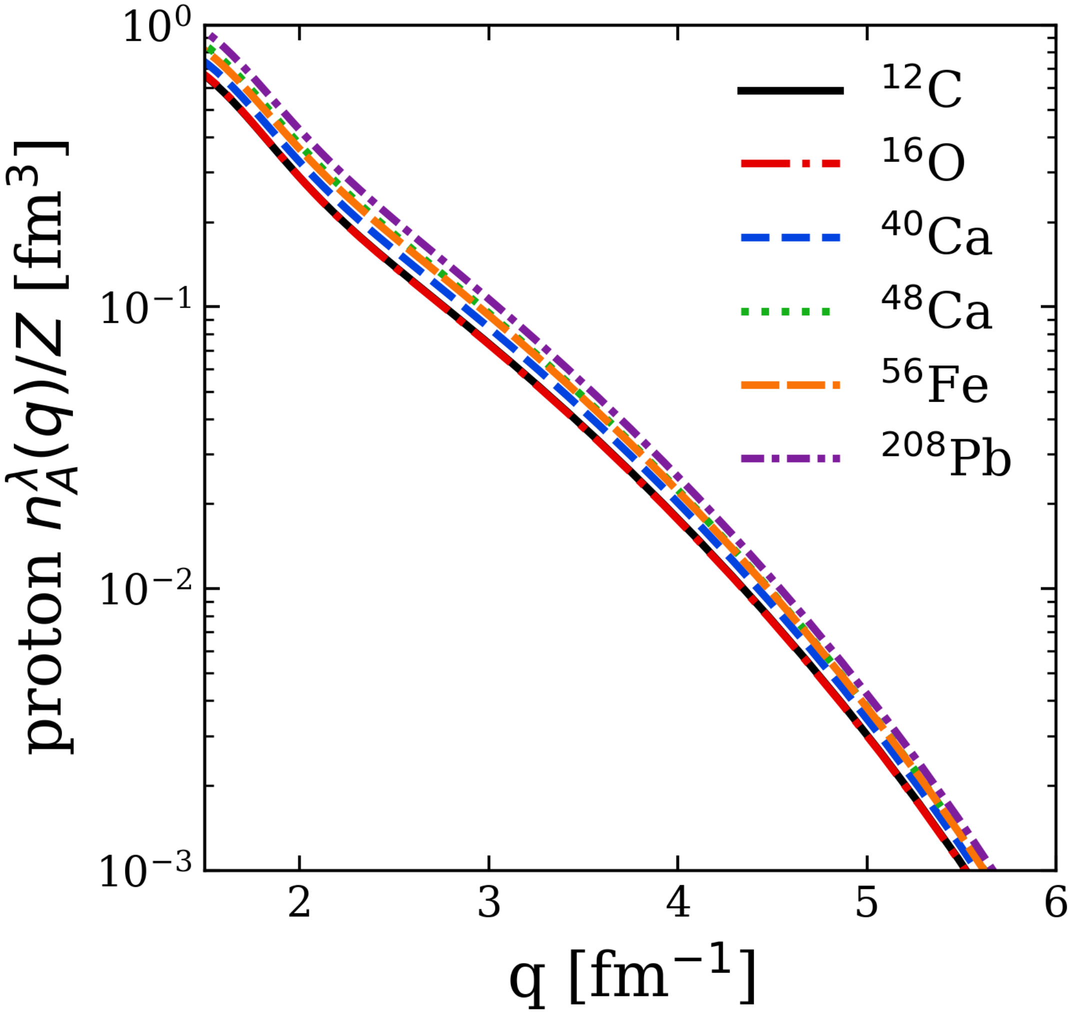

Fig. 7: Proton momentum distributions under HF+LDA with AV18 and $\lambda = 1.35$ fm^{-1}, showing several nuclei.

- Universality: High-q dependence from universal function $\approx \left|F_\lambda^{hi}(q)\right|^2$ fixed by 2-body and insensitive to nucleus

Tropiano et al. (2021)

Example: proton momentum distributions

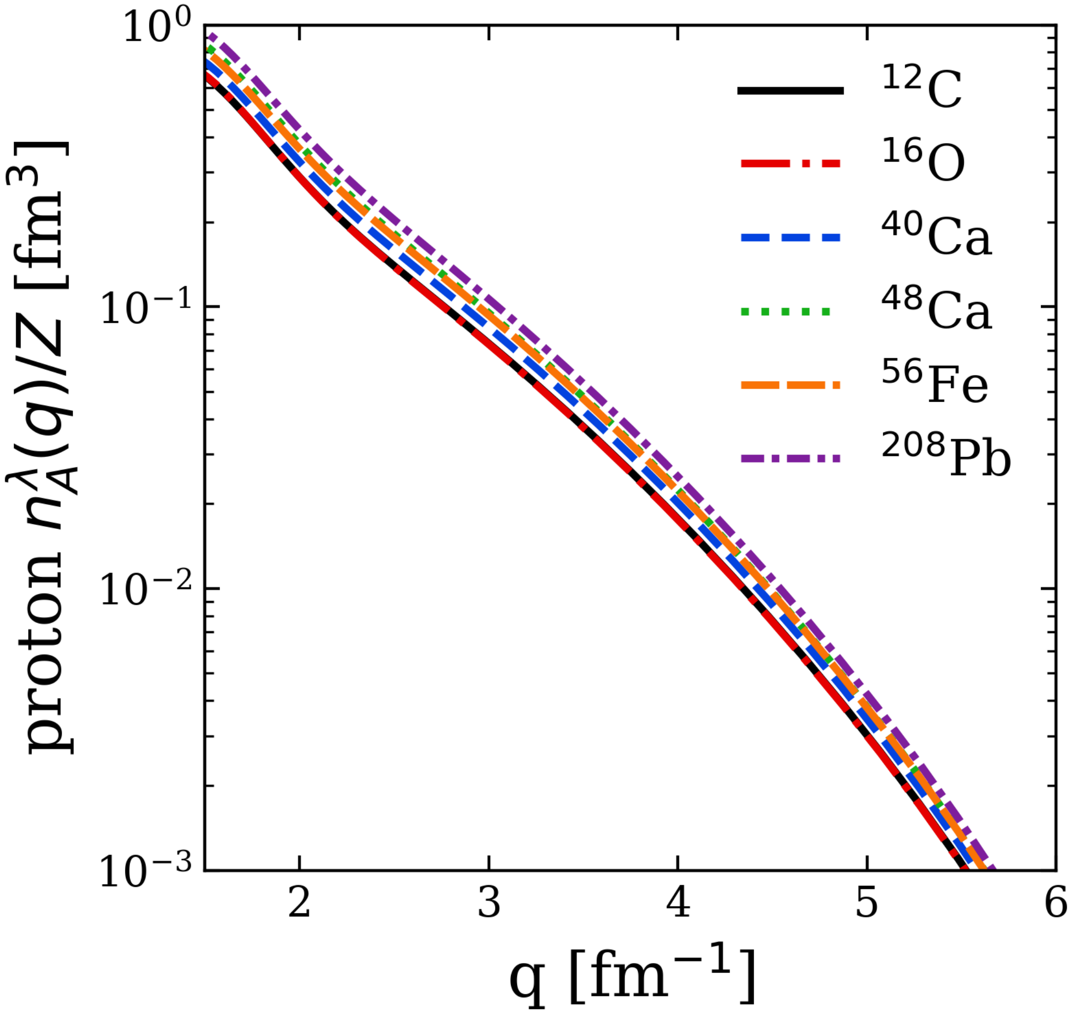

Fig. 7: Proton momentum distributions under HF+LDA with AV18 and $\lambda = 1.35$ fm^{-1}, showing several nuclei.

Wiringa et al., PRC (2014)

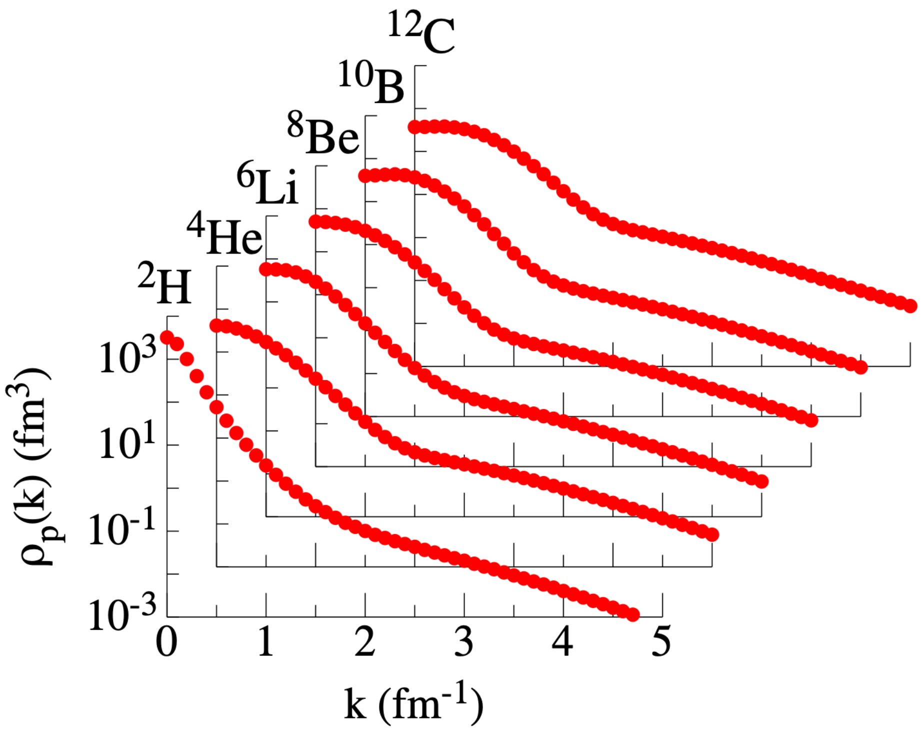

Consistent with universal high-q tails from QMC calculations of R. B. Wiringa et al., Phys. Rev. C **89**, 024305 (2014)

Tropiano et al. (2021)

SRC scaling factors

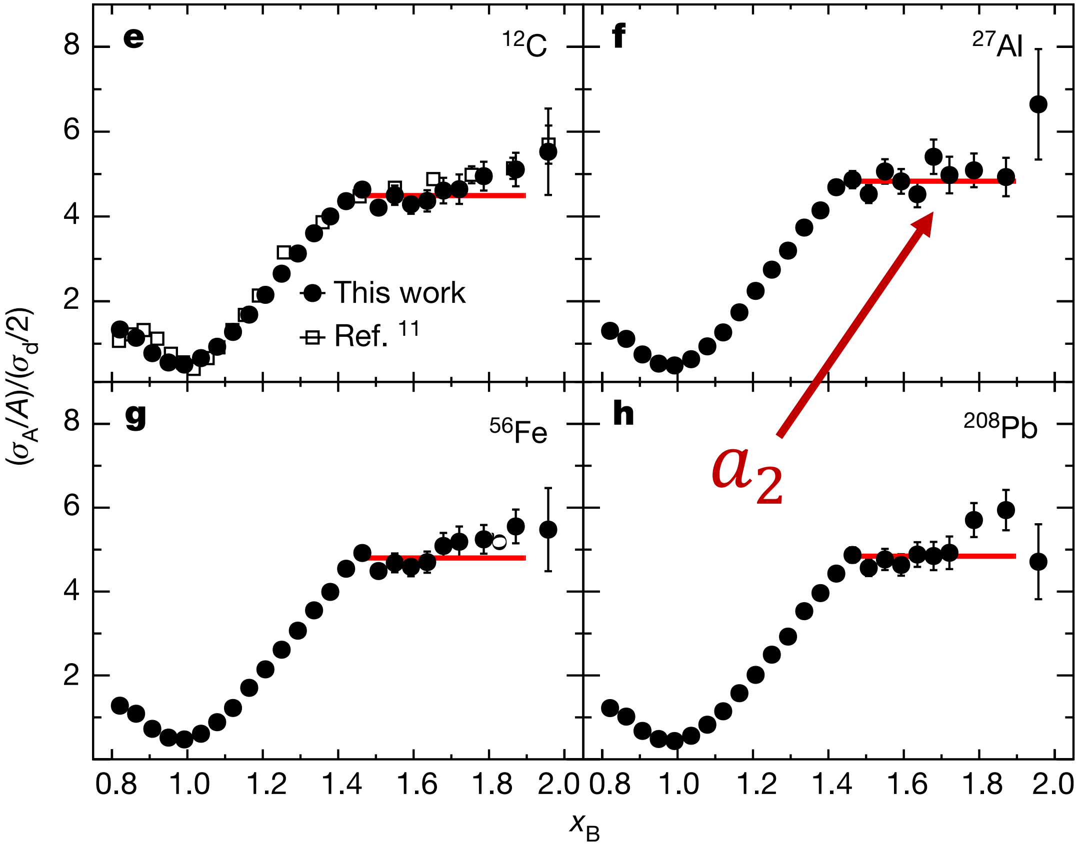

Fig. 8: Ratio of per-nucleon electron scattering cross section of nucleus A to that of deuterium, where the red line indicates a constant fit. Figure from B. Schmookler et al. (CLAS), Nature **566**, 354 (2019).

- SRC scaling factors a_2 defined by plateau in cross section ratio $\frac{2\sigma_A}{A\sigma_d}$ at $1.45 \leq x \leq 1.9$
- Closely related to the ratio of bound-nucleon probability distributions in the limits of vanishing relative distance (infinitely high relative momentum)
- Extract a_2 from momentum distributions[1]

$$a_2 = \lim_{q\to\infty} \frac{P^A(q)}{P^d(q)} \approx \frac{\int_{\Delta q^{high}} dq P^A(q)}{\int_{\Delta q^{high}} dq P^d(q)}$$

where $P^A(q)$ is the single-nucleon probability distribution in nucleus A (cf. LCA)

[1]J. Ryckebusch et al., Phys. Rev. C **100**, 054620 (2019)

[1]E. Chabanat et al., Nucl. Phys. A **635**, 231 (1998)
[2]J. Decharge et al., Phys. Rev. C **21**, 1568 (1980)
[3]B. Schmookler et al. (CLAS), Nature **566**, 354 (2019)
[4]J. Ryckebusch et al., Phys. Rev. C **100**, 054620 (2019)

SRC scaling factors

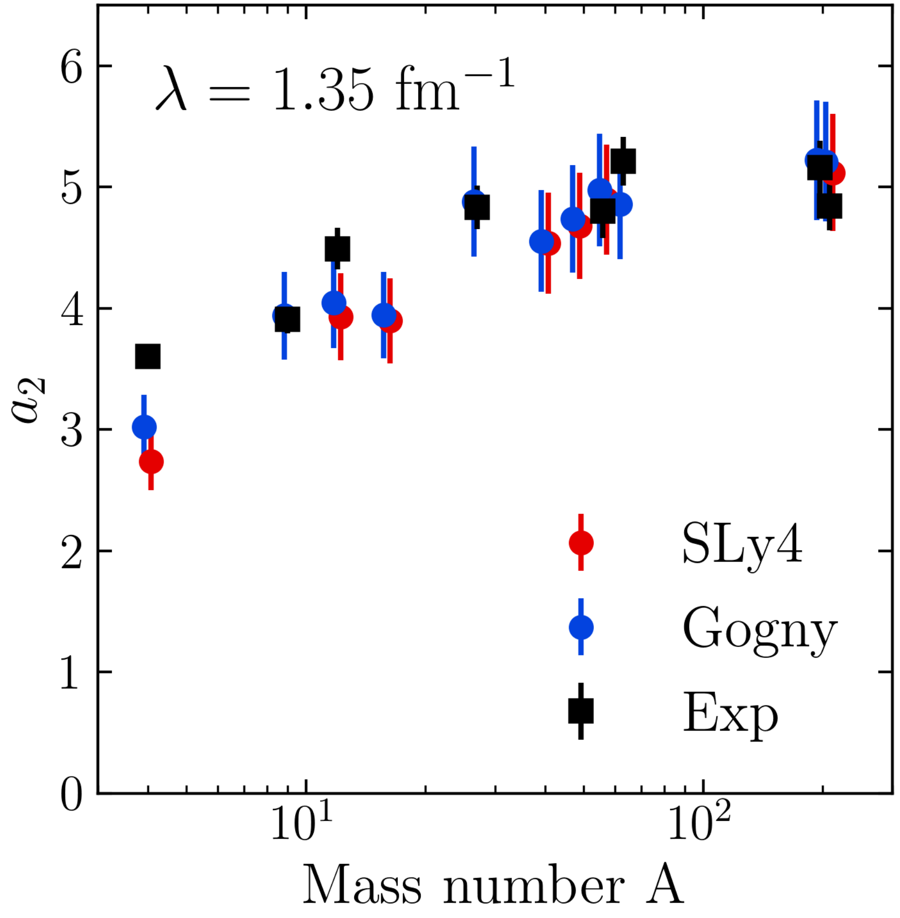

Fig. 9: a_2 scale factors using single-nucleon momentum distributions under HF+LDA (SLy4 in red[1], Gogny[2] in blue) with AV18 and $\lambda = 1.35$ fm^{-1} compared to experimental values[3].

$$a_2 = \lim_{q\to\infty} \frac{P^A(q)}{P^d(q)} \approx \frac{\int_{\Delta q^{high}} dq P^A(q)}{\int_{\Delta q^{high}} dq P^d(q)}$$

- High momentum behavior is characterized by 2-body $\left|F_\lambda^{hi}(q)\right|^2$ which cancels leaving ratio of mean-field (low-k) physics
- Good agreement with a_2 values from experiment[3] and LCA calculations[4] using two different EDFs
- Error bars from varying Δq^{high}

Tropiano et al. (2021)

SRC phenomenology

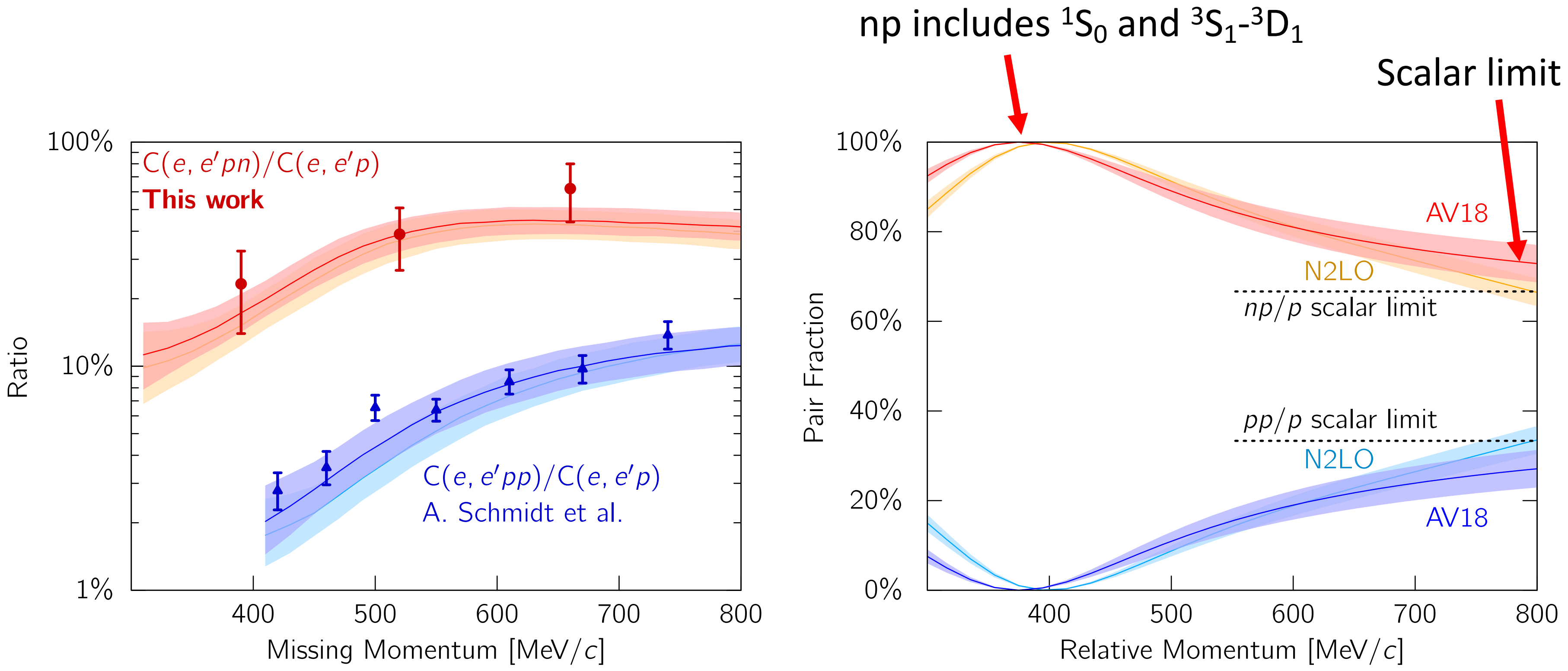

Fig. 10: (a) Ratio of two-nucleon to single-nucleon electron-scattering cross sections for carbon as a function of missing momentum. (b) Fraction of np to p and pp to p pairs versus the relative momentum. Figure from CLAS collaboration publication[1].

- At high RG resolution, the tensor force and the repulsive core of the NN interaction kicks nucleon pairs into SRCs
- np dominates because the tensor force requires spin triplet pairs, whereas pp are spin singlets
- Do we describe this physics at low RG resolution?

[1] I. Korover et al. (CLAS), arXiv:2004.07304 (2014)

SRC phenomenology

- At low RG resolution, SRCs are suppressed in the wave function and shifted into the operator

$$\hat{n}^{lo}(\boldsymbol{q}) = \hat{U}_\lambda a_{\boldsymbol{q}}^\dagger a_{\boldsymbol{q}} \hat{U}_\lambda^\dagger \rightarrow U_\lambda(\boldsymbol{k},\boldsymbol{q}) U_\lambda^\dagger(\boldsymbol{q},\boldsymbol{k}')$$

- Take ratio of $^3S_1$ and $^1S_0$ SRG transformations fixing low-momenta to $k_0 = 0.1$ fm^{-1}
- This physics is established in the 2-body system – will apply to any nucleus!

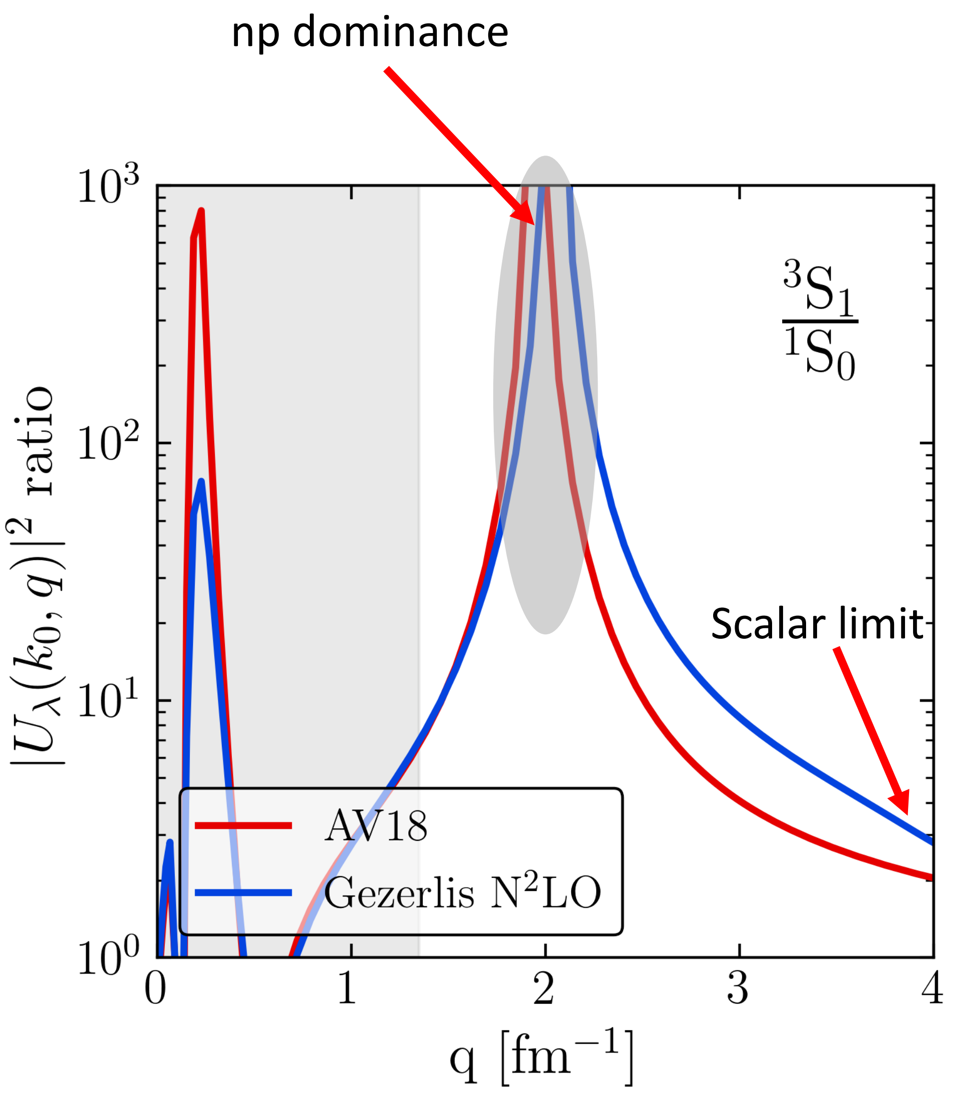

Fig. 11: $^3S_1$ to $^1S_0$ ratio of SRG-evolved momentum projection operators $a_q^\dagger a_q$ where $\lambda = 1.35$ fm^{-1}.

Tropiano et al. (2021)

SRC phenomenology

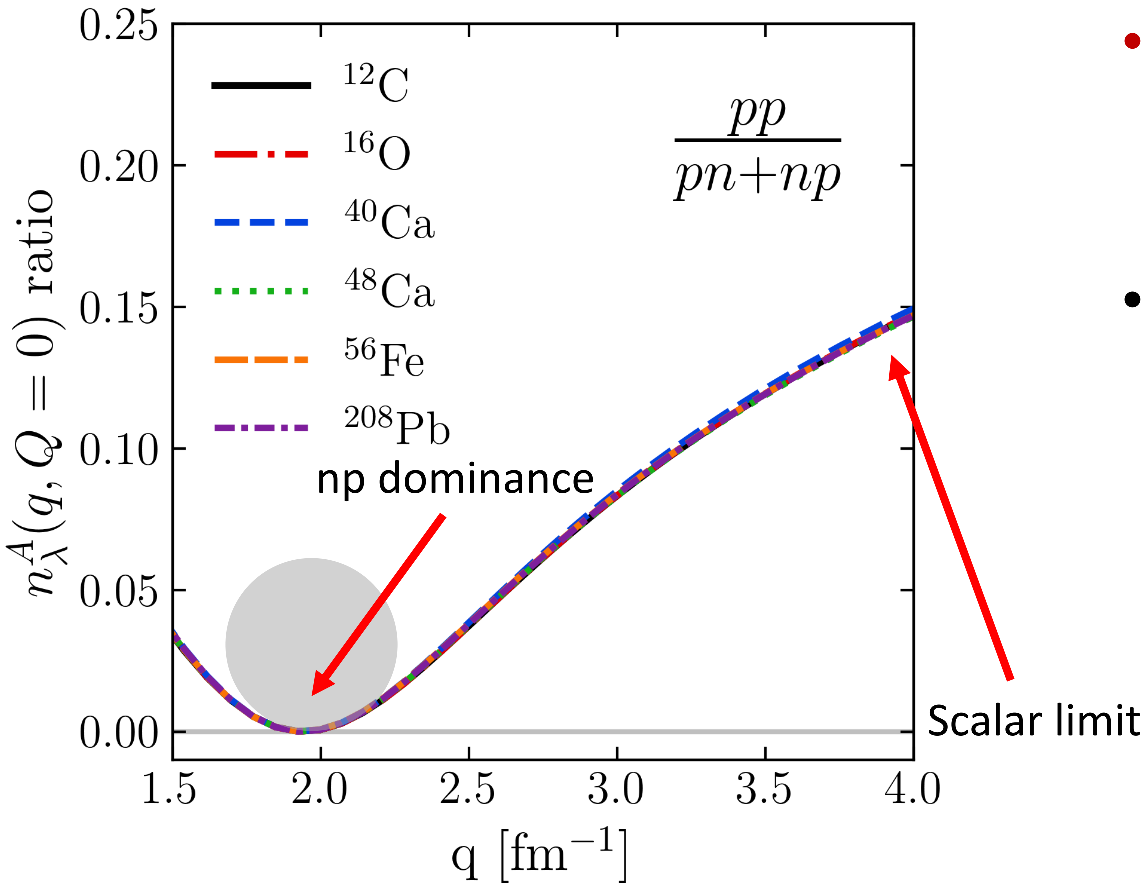

Fig. 12: pp/pn ratio of pair momentum distributions under HF+LDA with AV18 and $\lambda = 1.35$ fm^{-1}.

- Low RG resolution picture reproduces the characteristics of cross section ratios using simple approximations
- Weak nucleus dependence from factorization

$$\text{Ratio} \approx \frac{\left|F_{pp}^{hi}(\boldsymbol{q})\right|^2}{\left|F_{np}^{hi}(\boldsymbol{q})\right|^2} \times \cancel{\frac{\left\langle \Psi_\lambda^A \middle| \sum_{\boldsymbol{k},\boldsymbol{k}'}^{\lambda} a^\dagger_{\frac{\boldsymbol{Q}}{2}+\boldsymbol{k}} a^\dagger_{\frac{\boldsymbol{Q}}{2}-\boldsymbol{k}} a_{\frac{\boldsymbol{Q}}{2}-\boldsymbol{k}'} a_{\frac{\boldsymbol{Q}}{2}+\boldsymbol{k}'} \middle| \Psi_\lambda^A \right\rangle}{\left\langle \Psi_\lambda^A \middle| \sum_{\boldsymbol{k},\boldsymbol{k}'}^{\lambda} a^\dagger_{\frac{\boldsymbol{Q}}{2}+\boldsymbol{k}} a^\dagger_{\frac{\boldsymbol{Q}}{2}-\boldsymbol{k}} a_{\frac{\boldsymbol{Q}}{2}-\boldsymbol{k}'} a_{\frac{\boldsymbol{Q}}{2}+\boldsymbol{k}'} \middle| \Psi_\lambda^A \right\rangle}}$$

Tropiano et al. (2021)

SRC phenomenology

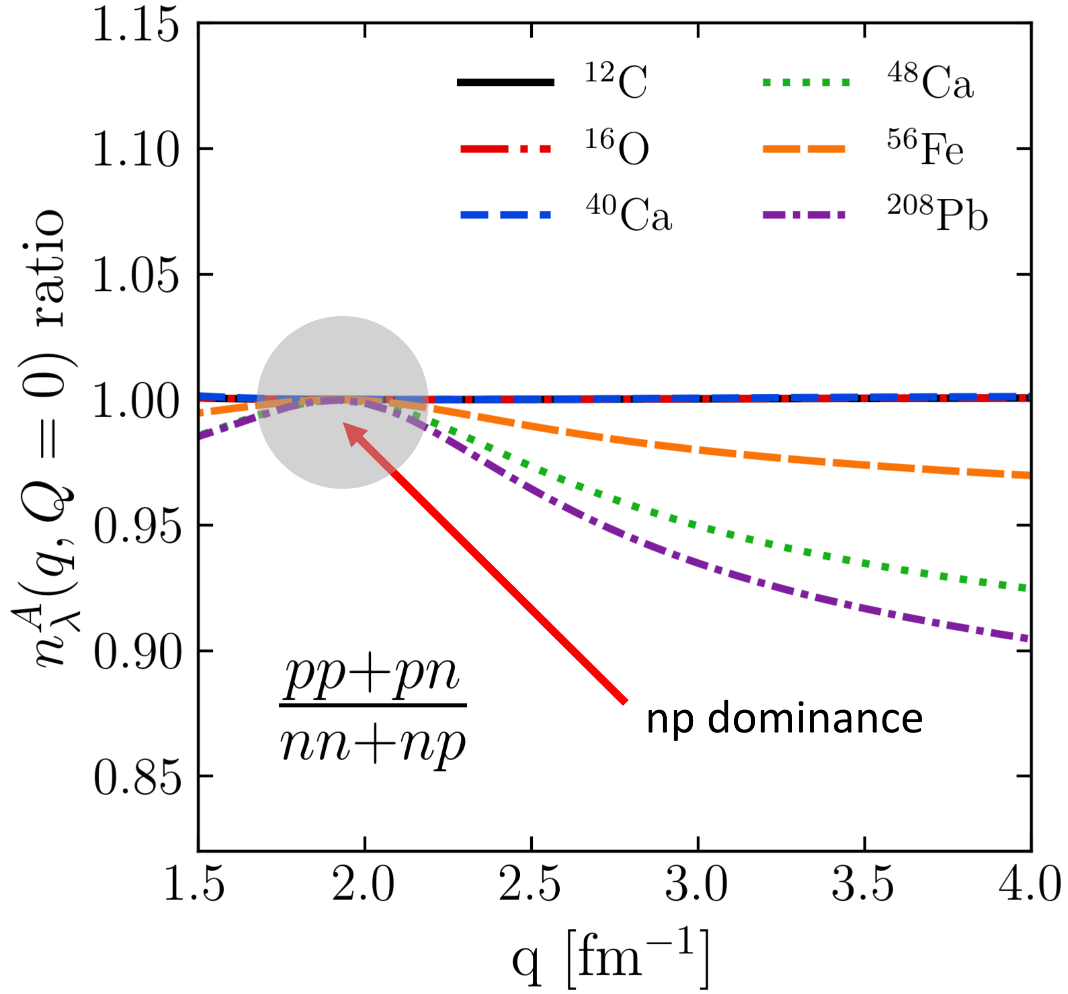

Fig. 13: (pp+pn)/(nn+np) ratio of pair momentum distributions under HF+LDA with AV18 and $\lambda = 1.35$ fm^{-1}.

- Ratio ~1 independent of N/Z in np dominant region
- Ratio < 1 for nuclei where N > Z and outside np dominant region

Tropiano et al. (2021)

Quasi-deuteron model

- Introduced by Levinger to explain knock-out of high-energy protons in photo-absorption on nuclei at energies of order 100 MeV
- High RG resolution: emitted protons from *pn* SRCs with deuteron quantum numbers ("quasi-deuterons")
- So cross section should be proportional to photo-disintegration of deuteron:

$$\frac{\sigma_A(E_\gamma)}{\sigma_d(E_\gamma)} \approx L\frac{NZ}{A}$$

- Defines Levinger constant *L*
- GCF (R. Weiss et al., 2015,2016): *L* given by ratio of high-momentum distributions (similar to a_2) → depends on "contacts"
- Low RG resolution: take ratio of evolved operators

Tropiano et al. (2022)

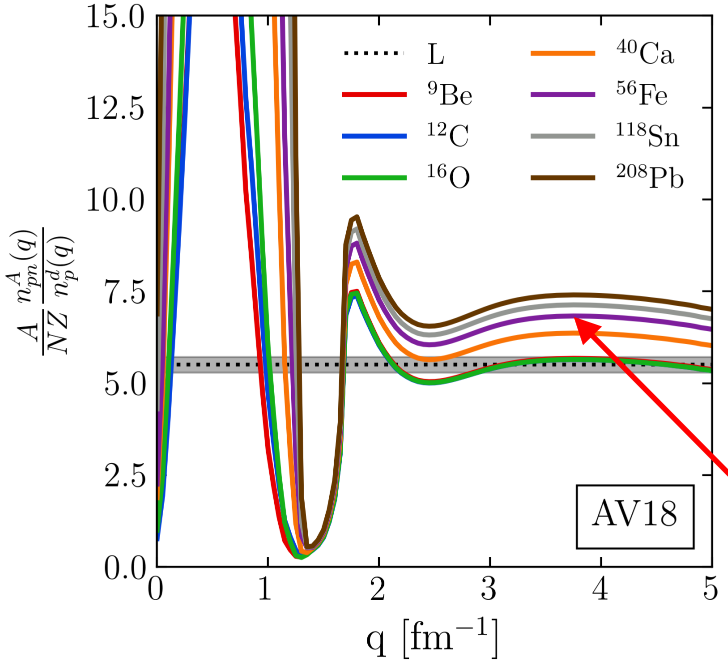

Ratios of evolved mom. dists. to *d*

Plateau despite >100 variation in this range of *q*

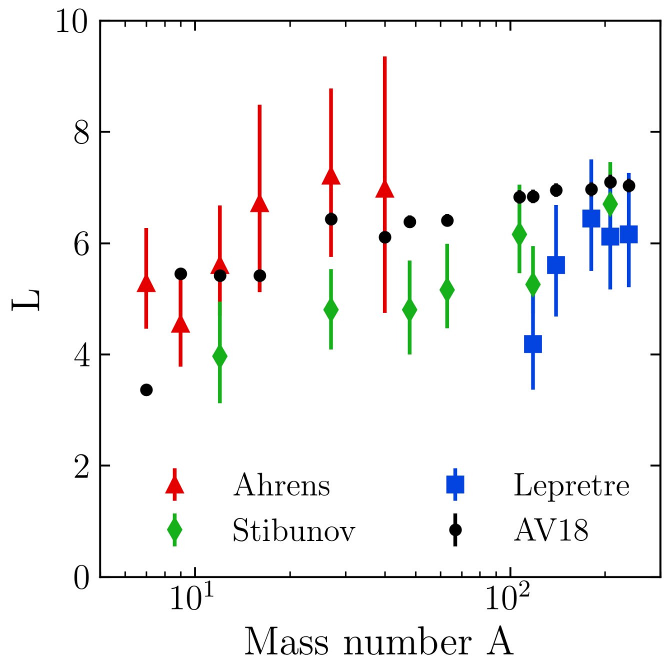

Colored points: *L* extracted from data

Black points: *L* from evolved mom. dists.

Levinger constant: Scale and scheme dependence

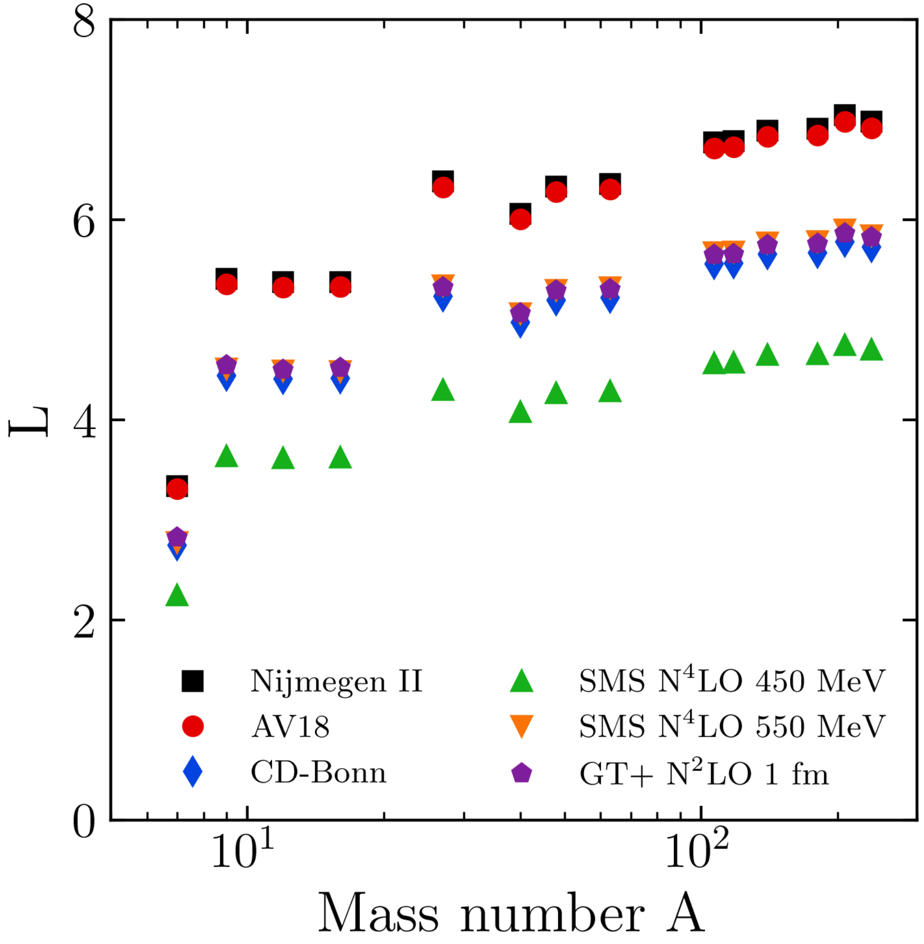

Average Levinger constant for several nuclei comparing different NN interactions.

- Varying the NN interaction changes the values of L
- Hard interactions give high L values and soft interactions give low L values
- But a ratio of cross sections should be RG invariant! So why is there sensitivity to the interaction?
  - We've assumed only an initial one-body operator!
- **Strategy**: Match results using a reference momentum distribution (AV18)
  - One-body initial operator for AV18
  - Two-body initial operator for soft potentials

Tropiano et al. (2022)

Matching interactions

- Use inverse SRG to match potentials at a scale λ_m:

$$H_{\text{soft}}(\lambda_m) = U^{\dagger}_{\text{hard}}(\lambda_m) H_{\text{soft}}(\infty) U_{\text{hard}}(\lambda_m)$$

- Use deuteron wave functions to find matching scale λ_m (other matching procedures also work)

Inverse-SRG evolution of the deuteron wave function from SMS N^{4}LO 550 MeV comparing to AV18. The solid lines correspond to the S states, and the dashed lines correspond to the D states.

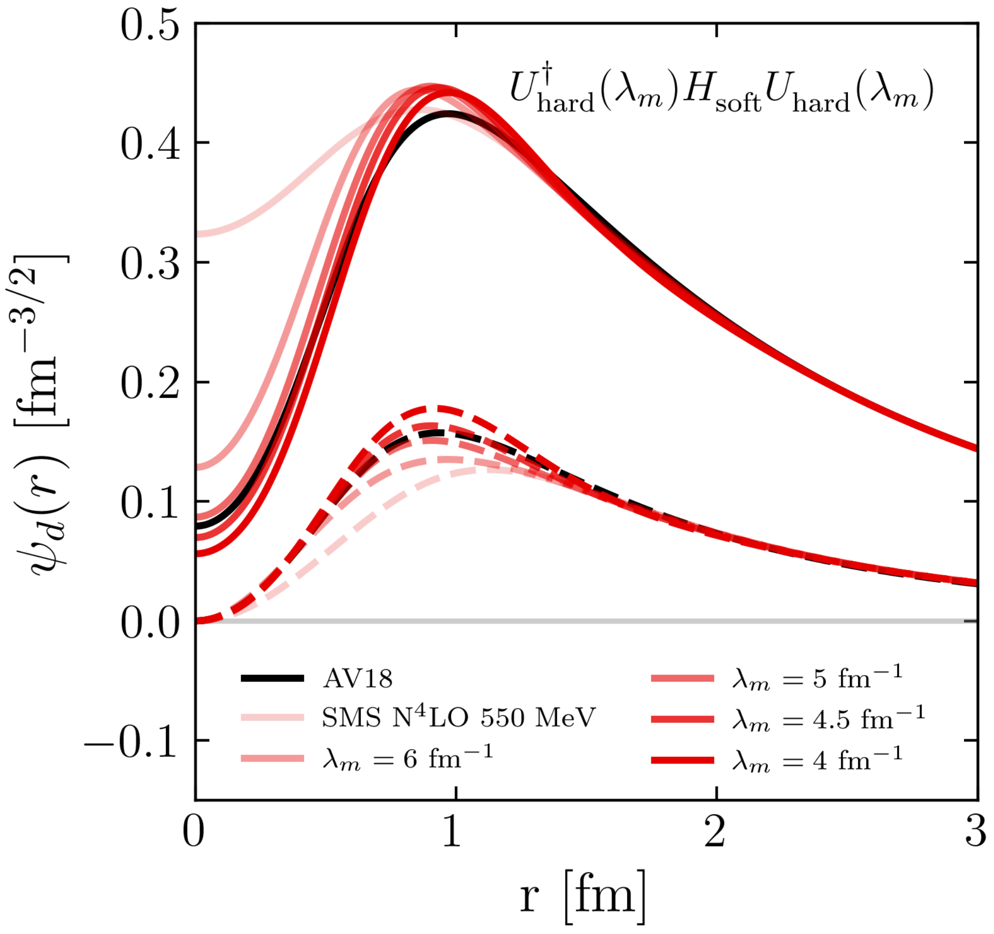

Tropiano et al. (2022)

Matching interactions

Average Levinger constant for several nuclei comparing the SMS N4LO 550 MeV and AV18 potentials. Results are also shown for the SMS N4LO 550 MeV potential with an additional two-body operator due to inverse-SRG transformations from AV18.

- Use inverse SRG to match potentials at a scale λ_m

$$H_{\text{soft}}(\lambda_m) = U^{\dagger}_{\text{hard}}(\lambda_m) H_{\text{soft}}(\infty) U_{\text{hard}}(\lambda_m)$$

- Use deuteron wave functions to find matching scale λ_m (other matching procedures also work)
- Transformations of the harder potential (AV18) determine the additional 2-body operator for calculations with soft potentials

$$O^{2\text{-body}}_{\text{soft}}(\lambda_m) = U_{\text{hard}}(\lambda_m) O^{1\text{-body}}_{\text{hard}}(\infty) U^{\dagger}_{\text{hard}}(\lambda_m)$$

- Apply same procedure following the previous point
- Lowering $\lambda_m \to 4.5$ fm^{-1} raises soft L to match hard L
- Moral: additional 2-body operator needed to calculate consistent values of L for soft potentials; found by matching!

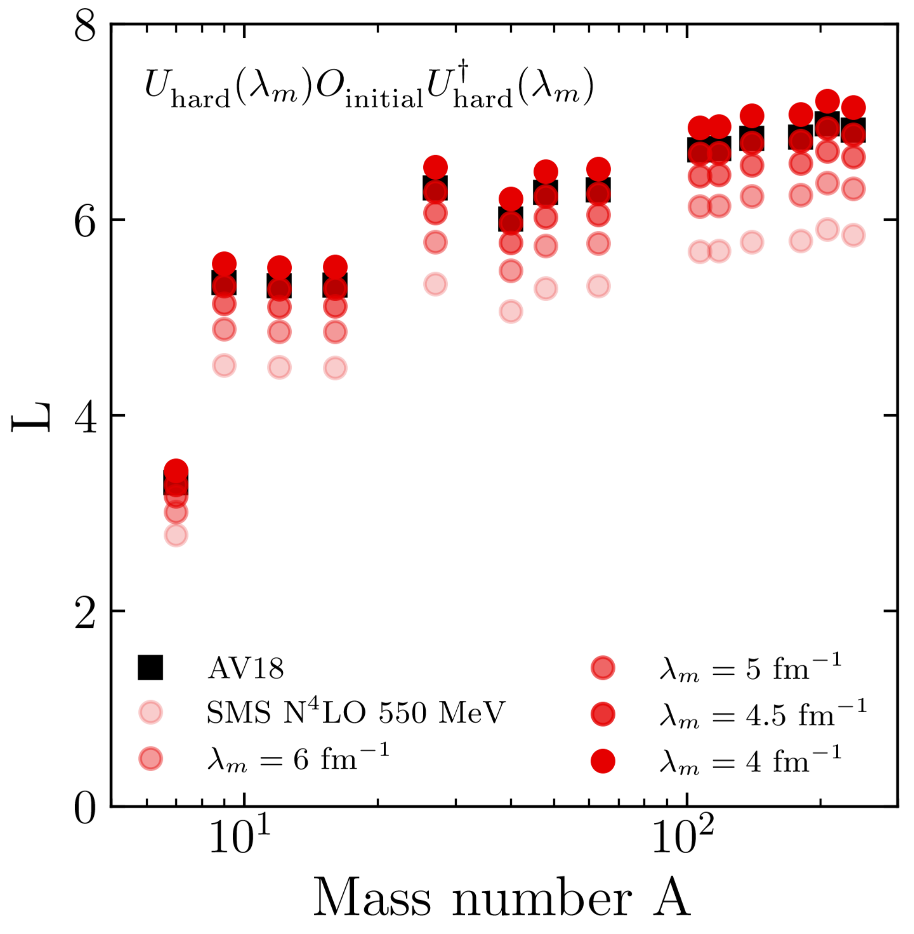

Tropiano et al. (2022)

Summary and outlook

- At low renormalization group (RG) resolution, simple approximations to SRC physics work and are systematically improvable
- Results suggest that we can analyze high-energy nuclear reactions using low RG resolution structure (e.g., shell model) and consistently evolved operators
    - Matching resolution scale between structure and reactions is crucial! (cf. quenching)
    - NN interactions can be “smoothly” connected by RG transformations

Summary and outlook

- At low renormalization group (RG) resolution, simple approximations to SRC physics work and are systematically improvable
- Results suggest that we can analyze high-energy nuclear reactions using low RG resolution structure (e.g., shell model) and consistently evolved operators
  - Matching resolution scale between structure and reactions is crucial! (cf. quenching)
  - NN interactions can be "smoothly" connected by RG transformations
- Ongoing work:
  - Extend to $(e, e'p)$ knockout *cross sections* and test scale/scheme dependence
  - Investigate impact of various corrections: 3-body terms, many-body physics, etc.
  - Apply to more complicated knock-out reactions; first steps: Hisham et al., *RG evolution of optical potentials*, PRC 106 (2022)
  - Benchmark against QMC calculations

Thank you!

Extra slides

Extras

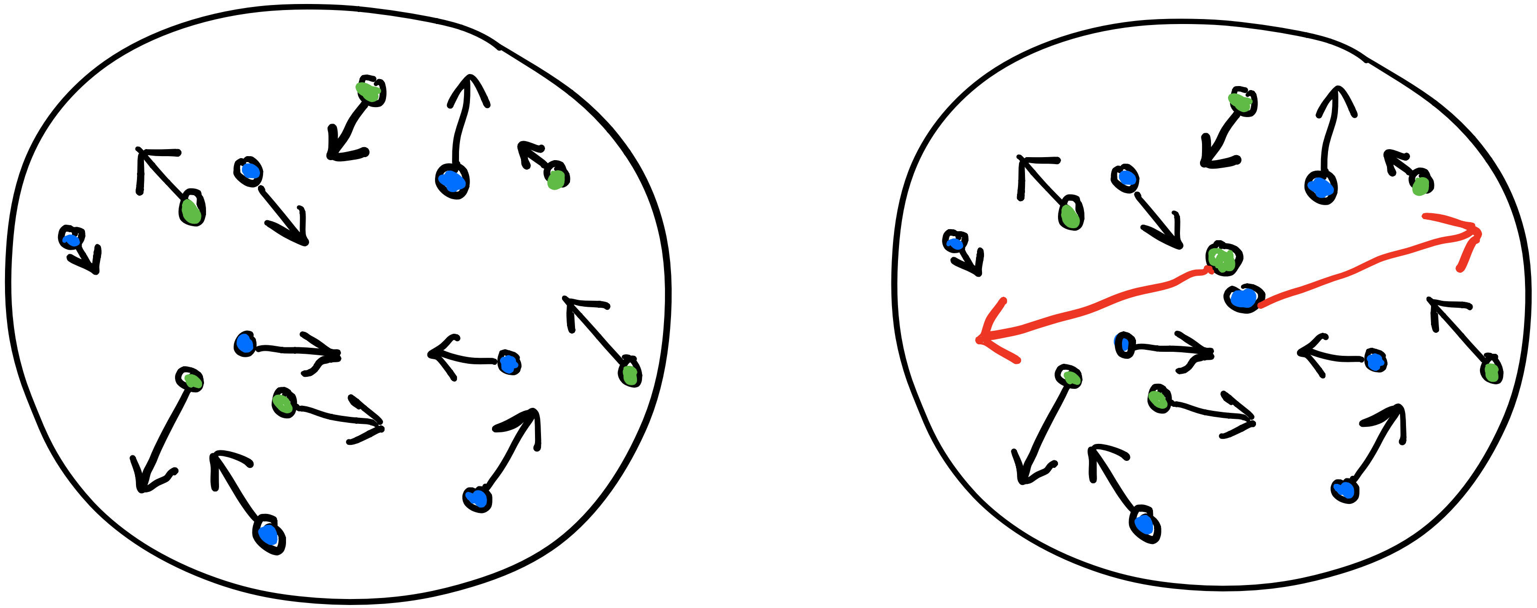

Fig. 16: Cartoon snapshots of a nucleus at (left) low-RG and (right) high-RG resolutions. The back-to-back nucleons at high-RG resolution are an SRC pair with small center-of-mass momentum.

Extras

Universality: Low-energy physics of different interactions becomes the same at low RG resolution

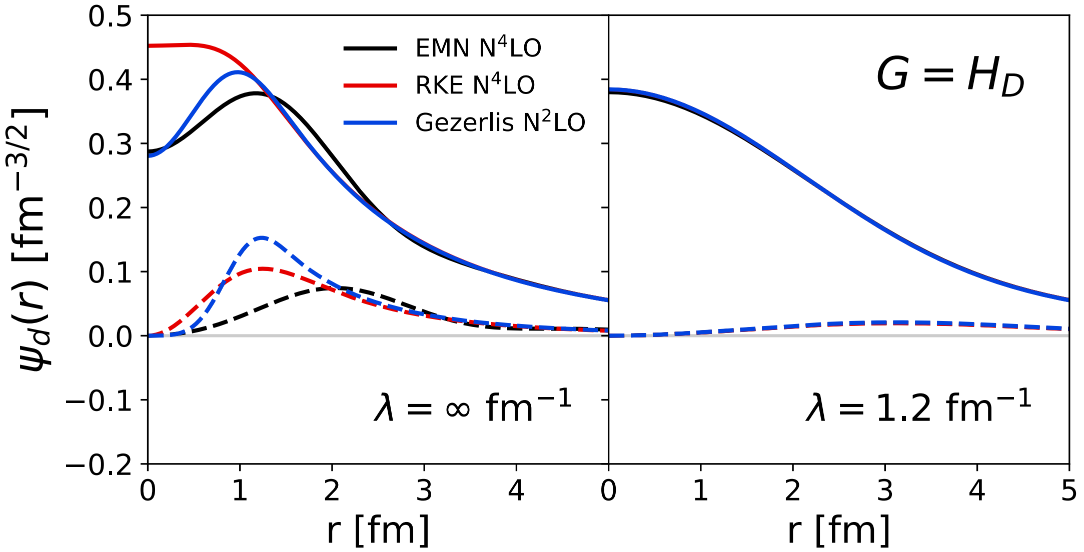

Fig. 17: Initial and SRG-evolved deuteron wave functions in coordinate space for several chiral interactions.

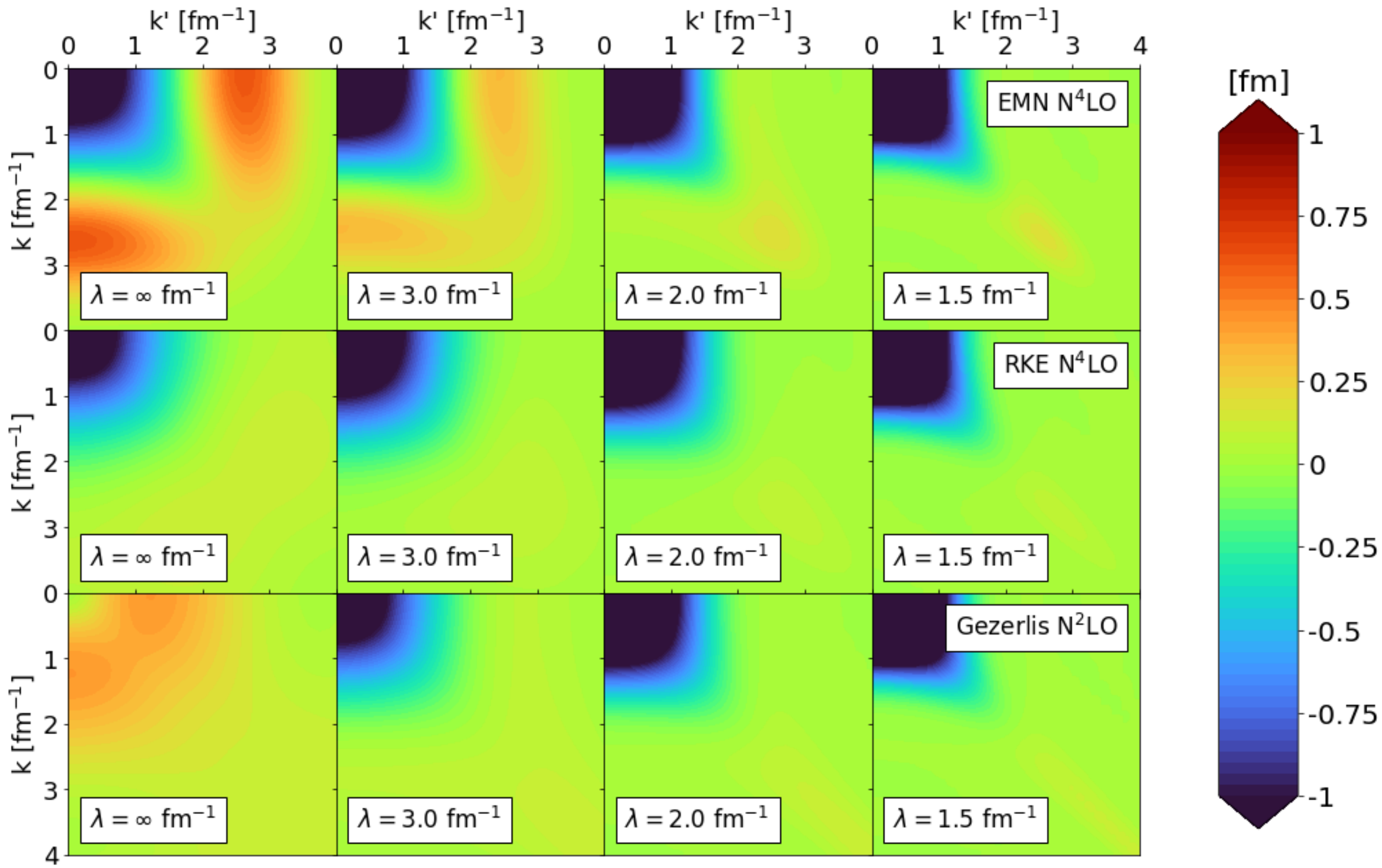

Fig. 18: SRG evolution for several chiral interactions in the $^3S_1$-$^3S_1$ channel.

Extras

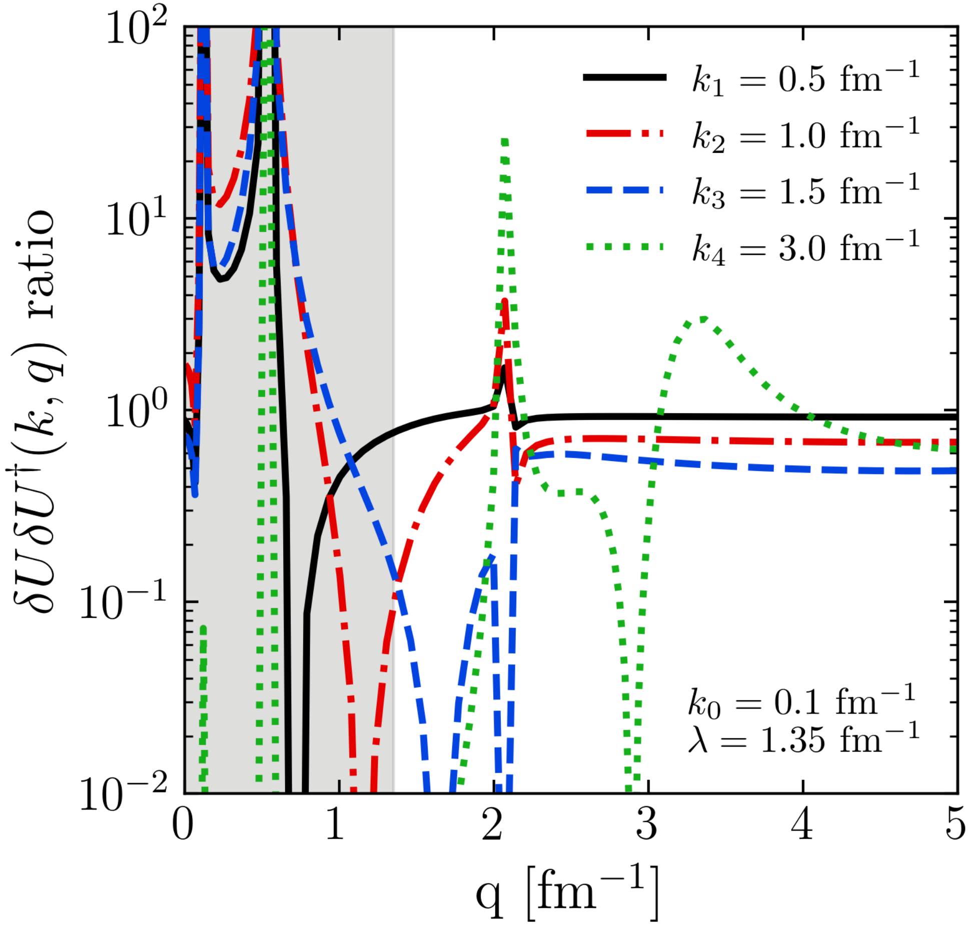

Fig. 19: Ratio of $\delta U \delta U^\dagger(k,q)$ for fixed k and λ.

- Consider an operator dominated by high momentum q where $k < \lambda$ and $q \gg \lambda$
- Expand the eigenstates ψ_α^∞ of the initial NN Hamiltonian in terms of the SRG-evolved states ψ_α^λ

$$\psi_\alpha^\infty(q) \approx \gamma^\lambda(q) \int_0^\lambda d\tilde{p} Z(\lambda) \psi_\alpha^\lambda(p) + \eta^\lambda(q) \int_0^\lambda d\tilde{p} p^2 Z(\lambda) \psi_\alpha^\lambda(p) + \cdots$$

- Substitute leading-order term of operator product expansion (OPE) in spectral representation of SRG transformation

$$\begin{aligned} U_\lambda(k,q) &= \sum_\alpha^\infty \langle k|\psi_\alpha^\lambda\rangle\langle\psi_\alpha^\infty|q\rangle \\ &\approx \Big[\sum_\alpha^{|E_\alpha| \ll |E_{QHQ}|} \langle k|\psi_\alpha^\lambda\rangle \int_0^\lambda d\tilde{p} Z(\lambda) \psi_\alpha^{\lambda\dagger}(p) \Big] \gamma^\lambda(q) \\ &\equiv K_\lambda(k) Q_\lambda(q) \end{aligned}$$

Why the SRG is a good thing for atomic nuclei

Deuteron wave function (s and d) original
(left) and evolved (

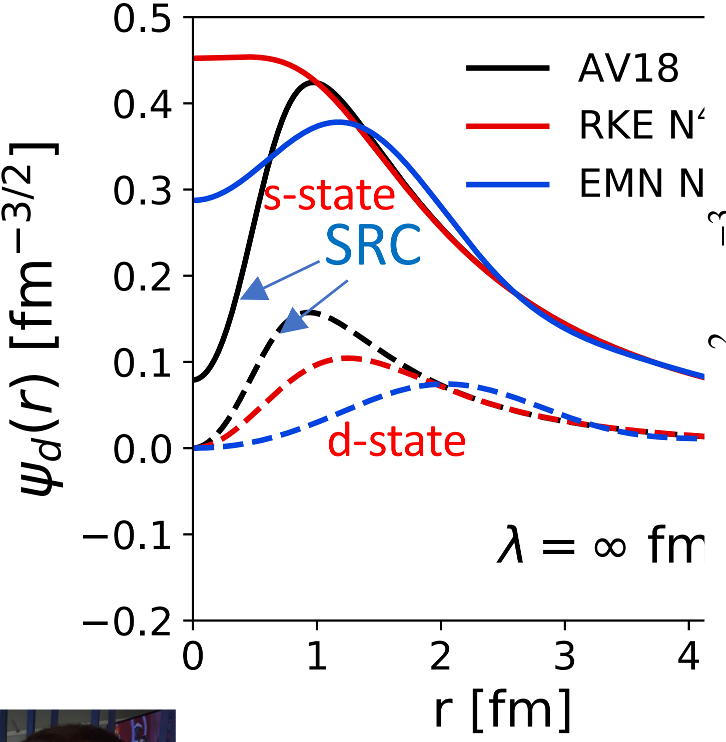

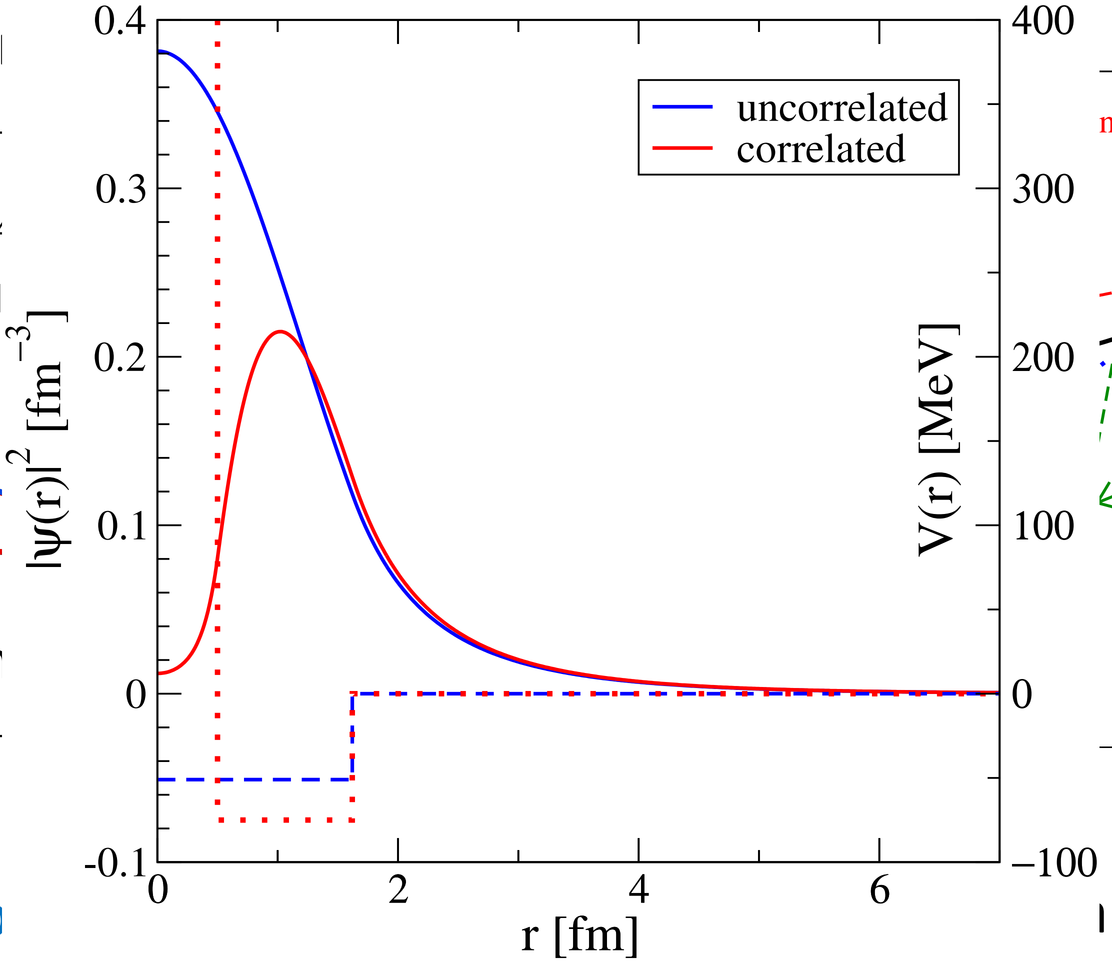

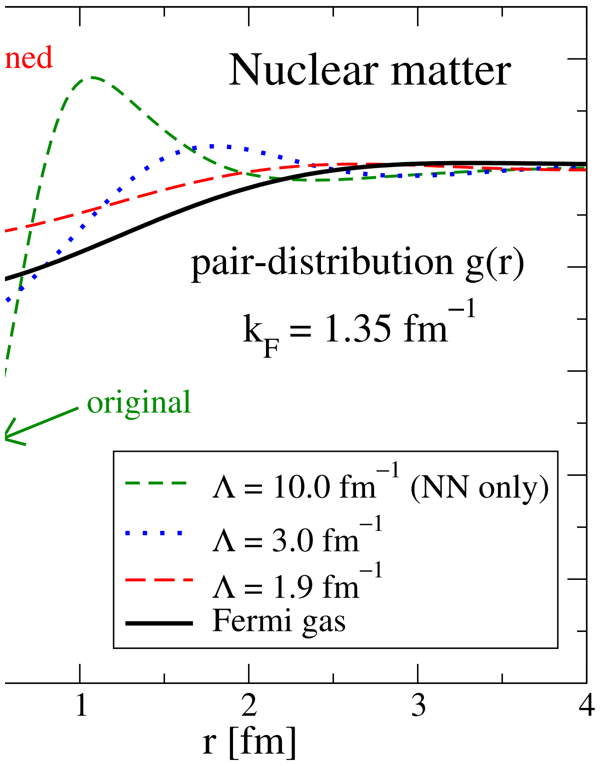

SRG evolution sup
core SRC physics, leaving observables unchanged

ırries over to nuclear
many-body systems

[see A. Tropiano et al (2020)]

SRG-evolved view of inclusive SRC ratios

Consider a high-momentum matrix element at high resolution (i.e., with SRCs) between *A*-body wave functions, divided by the same for the deuteron.

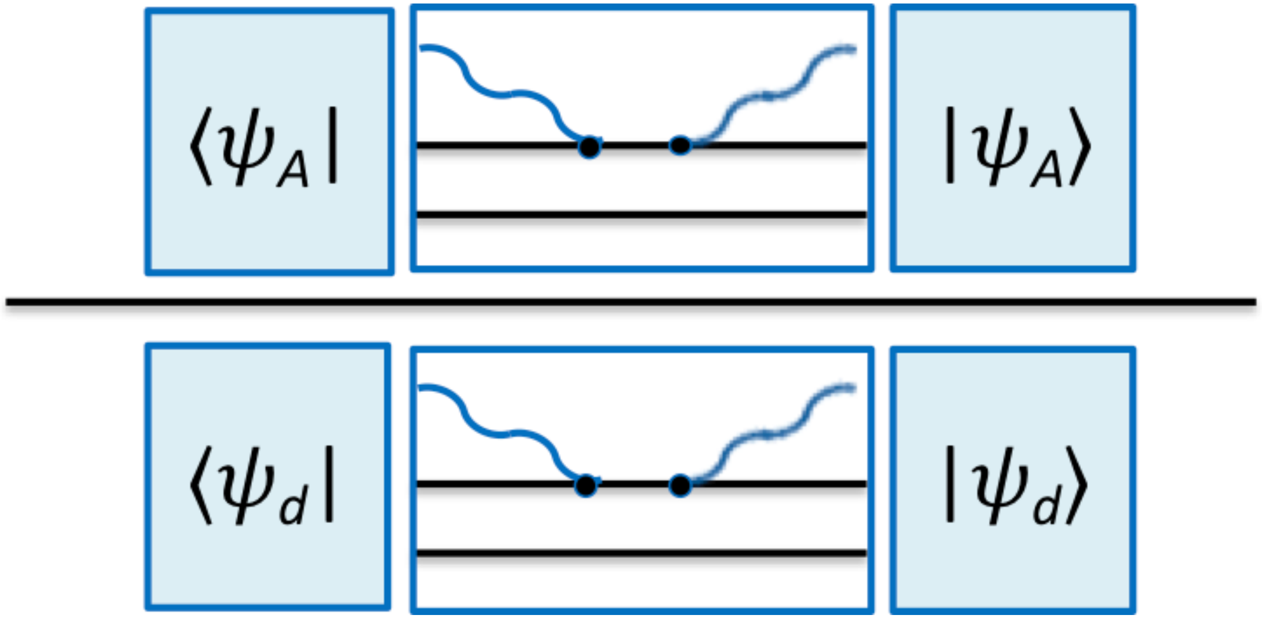

SRG-evolved view of inclusive SRC ratios

Consider a high-momentum matrix element at high resolution (i.e., with SRCs) between *A*-body wave functions, divided by the same for the deuteron.

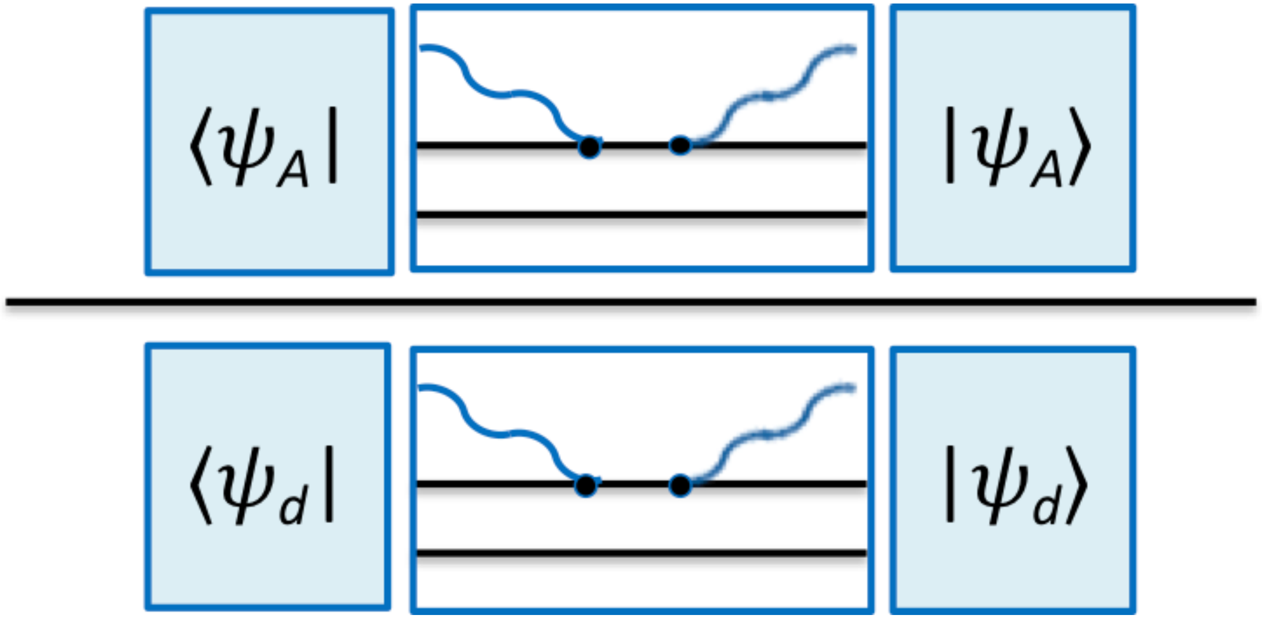

SRG unitary transformation where λ is resolution scale

$$\boxed{U_\lambda^\dagger(k,k')}\,\boxed{U_\lambda(k,k')} = 1$$

SRG-evolved view of inclusive SRC ratios

Consider a high-momentum matrix element at high resolution (i.e., with SRCs) between *A*-body wave functions, divided by the same for the deuteron.

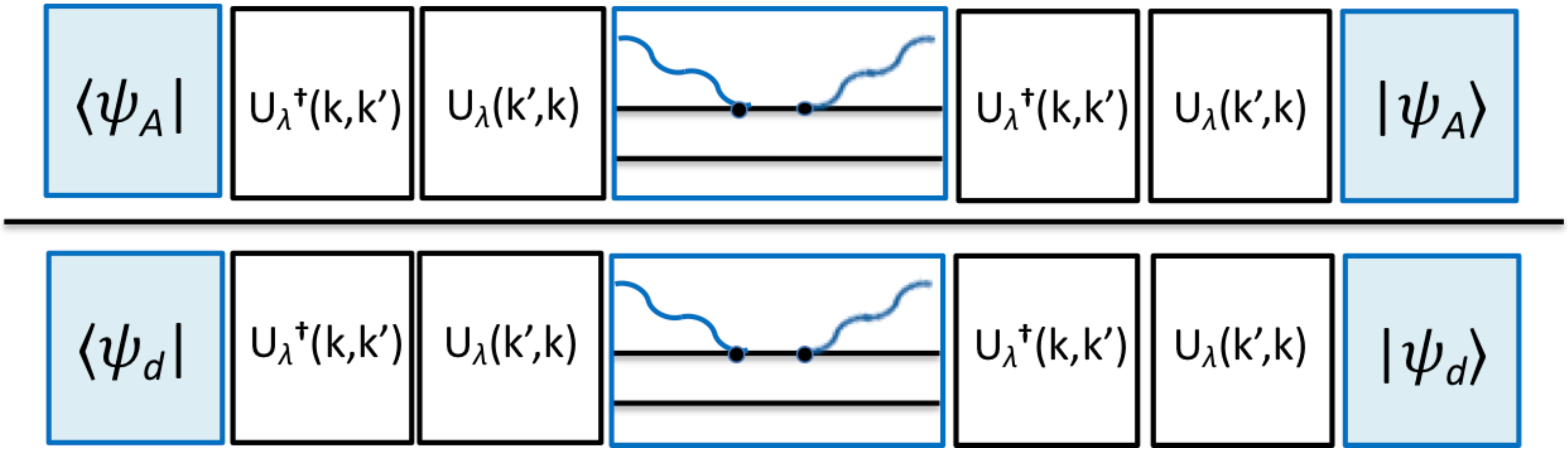

SRG unitary transformation where λ is resolution scale

$$\boxed{U_\lambda^\dagger(k,k')}\;\boxed{U_\lambda(k,k')} = 1$$

SRG-evolved view of inclusive SRC ratios

Consider a high-momentum matrix element at high resolution (i.e., with SRCs) between *A*-body wave functions, divided by the same for the deuteron.

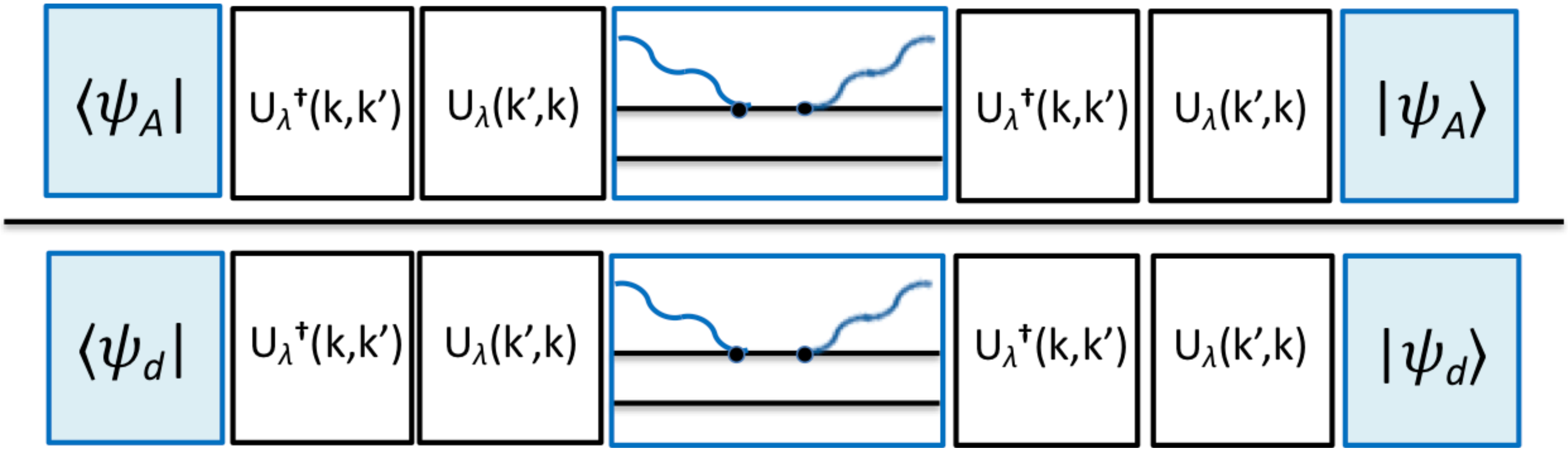

SRG unitary transformation where λ is resolution scale

$U_\lambda|\psi\rangle$ is a soft wave function

$$U_\lambda(k,k')\,|\psi_A\rangle = |\psi_A^\lambda\rangle$$

SRG-evolved view of inclusive SRC ratios

Consider a high-momentum matrix element at high resolution (i.e., with SRCs) between A-body wave functions, divided by the same for the deuteron.

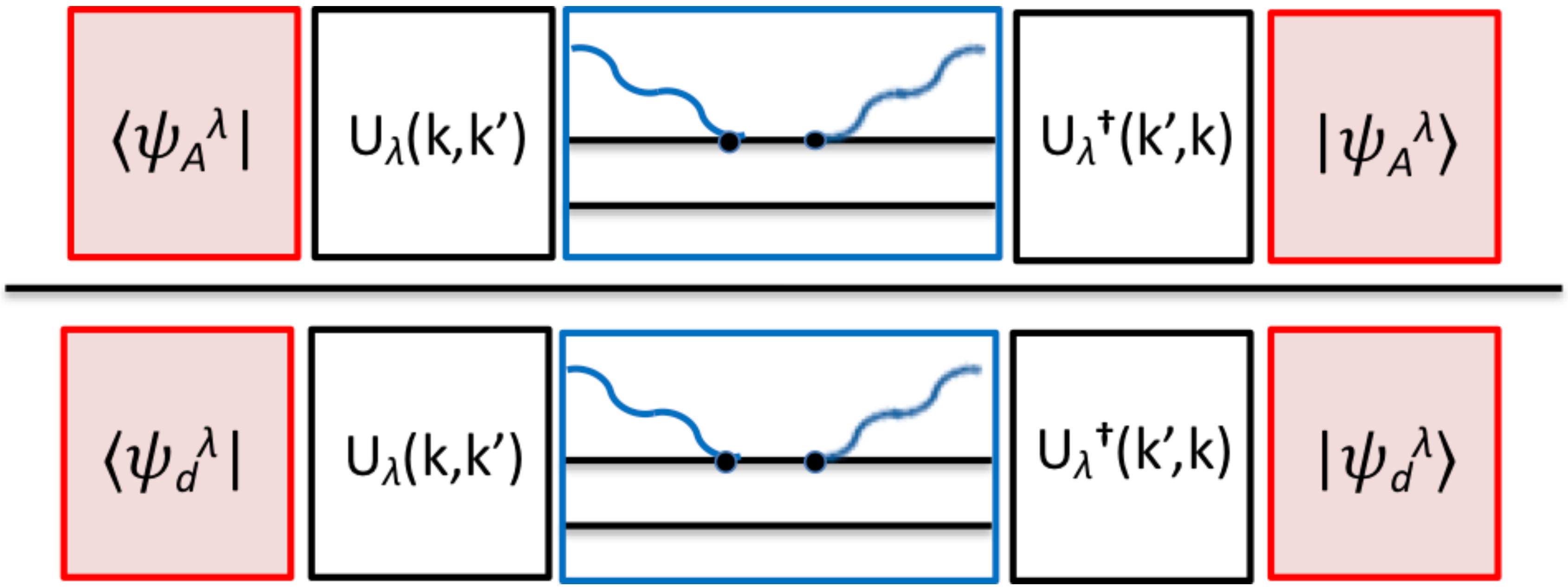

SRG unitary transformation where λ is resolution scale

$U_\lambda | \psi \rangle$ is a soft wave function

$$U_\lambda(k,k') \; | \psi_A \rangle = | \psi_A^\lambda \rangle$$

SRG-evolved view of inclusive SRC ratios

Consider a high-momentum matrix element at high resolution (i.e., with SRCs) between *A*-body wave functions, divided by the same for the deuteron.

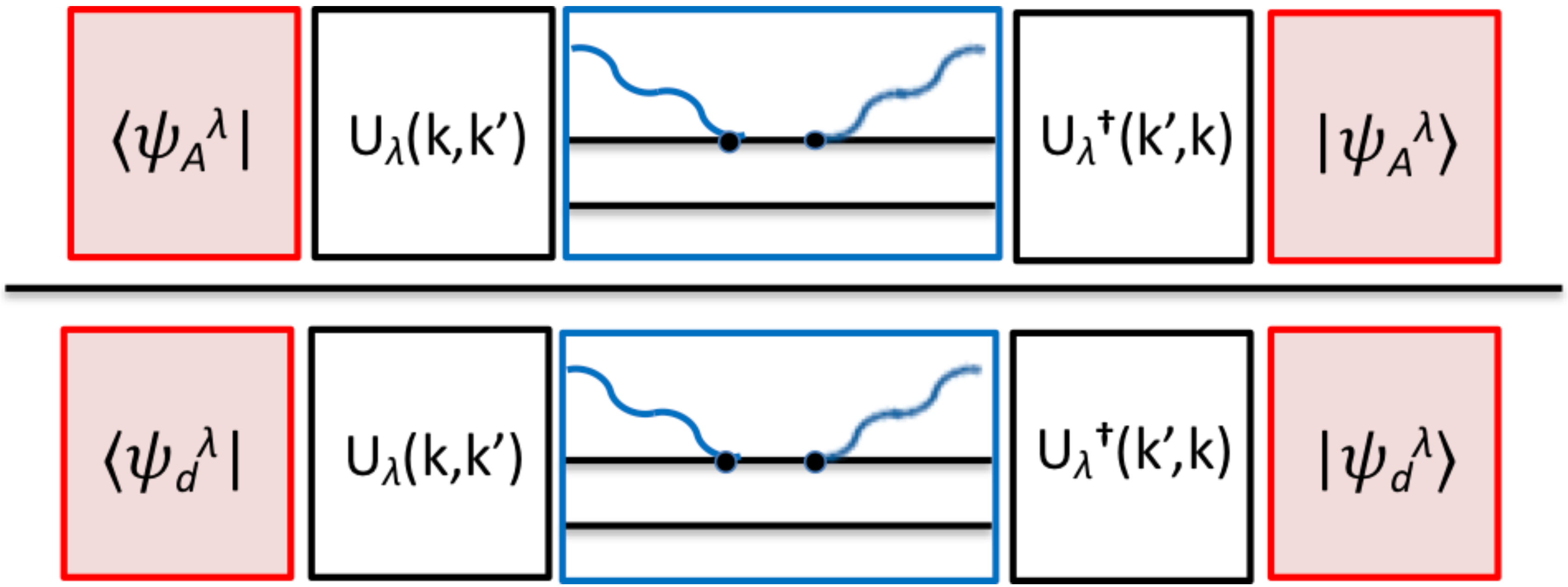

SRG unitary transformation where λ is resolution scale

If $k < \lambda$ *and* $k' > \lambda$, U_λ *factorizes*

$$U_\lambda(k,k') = F^{lo}(k)\, F^{hi}(k')$$

“Scale separation”

SRG-evolved view of inclusive SRC ratios

Consider a high-momentum matrix element at high resolution (i.e., with SRCs) between *A*-body wave functions, divided by the same for the deuteron.

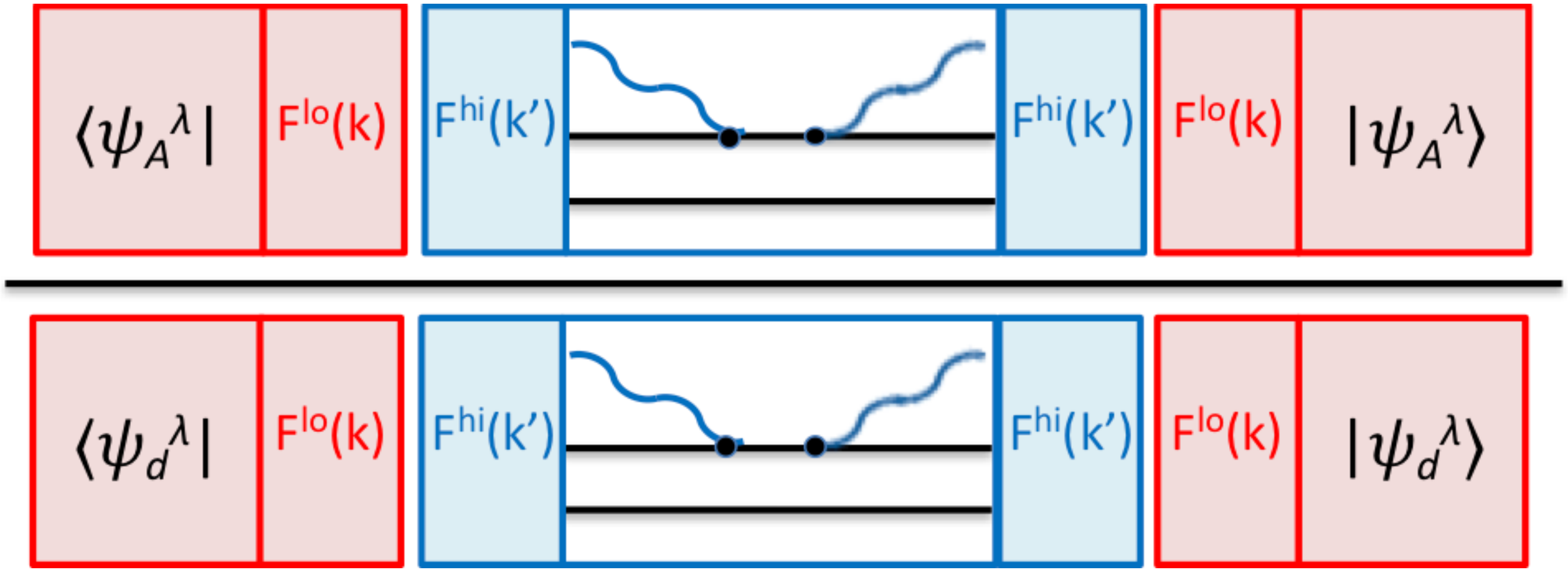

SRG unitary transformation where λ is resolution scale

If $k < \lambda$ *and* $k' > \lambda$, U_λ *factorizes*

$$\boxed{U_\lambda(k,k')} = \boxed{F^{lo}(k)}\,\boxed{F^{hi}(k')}$$

High-*q* dependence is independent of *A*

This is an operator product expansion (OPE), cf. EFT.

SRG-evolved view of inclusive SRC ratios

Consider a high-momentum matrix element at high resolution (i.e., with SRCs) between *A*-body wave functions, divided by the same for the deuteron.

Smooth operator in soft wf; can evaluate in LDA

$\langle \psi_A^\lambda |$ | $F^{lo}(k)$ | $F^{lo}(k)$ | $| \psi_A^\lambda \rangle$

$F^{hi}(k')$ 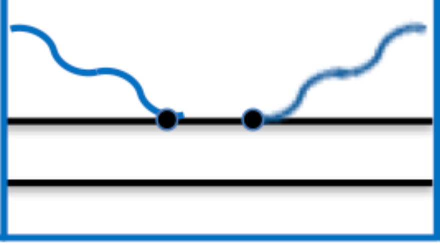 $F^{hi}(k')$

State-independent and dominated by two-body part

This is the GCF phenomenology derived, but generalizable and systematically improvable!

$$\rho_A^{NN,\alpha}(r) = C_A^{NN,\alpha} \times |\varphi_{NN}^{\alpha}(r)|^2$$
$$n_A^{NN,\alpha}(q) = C_A^{NN,\alpha} \times |\varphi_{NN}^{\alpha}(q)|^2$$

SRG unitary transformation where λ is resolution scale

If $k < \lambda$ *and* $k' > \lambda$, U_λ *factorizes*

$U_\lambda(k,k')$ = $F^{lo}(k)$ $F^{hi}(k')$

High-mom. dependence is independent of *A*

This is an operator product expansion (OPE), cf. EFT.

SRG-evolved view of inclusive SRC ratios

lement at high resolution (i.e., with SRCs)
divided by the same for the deuteron.

Wiringa et al., PRC (2014)

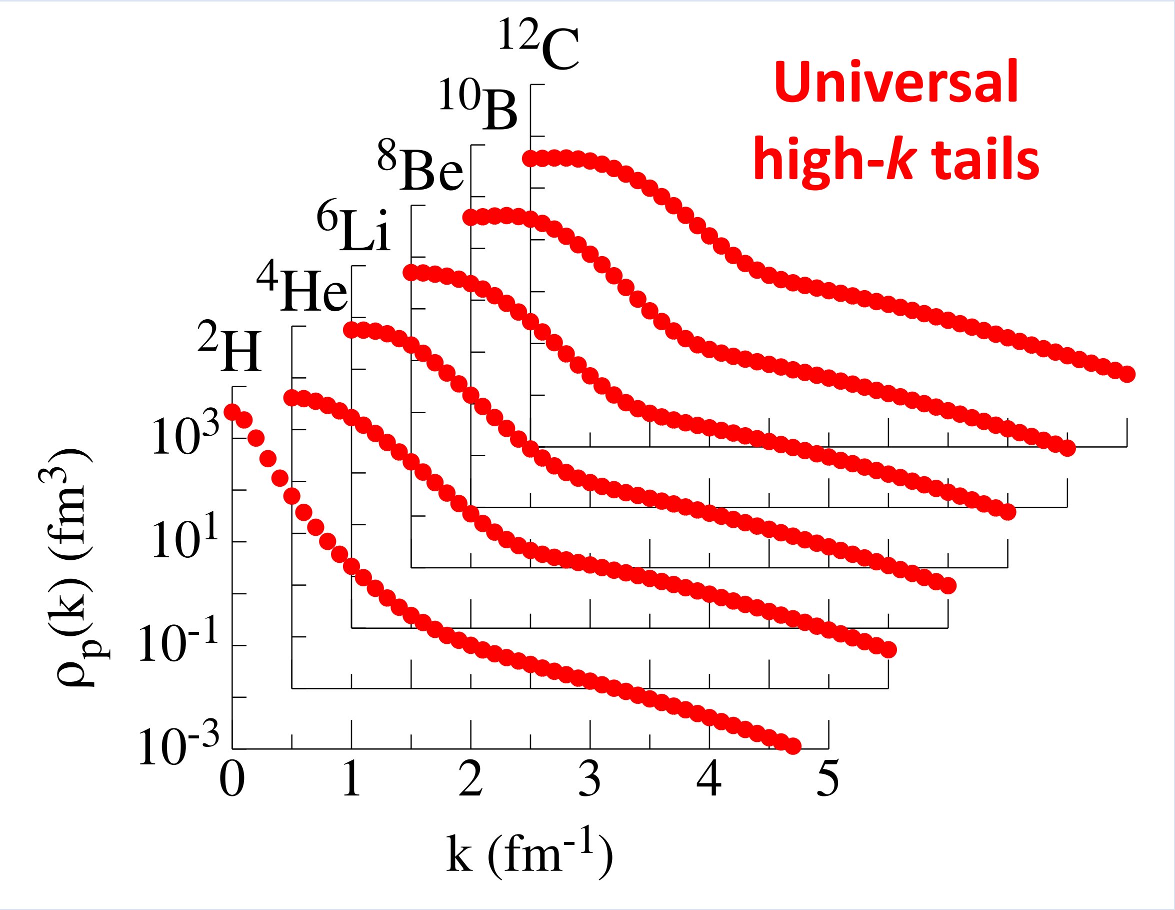

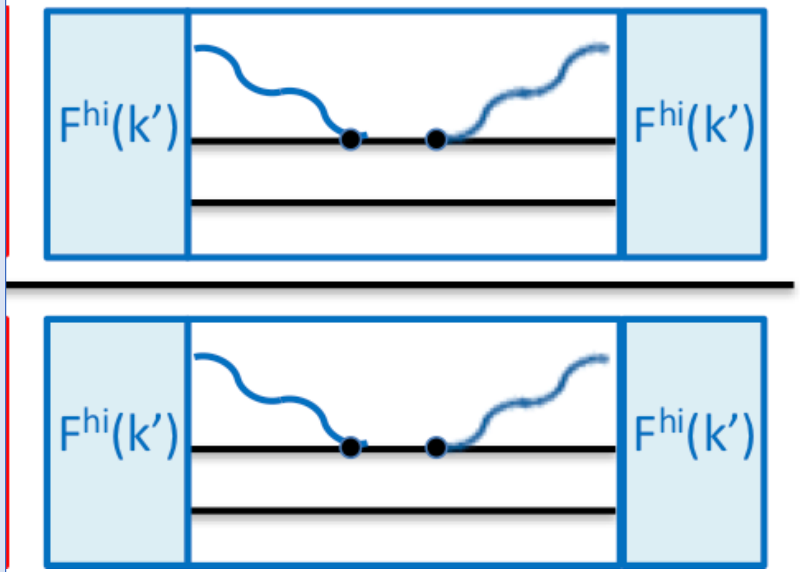

State-independent and dominated by two-body part

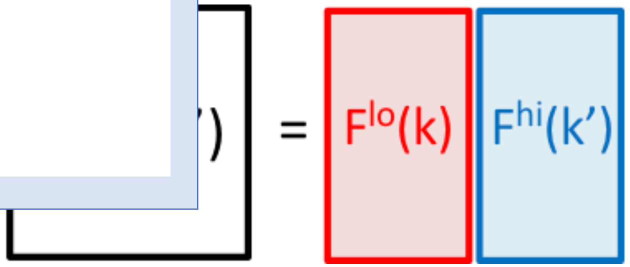

High-mom. dependence is independent of *A*

This is an operator product expansion (OPE), cf. EFT.

SRG-evolved view of inclusive SRC ratios

Consider a high-momentum matrix element at high resolution (i.e., with SRCs) between *A*-body wave functions, divided by the same for the deuteron.

Anderson et al., PRC (2010); Bogner/Roscher, PRC (2012); Chen et al., PRL (2017); Lynn et al., JPhysG (2020)

$$\frac{\langle\psi_A^\lambda|\; F^{lo}(k)\; F^{lo}(k)\; |\psi_A^\lambda\rangle}{\langle\psi_d^\lambda|\; F^{lo}(k)\; F^{lo}(k)\; |\psi_d^\lambda\rangle}$$

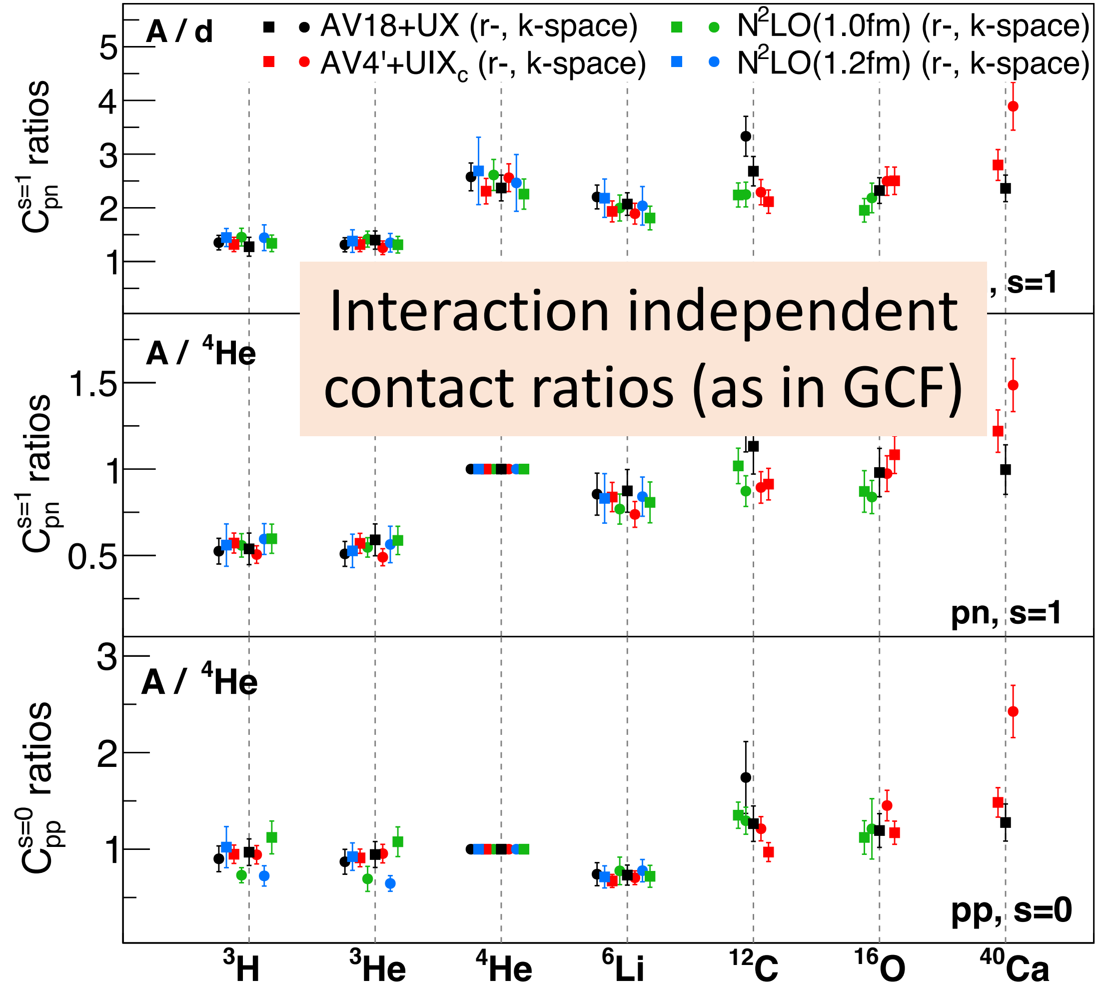

Interaction independent contact ratios (as in GCF)

Bottom line: to leading approxima
momentum matrix elements are de
physics and independent o

SRG-evolved view of inclusive SRC ratios

Consider a ratio of high-momentum matrix elements at high resolution (i.e., with SRCs) allowing both different A and different operators.

Correlation Probability:
Neutrons saturate Protons grow

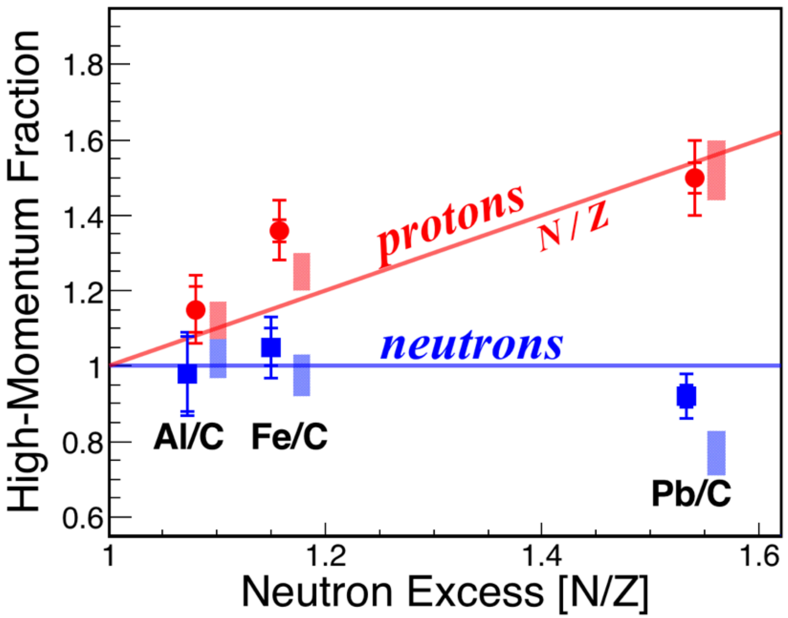

Duer Nature (2018)

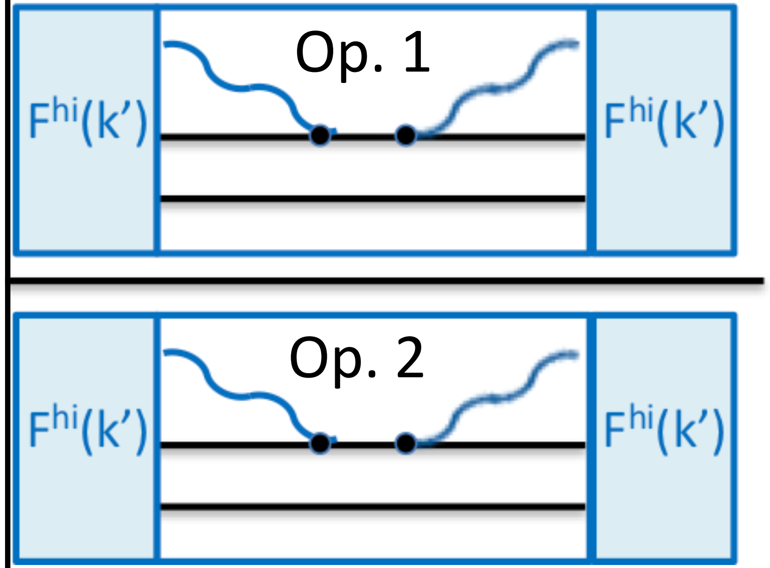

State-independent ratio of operators

Consider pair distributions for protons and neutrons